Deltares

The impact of Groundwater Extractions in the Roer Valley Graben

The impact of Groundwater Extractions in the Roer Valley Graben

Author(s)
Peter Vermeulen
Tess op den Kelder

Influences of Groundwater Extractions in the Roer Valley Graben

Client	Provincie Limburg
Contact	E. Castenmiller
Keywords	Groundwater extraxction, Rur-Scholle / Roer Valley Graben, iMOD

Document control

Version	0.3
Date	22-01-2020
Project nr.	11204053-002
Document ID	11204053-002-BGS-0001
Pages	111
Status	Final

Author(s)

	Peter Vermeulen	
	Tess op den Kelder	

Doc. version	Author	Reviewer	Approver	Publish
0.1	Peter Vermeulen	Gijs Janssen	Otto de Keizer	
	Tess op den Kelder			

Executive summary

This report describes the modelling activities carried out to improve the IBRAHYM v2 model to explore the mutual effects in the Roer Valley Graben (Rur-Scholle) of total groundwater extractions by the Province of Limburg, Province of Noord-Brabant, Waterboard Erfverband, Belgium and the open-pit mines Inden and Hambach in Germany. The geology within the model has been improved significantly based on recent geological mappings of the border regions. The extraction regimes have been improved and extended in time, as well as the boundary conditions that represent the open-pit mining activities in Germany. The model eventually computes the groundwater dynamics on a yearly base from 1955 up to 31st of December 2018. The adapted model proved to be able to compute a reliable and plausible estimate for the effects of the groundwater extractions in the Roer Valley Graben. The accuracy of the transient model, compared to measurements is statistically sound.

The effect on drawdown of all extractions on the groundwater level is significant along both rivers of the Rode Beek and the Saeffelerbach. Along the Rode Beek, a total drawdown of ~1-2 meter is expected as for the upper-stream of the Saeffelerbach this is can be significantly more in the order of magnitude of ~3-5 meter. The area in between the Rode Beek and the Saeffelerbach, the drawdown varies between 0 and ~5 meters. In the deeper aquifers, this drawdown is even ~10 meters. It has been found that the drainage capacity of the Rode Beek and Saeffelerbach are reduced with 65% and 52% since the 70s. For the downstream and south section of the Rode Beek it seems to be that the extractions of Limburg are mainly responsible as for the further upstream section the groundwater level is most influenced by the open pit mines. The Saeffelerbach is for a larger stretch mostly influenced by the open-pit mines.

With this model it has been demonstrated that groundwater extractions in The Netherlands and Germany largely influence drawdown mutually. Due to the enormous resistances in the aquitards the effect of extractions underneath those aquitards reaches 10-100 kilometers. Therefore, drawdown due to the open-pit mines in Germany determine still 40% and 25% in Limburg and Noord Brabant, respectively. On the other hand, Limburg effects the drawdown locally in Germany up to ~30% as it influences the drawdown in Noord Brabant less, ~25%. For almost half of Limburg, Noord Brabant determines most of the draw down with percentages of maximal 80%, it even influences the total drawdown in Germany for ~5-10%. The extraction of Belgium and Erfverband influence significant less of their neighboring countries.

The model is capable of exploring more measures to reduce drawdown. Due to the non-linearities in the model, it is advised to compute total drawdown as a function of a total set of measurements instead of superposition of individual measures.

About Deltares

Deltares is an independent institute for applied research in the field of water and subsurface. Throughout the world, we work on smart solutions, innovations and applications for people, environment and society. Our main focus is on deltas, coastal regions and river basins. Managing these densely populated and vulnerable areas is complex, which is why we work closely with governments, businesses, other research institutes and universities at home and abroad. Our motto is ‘Enabling Delta Life’.
As an applied research institute, the success of Deltares can be measured in the extent to which our expert knowledge can be used in and for society. As Deltares we aim at excellence in our expertise and advice, where we always take the consequences of our results for environment and society into consideration.

All contracts and projects contribute to the consolidation of our knowledge base. We look from a long-term perspective at contributions to the solutions for now. We believe in openness and transparency, as is evident from the free availability of our software and models. Open source works, is our firm conviction.
Deltares is based in Delft and Utrecht, the Netherlands. We employ over 800 people who represent some 40 nationalities. We have branch and project offices in Australia, Indonesia, New Zealand, the Philippines, Singapore, the United Arab Emirates and Vietnam. In the USA Deltares also has an affiliated organization.

www.deltares.nl

Contents

1 Introduction

1.1 Background

This report describes the modelling process of modifying the existing IBRAHYM v2 model (Vermeulen et al, 2015) and the quantification of the effects of regional extractions on the groundwater levels in the Roer Valley Graben / Rur-Scholle.

Since 2015, Deltares has been commissioned by the Province of Limburg to update the IBRAHYM model (Vermeulen *et al.*, 2007/2015) with data from representatives of Nordrhein-Westfalen (GD-NRW, Waterboard Erftverband, RWE-Power and LANUV). In 2018 a calibrated time-dependent (01-01-1955 / 31-12-2012) groundwater model (called IBRAHYM-ROERDAL model) with annual time steps was delivered with acceptable differences between the measured and calculated groundwater levels and pressure heads (Vermeulen, 2018). In 2019, this project was funded by the Province of Limburg, Province of Noord Brabant, Vlaamse Milieu Maatschappij (VMM) and Landesamt für Natur, Umwelt und Verbraucherschutz Nordrhein-Westfalen (LANUV) to improve the IBRAHYM-ROERDAL model even more and extend its application to make exploratory calculations for the quantification of the influence of the groundwater levels and pressure heads in the Roer Valley Graben by various extractors of groundwater, see *Figure 2.1*.

The following two questions are formulated:

1) What is the impact of the groundwater extractions on the Rode Beek and Saeffelerbach?

Initially, the project aimed to quantify the effects for two streams along the Dutch-German border; the Rode Beek and the Saeffelerbach, see inset figure on *Figure 1.1*. It is unknown whether developments along the Rode Beek (NL) and Saeffelerbach (GER) are influenced by groundwater effects of drinking water extraction in The Netherlands and withdrawals related to extractions in Germany and then particular the extractions at the brown coal mining in Germany. In 1995 a report from AHU AG Aachen was published, in which external deficits of surface water discharge of approximately 10 million m^3 / year were found and future damage to the existing nearby wetlands was not excluded. Both rivers are within the Roer Valley Graben / Rur-Scholle.

2) What is the impact of the groundwater extractions on the regional groundwater level and deeper pressure heads

In deeper aquifers of the Roer Valley Graben / Rur-Scholle, falling groundwater levels and water supply shortages are present as well. This raised the additional question what the total influence would be of all existing extractions in the Roer Valley Graben and what their total and mutual effect is on the groundwater levels as well as on deeper pressure heads. It is unknown what the mutual influences are between The Netherlands and its neighboring countries. A realistic estimate of the influence is up to now not available, mainly because the effects tend to spread out over such large distances – due to the enormous resistances of clayey sediments – that no existing groundwater model is large enough, except IBRAHYM.

The actions and results are described in the coming sections.

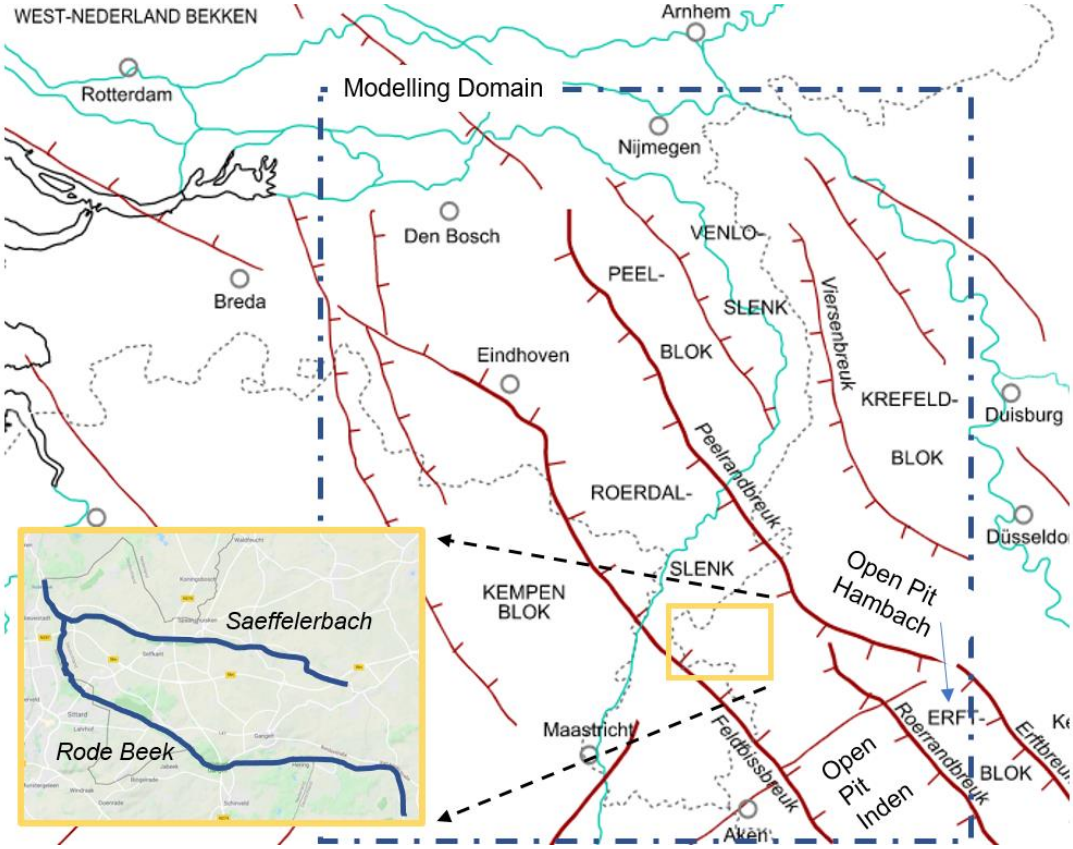

Figure 1.1 Model area and locations of the Saeffelerbach (GER) and Rode Beek (NL) (source: Door Woudloper - Eigen werk, CC BY-SA 1.0, https://commons.wikimedia.org/w/index.php?curid=4848971)

1.2 iMOD

In the Netherlands, the software package iMOD (Interactive MODeling) was developed to support the usage and creation of high resolution large-scale groundwater flow models (Vermeulen, *et al.*, 2019). The concept of iMOD avoids the inefficient and highly costly practice of building many individual special-purpose models within a region and facilitates engagement of the stakeholders in the model building process. To make this happen iMOD provides the necessary functionalities to manage groundwater flow models efficiently, including the generation of multiple scenarios. These features are essential in the current modeling study.

1.3 Groundwater Flow

To describe groundwater flow in three dimensions we use the partial differential equation based upon Darcy's law and the equation of continuity (McDonald and Harbaugh, 2005):

$$\frac{\partial}{\partial x}\left(T_x\frac{\partial h}{\partial x}\right)+\frac{\partial}{\partial y}\left(T_y\frac{\partial h}{\partial y}\right)+\frac{\partial}{\partial z}\left(T_z\frac{\partial h}{\partial z}\right)-q=S\frac{\partial h}{\partial t}$$

where h [L] is the piezometric head, x, y and z [L] are Cartesian coordinates, t [T] is the time, $T_{x/y/z}$ [L^2/T] are the conductivities in x, y and z directions of the subsoil, S [L^2/T] is the storage coefficient and q [L^3/T] is the discharge or recharge term. Any feature that interacts with groundwater is described in the discharge or recharge term q, which can be dependent on groundwater head.

For the IBRAHYM-ROERDAL model, this *q* is used to describe the interaction of:

- groundwater extraction volumes from various companies;
- the net recharge and net inflow from a part of Germany;
- river- and/or drainage canals, which are widespread in the area.

The river- and or drainage systems exchange water between surface and groundwater. The amount of exchange depends on the difference between the surface water level and the computed groundwater level. The interaction of this with groundwater is modelled using a so-called *Cauchy Boundary* condition. This boundary condition assumes that there is a nonlinear-relation between the amount of groundwater flow and the difference in groundwater level and seawater level, so:

$$q = C(h_{channel}) \times (h_{channel} - h_{groundwater}),$$

here $C(h_{channel})$ is a conductance that depends on the wetted surface in the channel and determines the steepness of the relation, the higher *C* the more groundwater exchanges with differences in head.

2 Modelling

2.1 Model boundaries

2.1.1 Spatial and Temporal Dimensions

The model is constructed for the window between the lower left coordinate of x=120000 and y=298000 and the upper right coordinate of x=240000 and y=430000. The total active modelling area is 6428 km^2. The highest spatial resolution for which the model ran, is 250 x 250 meter, see *Figure 2.1*. Effects are presented for the Roer Valley Graben and Rur-Scholle only.
The model simulates groundwater flow at an annual temporal resolution for a modelling period that starts at the 1st of January 1955 and end at the 31th of December 2018; yielding 64 stress periods in total. Prior to the simulation, an initial steady-state simulation is applied. This steady-state simulation represents the undisturbed geohydrological situation without any groundwater extraction and an absence of the open-pit mining areas in Germany.

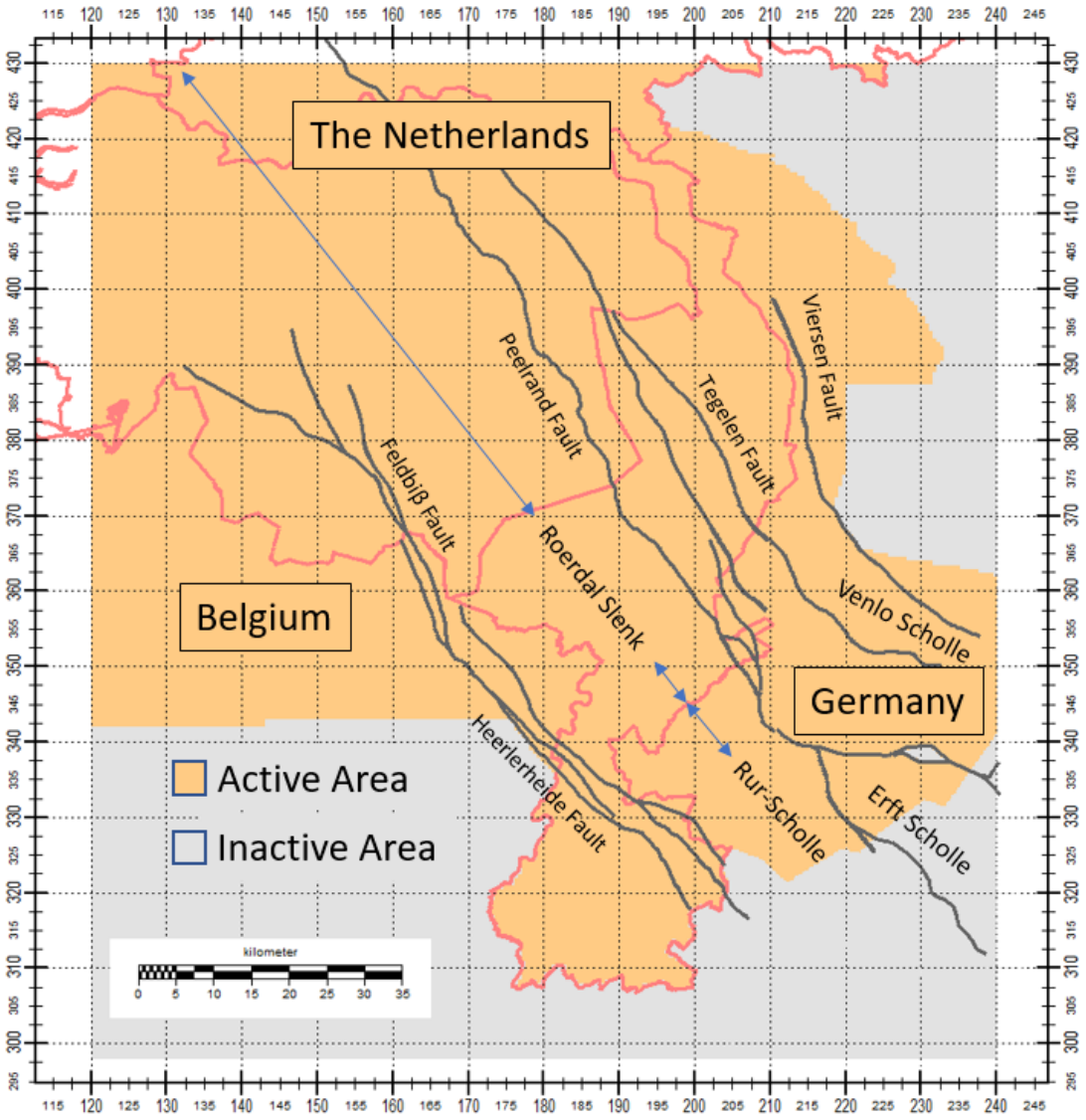

Figure 2.1 Overview of the location of the active- and inactive areas of the model as well as the location of the Roer Valley Graben (Roerdal Slenk), Rur-Scholle and important faults.

2.1.2 Boundary Conditions

Three types of boundary conditions are used in the current model (Figure 2.2): a *closed boundary condition* which is defined as a modeling boundary over which no groundwater flow is passing, an *open boundary condition* which is defined as a boundary over which groundwater flow is passing and on which a fixed or *specified head* is imposed (Dirichlet Boundary), and a *constant flux boundary* (Neumann Boundary) for which a fixed flux passes the boundary.

2.1.2.1 Closed Boundary Condition

The closed model boundary condition is present along most of the model boundary. As a result, no groundwater flows into or out of the model as it is assumed that the inflow is either sufficiently low to be relevant (e.g. at the location of a watershed that is aligned with the model boundary) or too far away to contribute significantly to the groundwater situation in the Rur-Scholle (e.g. the minor inflow from the south border in Southern part of Limburg). Furthermore, the western boundary is closed as the major flow direction is south-north and therefore perpendicular to that boundary. The location of the closed boundaries is depicted as a black solid line in *Figure 2.2*.

Finally, there is a no-flow boundary condition on the bottom of the lower-most model layers. There is no groundwater exchange with geological layers underneath the base of the model.

2.1.2.2 Open Boundary Conditions – Dirichlet Boundary

There is an inflow of potential groundwater along the Peelrand Fault on the German territory. To simulate that, the hydraulic heads are fixed to allow in- and/or outflow. Those fixed hydraulic heads are extracted from the RWE-model (RWE AG, 2013) and positioned on the eastern side of the Peelrand Fault and on the western side of the open-pit Mining areas of Inden and Hambach. For the period 2013 up to 2017, a prognosis has been computed. The fixed hydraulic head is specified as a yearly value for the entire simulation window. The undisturbed situation (no open-pit mining before 1955) and the start and progress of the open-pit mining since the 70^{s} is represented by the fixed hydraulic heads. For the undisturbed situation these are gathered from an isohypses map of 1955 (shapefile of contours received from RWE AG and LANUV NRW). The run-up from 1970 (start of the open-pit mining in Inden) towards 2010 is not reliable enough (personal comment, RWE Power). Also, the groundwater injections near the Meinweg are represented by the fixed hydraulic heads. The Peelrand Fault is modelled explicitly as a Fault with a high resistance, and the yielding effective in- and/or outflow over this fault is an outcome of the model. The location of the open model boundaries is depicted as a blue solid line in *Figure 2.2*.

A major advantage of the chosen methodology is that the complex configuration of extractions and infiltrations along the open-pit minding areas, are not modelled explicitly but represented by the simulated hydraulic heads from the RWE Power model (RWE AG, 2013). To check the water balance, the modeled fluxes over the Peelrand Fault are compared with those computed by the RWE AG model.

2.1.2.3 Constant Flux Conditions – Neumann Boundary

On the south-east side, near the border between the Netherlands and Germany, there is a significant inflow of 1.35- and 0.30 million m^3/year (LANUV, D. Hüsener) for the shallow and deep aquifers underneath the Frimmersdorf (see Geology section 2.1.6). This amount is weighted divided by transmissities among the appropriate model layers. The location of the constant flux boundaries is depicted as a green solid line in *Figure 2.2*.

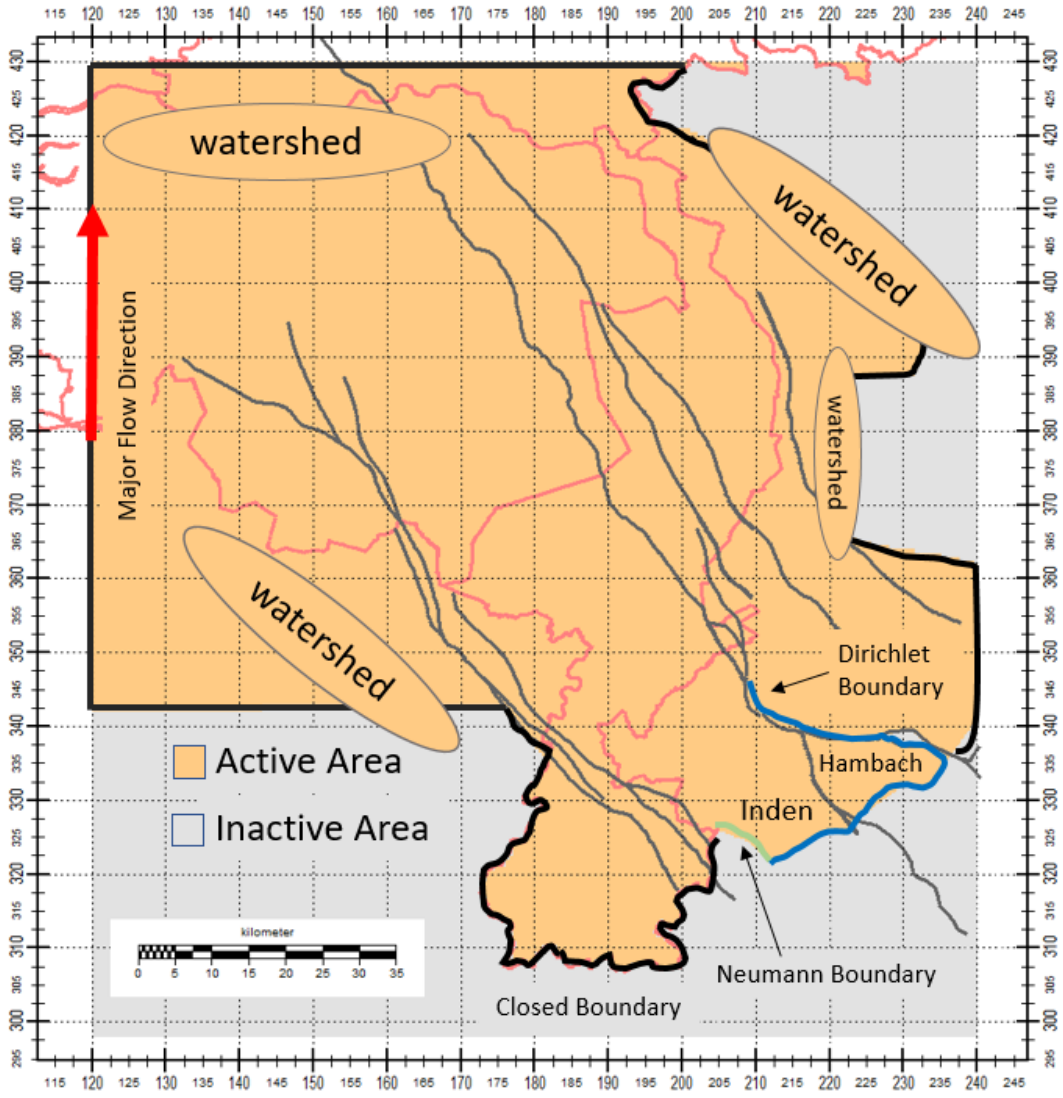

Figure 2.2 Overview of the location and type of model boundary conditions used.

2.1.3 Recharge

Recharge is the net groundwater replenishment from precipitation and evapotranspiration. For IBRAHYM, the averaged groundwater recharge is computed from the transient groundwater flow model coupled with the unsaturated zone package MetaSWAP (Walsum and Veldhuizen, 2010). This average value is multiplied for each year with an appropriate factor (source: Waterboard Erftverband, 2019), see *Figure 2.3*. For the period 1955 up to 1969 nor recharge multipliers are available; therefore, similar recharge multipliers as applied to 1970 up to 1984 are used. For the most northern- and western model side, no results from IBRAHYM were available, therefore, an average value of 0.7 mm/day is applied.

The focus of the current modeling project is to compute the hydraulic effects of the brown coal and drinking water abstractions, high temporal resolution of the precipitation dynamics is not relevant here.

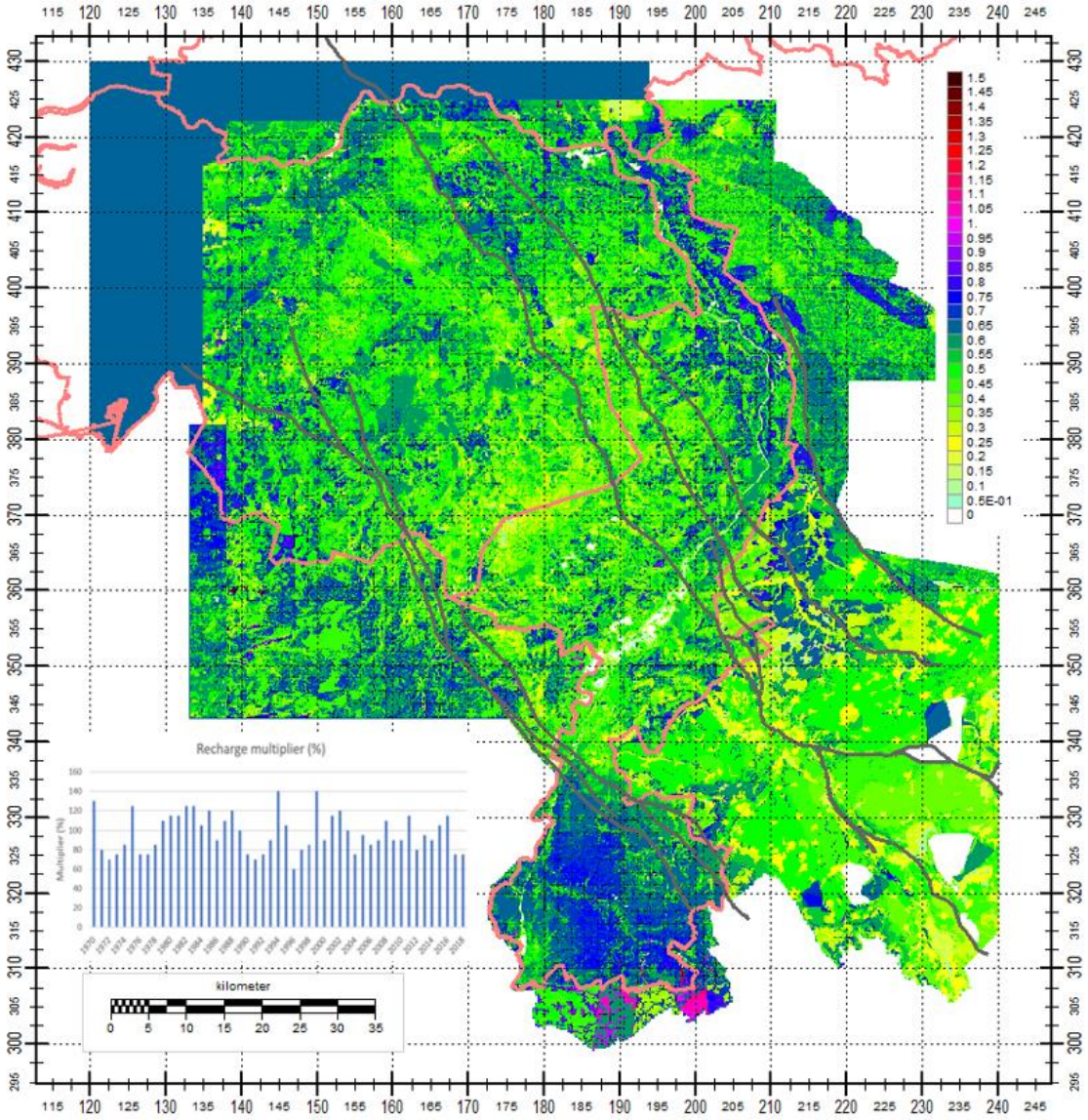

Figure 2.3 Spatial averaged net recharge (mm/day) and (left inset figure) the multiplication factors per year for the net recharge per year.

2.1.4 Surface Water Systems

Commonly, $h_{channel}$ varies over time, however, in this model all river- and drainage stages are kept constant in time. This is supported by the yearly time steps, on that timescale the entire surface water system (including the Maas) does not vary over time. Important to note is that the Saeffelerbach is modelled as a stream that can only drain water; infiltration is not supported in the model as the water bearing of the stream is not guaranteed always. This contrasts with the Rode Beek, which can in- and exfiltrate groundwater.

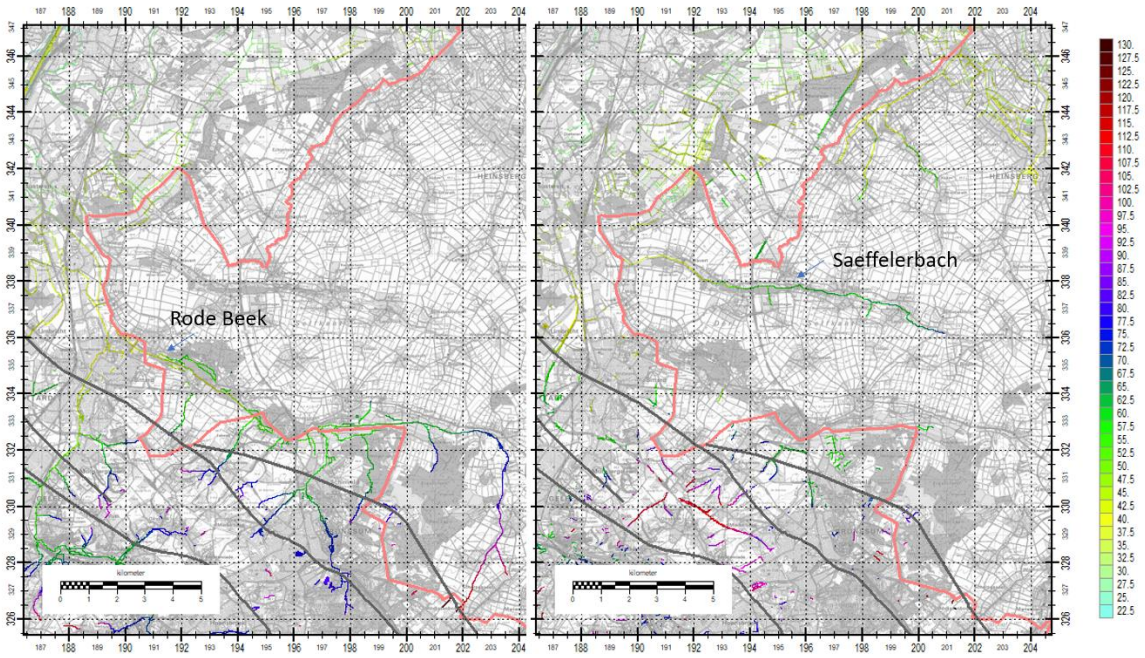

Figure 2.4 Overview of the applied surface water stage (m+MSL) for (left) water bearing- and (right) non-water bearing streams for the area of the Rode Beek and the Saeffelerbach.

2.1.5 Groundwater Extractions

The groundwater extraction rates are subdivided into several categories to support easy modification in the scenario analysis. In *Figure 2.6* the location of each individual extraction is depicted. Although the extractions in the waterboard Niersverband are part of the IBRAHYM model, they are not included in the report as they do not extract from the Roer Valley Graben.

The total, yearly extraction volumes are presented in *Figure 2.5* (top), as well as the total, yearly volume that is extracted solely from the Roer Valley Graben, (*Figure 2.5* bottom). In 2017, the total amount of extracted groundwater is approx. 325 million m^3/year, of which commercial drinking water companies in The Netherlands (WML and Brabant Water) extract in total 63%; the drinking water company in Germany (Erfverband) extracts 20% and the remaining 17% is extracted by industry in The Netherlands and Belgium. These contributions will be outlined briefly per category in the following subsections.

The extraction at the open-pit mine Inden and Hambach are not entered as a volume but the effect of the extractions is represented by simulated hydraulic heads from the RWE Power model (RWE Power, 2013). The order of magnitude for this extraction in 100 million m^3/year.

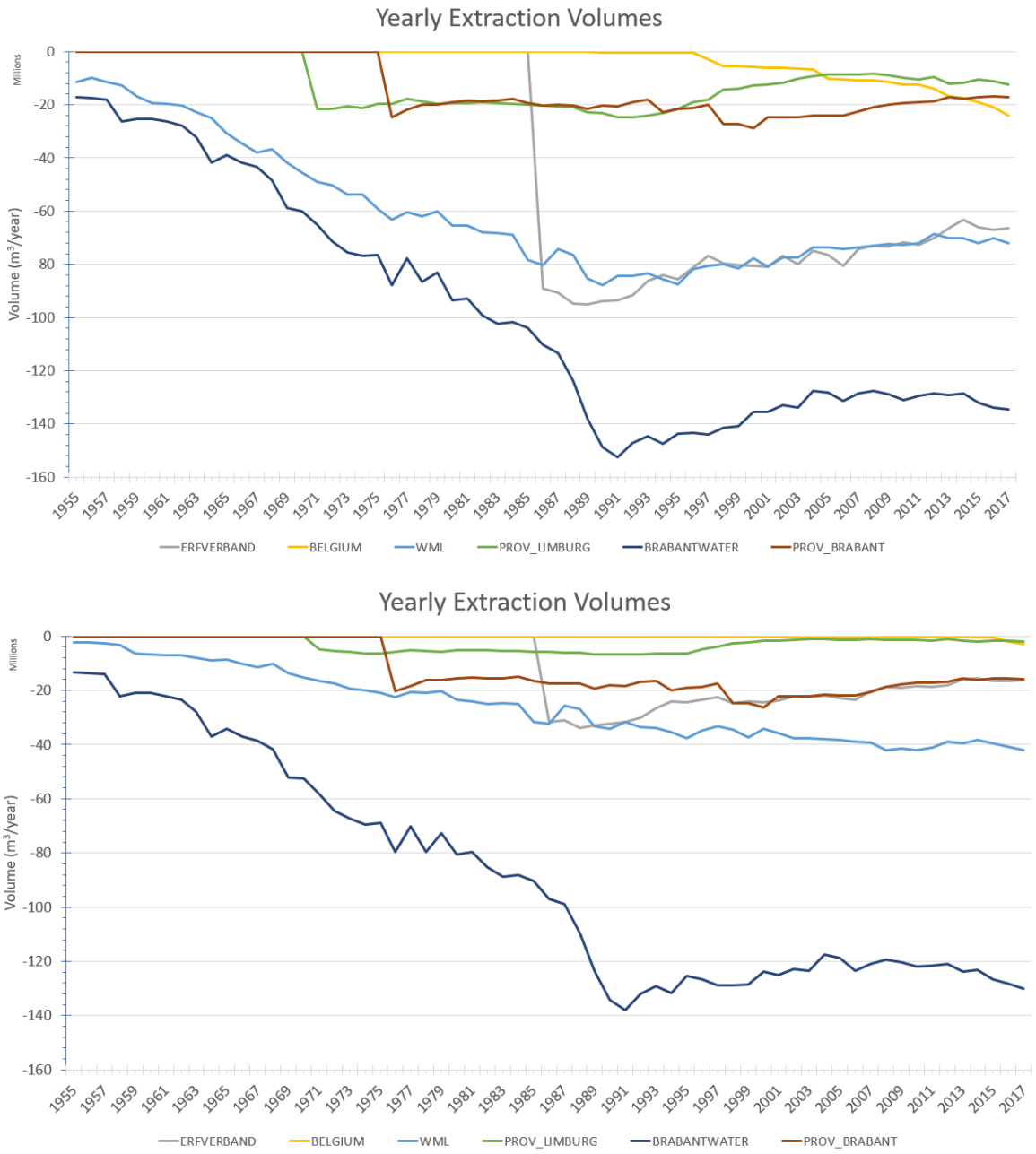

Figure 2.5 Overview of (top) the total yearly volumes extracted by the various categories; (bottom) the total amount extracted from the Roer Valley Graben, solely. Based on currently known data that is used in the model.

2.1.5.1 Province of Limburg (The Netherlands)

The pumping well data from the province of Limburg (The Netherlands) is provided by the province of Limburg (Mr. E. Castenmiller). Provided are the wells which have a permit of extracting more than 100.000 m^3/year. From the provided data the data for the extended period (2014-2017) is extracted and added to the existing dataset of the previous period up to 2014. A distinction is made between extraction for drinking water purposes (WML) and other extractions. For the industrial extractions of Limburg there were four wells that had an unknown screen depth, see A.1**Error! Reference source not found.**; these wells are excluded. After an analysis of the total q uantities of extraction, it showed that there were no extractions present in the dataset for the period 1981 and 1989. To fill in this gap, a linear interpolation has been carried out between the

last known extraction quantity of 1980/81 and the next known quantity in 1988/89. Unfortunately, there is no information on extractions before 1970. The filter upper- and lower elevations are given in m+MSL and are used to position the well vertically to the appropriate model layer

2.1.5.2 Water supply company Limburg WML (The Netherlands)

Up to 2012 the extraction rates of WML are used as those that were already processed in an earlier stage of this project (Vermeulen, 2018). For the period 2012 up to 2017, a new dataset is provided by the WML (Mrs. B. Putters). This dataset provides monthly values and is converted to pumping amounts in m^3/d. The filter upper- and lower elevations are given in m+MSL and are used to position the well vertically to the appropriate model layer. There is no difference in the level of detail between the two datasets.

2.1.5.3 Province of Brabant (The Netherlands)

The pumping well data from the province of Brabant (The Netherlands) is provided by the Province of Brabant (Mr. E. Kessels). Pumping amounts are given as total quarterly extractions for each year per INRNR number. If an INRNR number is linked to multiple wells, the extraction is subdivided equally over each well. The pumping amounts are converted to m^3/d and the filter upper- and lower elevations are converted from meters below ground surface to meters below NAP by subtracting the values from the upper elevation of the first model layer, which represents the ground surface. Unfortunately, there is no information on extractions before 1976.The filter upper- and lower elevations are given in m+MSL and are used to position the well vertically to the appropriate model layer.

2.1.5.4 Brabant Water (The Netherlands)

Extraction rates for each well per installation in the period before 1996 are provided by RHDHV (Mr. F. Verhagen) in IPF format that can be used directly in the IBRAHYM-ROERDAL model. These represent the extractions for the drinking water company Brabant Water back to the early decennia of last century. For the period after 1996, the original dataset is used that was already processed in an earlier stage of this project (Vermeulen, 2018). There is no difference in the level of detail between the two datasets. The filter upper- and lower elevations are given in m+MSL and are used to position the well vertically to the appropriate model layer.

2.1.5.5 Waterboard Erfverband (Germany)

Waterboard Erftverband has delivered its extraction wells in an ESRI shapefile containing the x and y coordinates, annual flows (1996-2013) and water-bearing package (*Stockwerk*) and geological layer (*Horizont*). For the period 1986-1997 and beyond 2013, the pumping well data is provided by LANUV (Mr. D. Hüsener). The yearly data is converted to extraction rates in m^3/d. Based on these data, IPF files are created to assign the extraction wells to the appropriate model layers. Therefore, a relationship is defined to connect *Stockwerk* to *Horizont* to model layers, see A.2. Unfortunately, there is no information on extractions before 1986.

2.1.5.6 VMM (Belgium)

The Flemish Environmental Agency (VMM) has provided an improved set of extraction data from the most important extractors in the Belgium part of the Roer Valley Graben (Mrs. C. Slenter). These are added to the model from 2007 onwards. For the period before 2007, the original dataset of IBRAHYM V2 is used (Vermeulen, *et al.* 2015). All extraction rates are equal to the licensed quantities; from experience, it is known that a factor or 0.75 is realistic to estimate the quantity that is truly extracted. Unfortunately, there is no information on extractions before 1983.

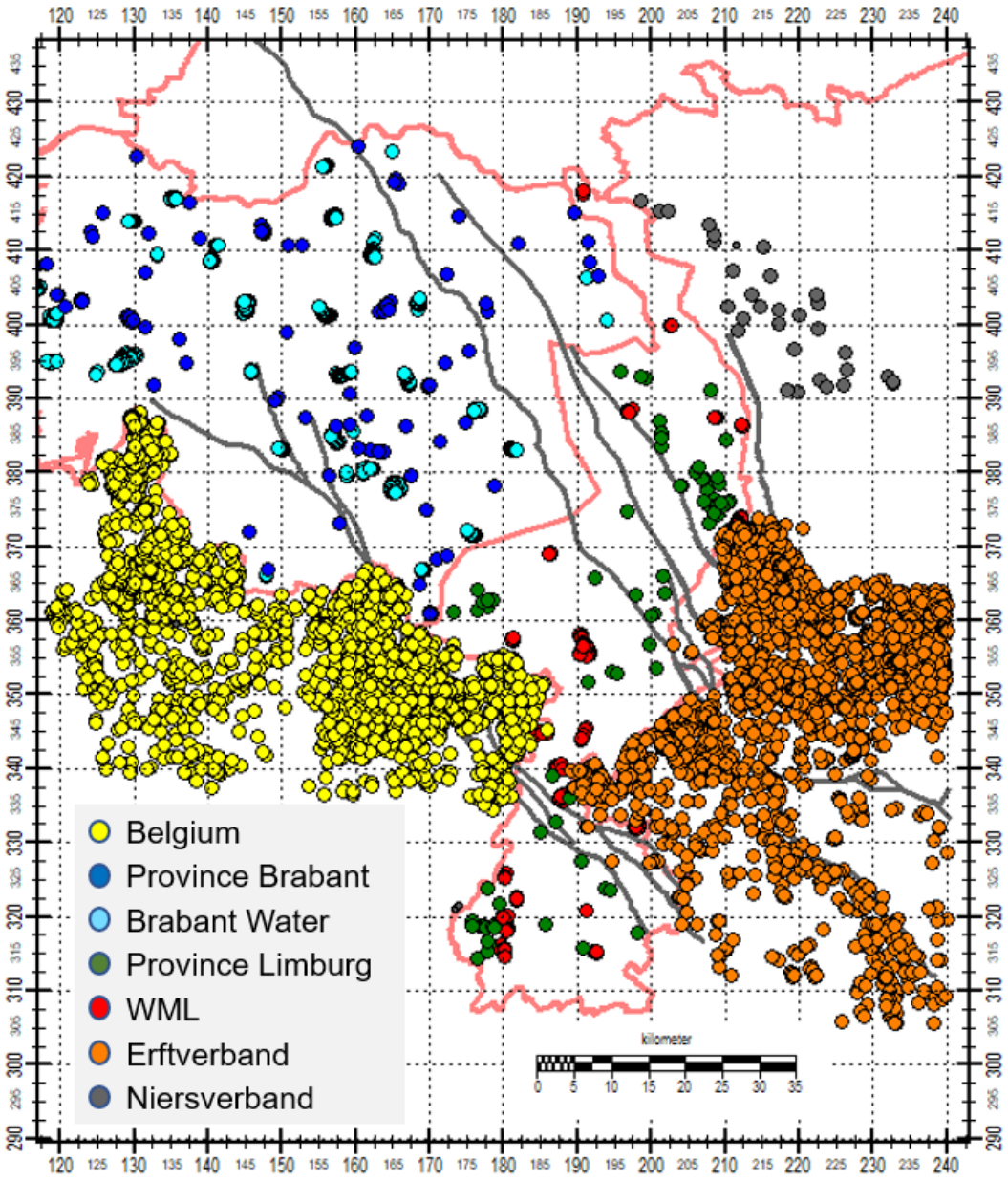

Figure 2.6 Overview of the location of the extractions in the model grouped in relevant categories.

2.1.6 Geology

This section describes the set-up of the geological model.

2.1.6.1 Phase I

In an earlier phase I of this project, the geology in the German part of IBRAHYM (Rur-Scholle and Venlo-Scholle) was replaced by the data of the GD-NRW (Geological Survey, Nordrhein-Westfalen) and LANUV (Landesamt für Natur, Umwelt und Verbraucherschutz Nordrhein-Westfalen), see *Figure 2.7* and appendix A.3. These were digital contour maps of the various geological formations which were converted to IDF files that could be connected to the interfaces of the IBRAHYM model, at the border of the Netherlands. Those connections were made by examining the vertical position of each the geological formations and connect them to the most appropriate interface of the IBRAHYM model. As the extent of the mentioned German geological models was limited in the east, beyond this, the geology from the original IBRAHYM model was used. It appeared to be difficult to correctly connect the Kiezelooliet Formation (Rotton Formation) as the number of layers that represent this formation differ in the Dutch and German side. So,

several of them, unfortunately were stopped abruptly at the German border. Also, it appeared that the area in Germany east of Sittard was not mapped, this has been filled in manually. The hydrological base (Boomse Clay Formation) was not mapped by the GD-NRW, the base was used from the RWE model (RWE Power AG, 2013).

The geological models did not contain permeabilities; those were used from the RWE model (RWE Power AG, 2013). From RWE an ESRI PersonalGeoDatabase was received that contained the upper- and lower elevation of their distinguished layers and their permeability (Kf) values in m/s. Based on the upper- and lower elevations of the geological layers, the permeability values of RWE were mapped to the nearest model layer of the IBRAHYM ROERDAL model.

After this phase it has been decided to improve the geological model with the joint geological mapping of the border between Belgium and The Netherlands, this is Phase II.

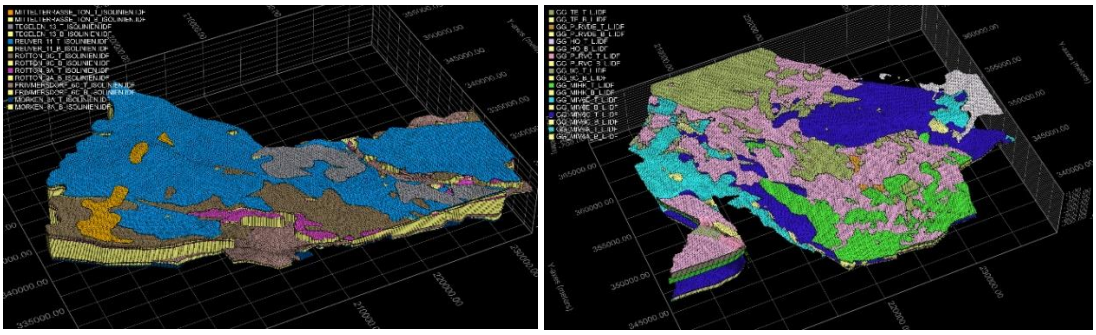

Figure 2.7 Overview of the geological data from the Rur-Scholle and Venlo-Scholle models.

2.1.6.2 Phase II

The H3O ROER VALLEY GRABEN project has been carried out by Dutch Geological Survey of the Netherlands (TNO-GDN) and Flemish Organization (VITO) in collaboration with the Belgian Geological Survey (BGD). The aim of the H3O project was to create a cross-border, up-to-date, three-dimensional geological and hydrogeological model of the Limburg, Southeast Brabant and Flemish part of the Roer Valley Graben (Jef, *et al.*, 2014). Much effort is put particularly into an improvement mapping of the various fault lines that exist along both sides of the Roer Valley Graben. Many additional boreholes and seismic lines are used to improve this interpretation. The connection of these fault lines between Belgium and The Netherlands has been improved significantly. The H3O project delivered improved mapping of geological formations in The Netherlands as well. The complete data of the H3O project was used to adjust the geological model from Phase I.

The H3O project did not map the Ville Formation (Frimmersdorf and Morken Formations in Germany and very limited in Belgium in the formations 0253-v1 and 0253-v2) in the central and very deep part of the Roer Valley Graben due to a lack of deep boreholes. The Ville Formation is, however, very important to the geohydrological model; it is used for the deep part, as mapped in the original IBRAHYM model. The hydrological base of the model is given by the Boomse Klei (The Netherlands) and the formation 0300 (Belgium). Furthermore, it is important to note the modification in the mapping of the Kiezelooliet K5, which is now the Inden K1. The new mapping of H3O resulted in an increase of the number of model layers from 19 to 20.

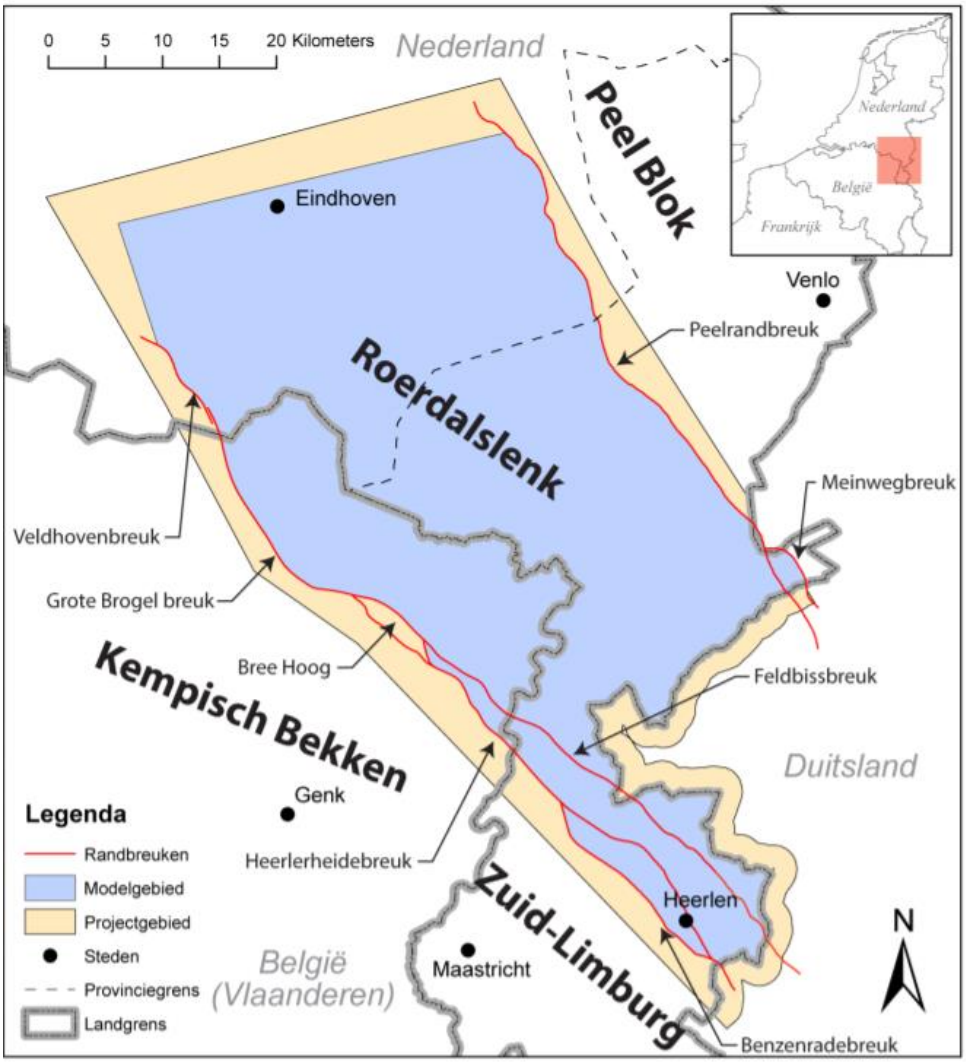

Figure 2.8 Location of the H3O ROERDAL Project.

2.1.6.3 Phase III

The geology in the area around the Dutch and German border, especially near Schinveld, is complex and discontinuous. The geology as mapped by both the GD-NRW and TNO-GDN in the previous phases, is not properly aligned. TNO-GND, in collaboration with VITO, BGD / RBINS, mapped the border area between the Netherlands and Germany in the so-called H3O-ROSE project, see Appendix A.4 and Appendix A.5. A preliminary result of the 3-D mapping of the H3O-ROSE (Roer Valley Graben South-East) project is received from LANUV (Mr. D. Hüsener) and incorporated in the current model configuration from Phase II. This preliminary result contained the lateral- and vertical position of the most important geological aquitards in the H3O-ROSE modeling area, which includes the area from the Dutch-German border up to the east flank of the river Meuse. No permeability values were received, but similar constant values per units were initially assigned to the formations as done in Phase II. Those are all subject to the model calibration, see section 3.5.1.

The final geology is presented in *Figure 2.10* (right). In the cross-section the enormous thickness of the Breda Formation is visible. This formation consists of low permeable marine sands, in which the brown coal layers Frimmersdorf and Morken (ViB1 and Vib2 formations) are present. The western extent of these coal layers? are highly uncertain as only a few boreholes were available to characterize them. The extractions of the Inden pit are mainly below these high resistance layers. On top of the Breda Formation the sandy and clayey sediments of the Inden Formation and

Kiezelooliet Formation are present. In Germany, the latter is referred to as the Reuver (KiK1) and the Rotton (Kik2 and Kik3). Above these, sandy and clayey sediments of the Peize-Waalre Formation are deposited, which extent to the upper west boundary of the model, as the deposit of the Kiezelooliet sediments vanishes near the Limburg-Brabant border. There is an area in which the Maassluis and Kiezelooliet Formation are both absent. In this area, the sandy and clayey sediment of the Peize-Waalre Formation predominate. Minor sandy and clayey sediments of the Sterksel and Stramproy Formation are in the shallow subsurface of the geological cross-section. Finally, sediments of the Beegden and Boxtel Formation conclude the geological profile. In Germany, a minor Tegelen Formation is present at the surface with a limited extent. A detailed cross-section near the Dutch-German border is depicted in *Figure 2.10* (left). It shows the so-called *Tonfenster-Uberpalenberg* which is a local area in which no clayey sediments of the Rotton- and Reuver Formation (Kiezelooliet Formation) are present. It is an important recharge area for the deeper aquifers.

Figure 2.11 shows a cross-section perpendicular to the Roer Valley Graben. Clearly visible are the faults and their influence on the depth and vertical shift of clayey sediments. Pump station Schinveld has been projected on the cross-section to illustrate the high level of detail in which those extractions are represented in the model and how this pump station penetrates multiple aquifers. Another pump station in Germany (43-003A1-3) is included as another example.

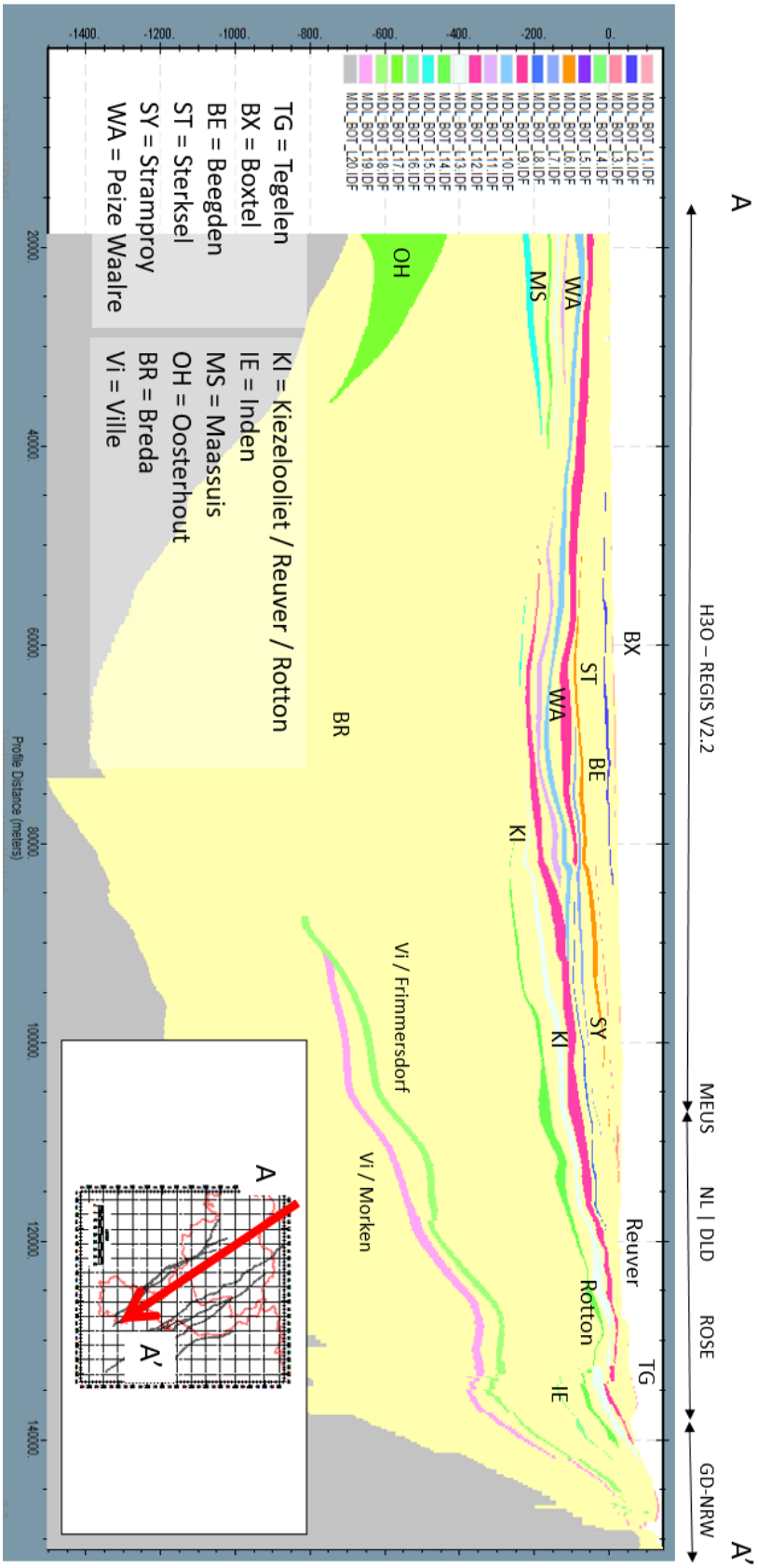

Figure 2.9 North-west South-east cross-section of the geology; a complete transect over the entire modelling domain.

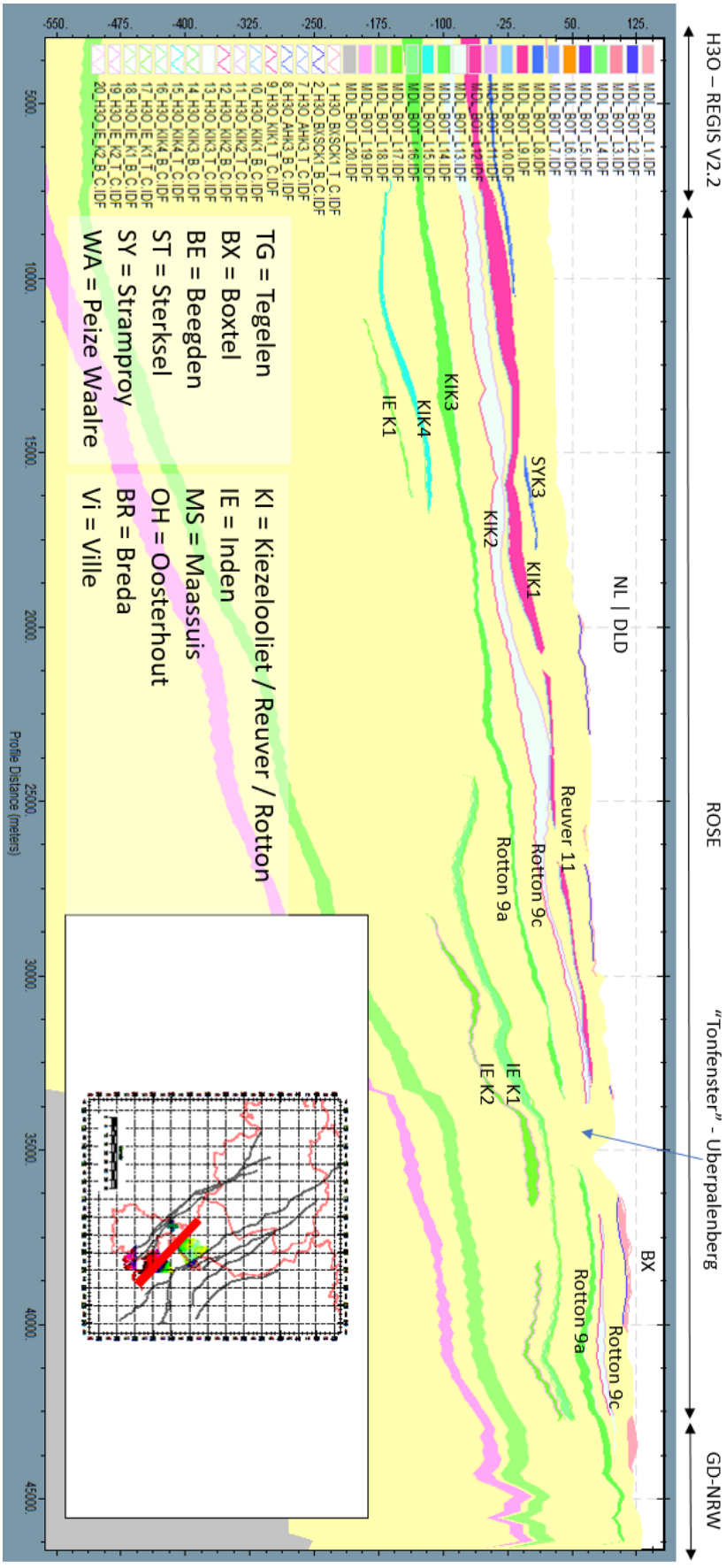

Figure 2.10 North-west South-east cross-section of the geology; a detail near the so-called Tonfenster Uberpalenberg.

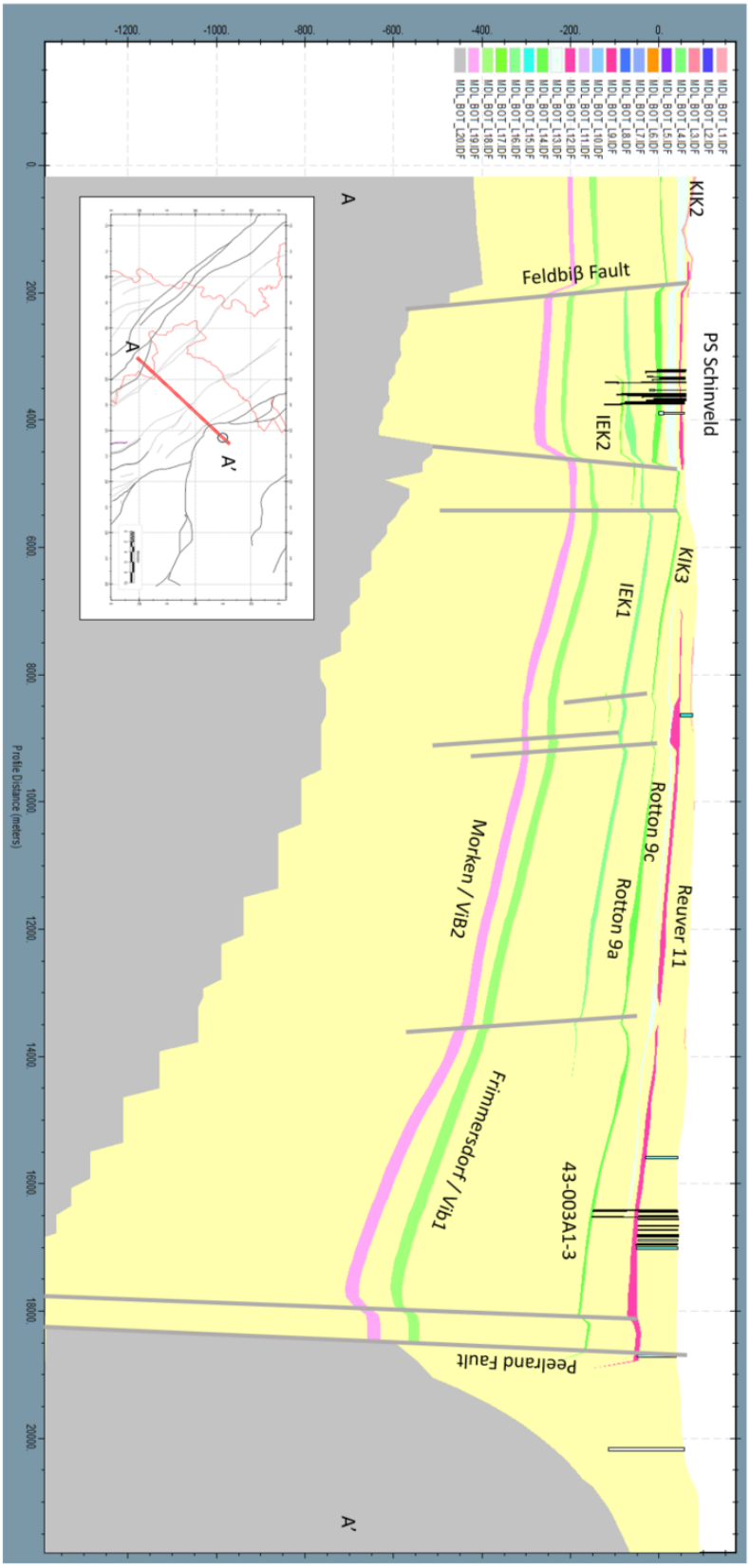

Figure 2.11 Cross-section in south-west to north-east direction including the fault lines and the location of filters for the extraction for pump station Schinveld and 43-003A1-3.

2.1.7 Faults

The model area is part of plate tectonics from the Northwest European rift system, a fractured sink area that cuts through western Europe from the North Sea to the Mediterranean Sea. The Roer Valley Graben forms the western segment of the Lower Rhine Slenk, in which sediment has accumulated to 1600 m depth for 28 million years. The Roer Valley Graben turns into the Ardennes-Eifel massif, which was uplifted at the same time as the Roerdal sunk; it became the main source of sediments in the Roer Valley Graben. This system is still active, as witnessed by the fractional steps that are visible in the landscape and the earthquakes that are mainly concentrated in the south of the Slenk (Jef *et al*., 2014). The Roer Valley Graben itself is characterized by a complex system of faults, see *Figure 2.12* for the most important faults. Most of them are oriented in a north-west towards south-east direction. Two major faults are the Peelrand Fault and Feldbiβ Fault on the north- and south border of the Roer Valley Graben.

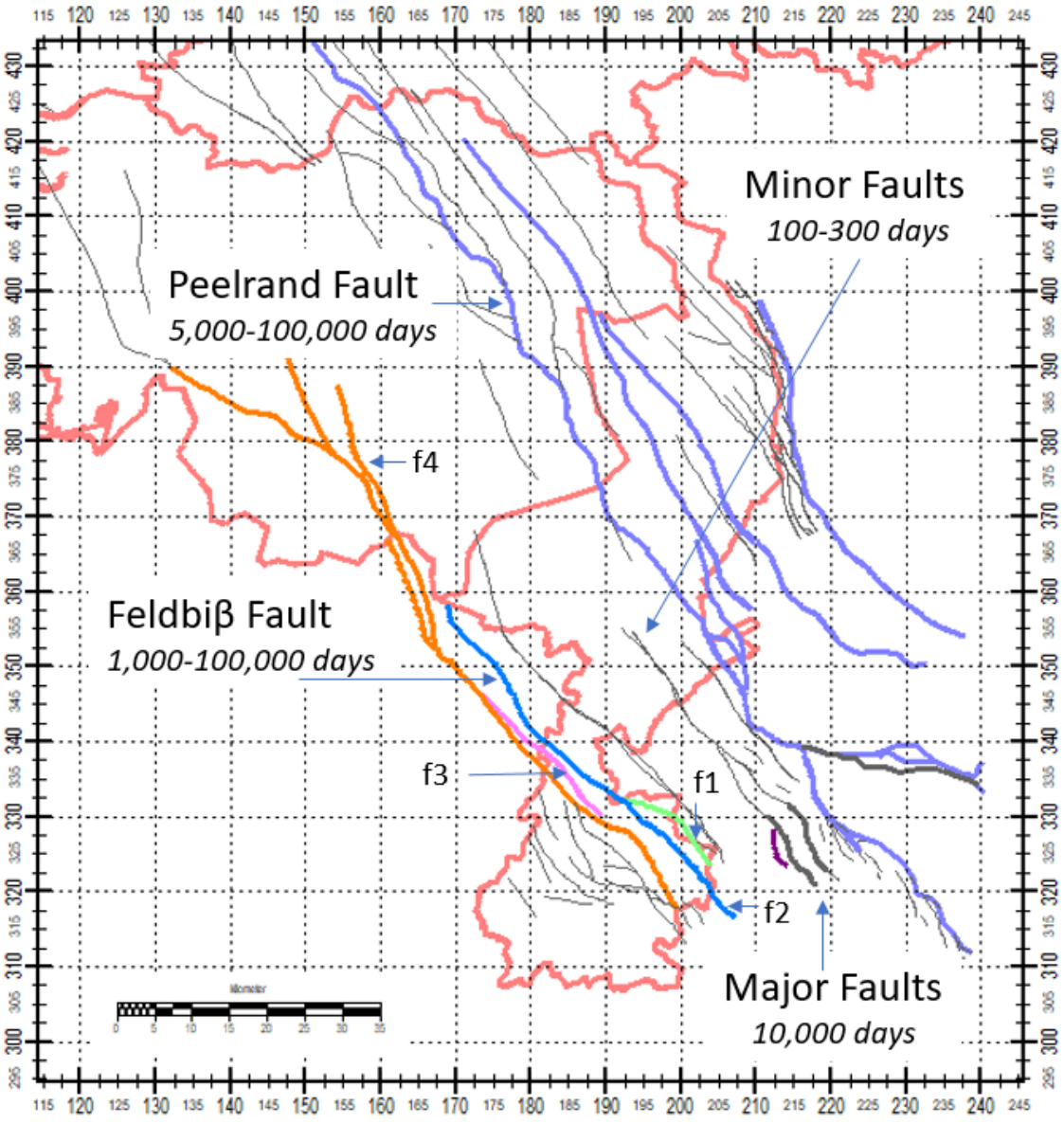

Figure 2.12 Location of important, major and minor faults and their initial lateral resistance. The f1, f2, f3 and f4 are sub parts of the Feldbiβ-fault used in the model optimization.

The vertical shift along those faults is significant and they act as a natural barrier for groundwater flow which clearly can be seen in the head difference between observations in between two side

of the faults. In the model, those faults have a resistance that varies spatially and over depth. The resistance for the Peelrand Fault ranges from 10,000 days (first and second aquifer) up to 100,000 days (Kiezelooliet Formation) to 10,000 days in the Formation of Breda and only 5,000 days underneath the Vib1 (Frimmersdorf) formation. Those resistances are taken from the IBRAHYM v2 model and some local modification is applied to faults in Germany where some key numbers were available on the exchange of groundwater over the fault, e.g. the flow in between the Rur-Scholle and Erft Scholle as computed with the RWE Model (RWE AG, 2013). A major modification was to reduce the resistance from the ViB1 Formation from 100,000 days to 5,000 days to increase the outflow from the Rur-Scholle into the Erft Scholle.

The Feldbiβ Fault has resistances of 1,000 days for the first and second aquifer and an increased resistance of 10,000 for all deeper aquifers. Minor faults have a resistance between 100 and 300 days. In the eastern part of the model, several faults have been assigned high resistances. This is supported by the isohypses which were constructed for the different aquifers, see *Figure 2.13*. Those faults have a resistance of 10,000 days, this value yields a similar jump in the hydraulic head computed by the model as observed in the isohypses.

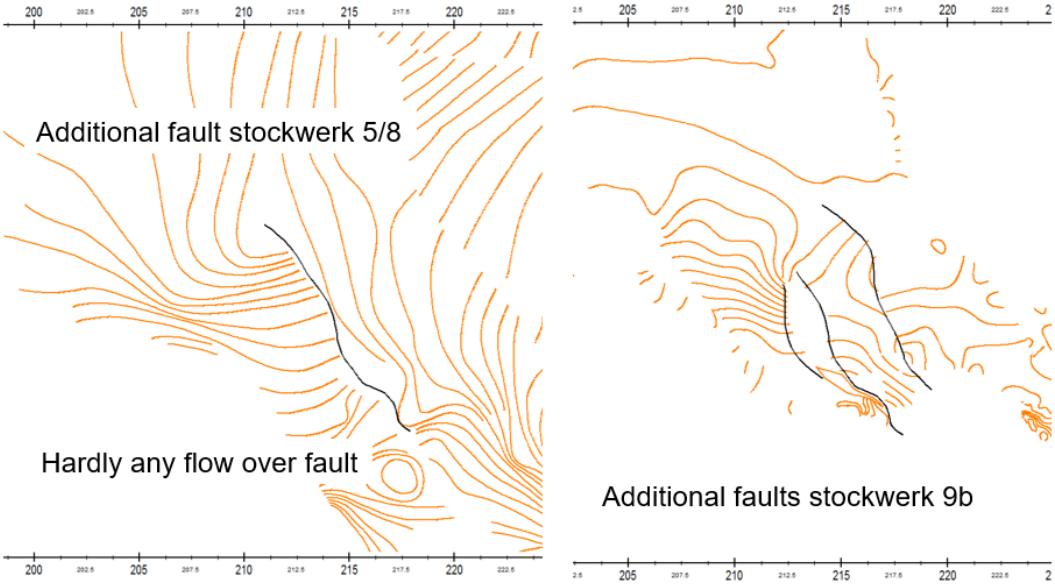

Figure 2.13 Location of the major faults (Germany) inside the Rur-Scholle which show significant drops in hydraulic levels and therefore indicate high lateral resistances.

From numerical experiments with the model, it has been shown that the lateral effect of changing resistances of faults is limited if the changes are within the same- or one order of magnitude difference. It is very difficult to determine the precise resistance due to lack of measurement on both side of the faults.

2.1.8 Initial Storage coefficient

The porosity (*ne*) of the German part of IBRAHYM is calculated with the formula $ne = 1.33 * kf^{0.22}$ (Helmbold, 1988) where *kf* is the permeability (*k-werte* in m/s). The Dutch part of IBRAHYM has a constant porosity of 0.15. This is subject to the parameter optimization as described in section 3. The initial specific yield coefficient for the confined model layers is equal to the values as specified in IBRAHYM V2, namely 0.1×10^{-5} x thickness of the model layer. This holds for the German and Belgium part of the model as well.

2.1.9 Geohydrology and initial permeability values

Geohydrology is a combination of geology and permeability. Geology represents the layering of sediments (formations) and permeability denotes the water bearing capability of these layers.

Geohydrology aims to subdivide these sediments into aquifers (high water bearing capability) and aquitards (low water bearing capability). These are the entries in the geohydrological groundwater flow model. IBRAHYM v2 is subdivided into 20 model layers (aquifers) and 19 aquitards (or interbeds as a part of the model layers that represents the vertical resistance between 2 subsequent model layers). Twenty model layers are the minimal number of model layers to capture all available and relevant aquitards in The Netherlands. Prior to the parameter optimization, each model layer and aquitard are given an initial value for permeability. The initial (prior estimated) permeability values are based upon the permeability distribution as given by the calibrated IBRAHYM v2 model. An exception is made for the Roer Valley Graben. Here, per layer, the permeability is given a single value which represents an average value of the original dataset, see *Table 2.1*.

Table 2.1 Overview of the initial (prior estimated) values for permeability.

Model layer	NLD / GER	Formations	SAND	CLAY	SAND	CLAY
			m/d		m/s	
1		BXZ1 / BEZ1	30	-	3.47E-04	-
	NLD / GER	BXK1 / BXLMK1	-	2.00E-03	-	2.31E-08
2		BXZ2 / BEZ2	30	-	3.47E-04	-
	NLD	BXK2 / BEK1 / STK1	-	2.00E-03	-	2.31E-08
3		BXZ2/ BEZ2	30	-	3.47E-04	-
	NLD	BEK1 / BEK2 / BXLMK1 / STK1	-	2.00E-03	-	2.31E-08
4		BEZ1 / BEZ2 / BXZ2	30	-	3.47E-04	-
	NDL / GER	STK1 BEK2 / JHK1	-	3.00E-04	-	3.47E-09
5		STZ1 / BEZ2	30	-	3.47E-04	-
	NLD	STK1 / SYK1 / RUK1 / RUK2	-	3.00E-04	-	3.47E-09
6		STZ2 / SYZ1 / RUZ1	30	-	3.47E-04	-
	NDL / GER	SYK1 / AHK2	-	3.00E-04	-	3.47E-09
7		SYZ1	15	-	1.74E-04	-
	NLD	SYK2	-	3.00E-04	-	3.47E-09
8		SYZ3	15	-	1.74E-04	-
	NDL / GER	SYK3 / WAK1 / AHK3	-	3.00E-04	-	3.47E-09
9		SYZ4 / WAZ2	30	-	3.47E-04	-
	NLD	SYK3 / WAK2	-	3.00E-04	-	3.47E-09
10		SYZ4 / WAZ2	30	-	3.47E-04	-
	NLD	WAK3	-	3.00E-04	-	3.47E-09
11		WAZ4	30	-	3.47E-04	-
	NLD	MSK1	-	3.00E-04	-	3.47E-09
12		MSZ1	25	-	2.89E-04	-
	NLD / GER	KIK1 / Reuver 11	-	3.00E-04	-	3.47E-09
13		KiZ1 / 10	25	-	2.89E-04	-
	NLD / GER	KIK2 / Rotton 9C	-	3.00E-04	-	3.47E-09
14		Sands of Pey / 9B	25	-	2.89E-04	-
	NLD / GER	KIK3 / Rotton 9A	-	3.00E-04	-	3.47E-09
15		Sands of Waubach / 8	10	-	1.16E-04	-
	NLD	KIK4	-	3.00E-04	-	3.47E-09
16		Sands of Waubach / 8	10	-	1.16E-04	-
	NLD / GER	IEK1 / 7F	-	3.00E-04	-	3.47E-09
17		Sands of Inden / 7E	5	-	5.79E-05	-
	NLD / GER	IEK2 / 7D	-	3.00E-04	-	3.47E-09
18		Sands of Inden / 6D	5	-	5.79E-05	-
	NLD / GER	ViB1 / Frimmersdorf / 6C	-	8.60E-06	-	9.95E-11
19		Heksenberg / 6B	2	-	2.31E-05	-
	NLD / GER	ViB2 / Morken / 6A	-	8.60E-06	-	9.95E-11
20		BR-Lower (Heksenberg / Vib2 / 5)	2	-	2.31E-05	-

3 Calibration

3.1 Introduction

The term “calibration” stands for optimizing a set of model parameters such that the misfit between measurements and model prediction is minimized according to a defined penalty function, called an objective function.

Commonly, the calibration is started as soon as the first model simulation ran, in which conceptual errors (e.g. missing information on drainage, wells, geology) are found and corrected. An automatic parameter optimization is the final step whenever there are no obvious conceptual errors in the model anymore. During the automatic parameter optimization, other conceptual errors might be found. So, the manual and automatic parameter optimization process is a cycle of many sequences.

It is important to note that the optimized parameters are directly related to all choices in the modelling, as well as de definition of the objective function and the set of available measurements. Any calibration is the result of those subjective decisions and the result is therefore one-of-the-many feasible model outcomes. The presented results in the coming sections, is the most plausible solution obtained from the calibration procedure given the abovementioned subjective decisions.

The focus point of the current calibration is the Roer Valley Graben, this means that residuals and or parameters that are outside the Roer Valley Graben are not involved, inspected and/or modified compared to the original IBRAHYM V2 model.

3.2 Methodology

Generally, for the Erftverband and RWE-Power it is customary to work towards an optimum match between calculated and measured groundwater levels. For this, additional zoning is applied repeatedly to change the permeability locally so that the local groundwater level better matches the measurement. In the Netherlands a more conservative approach is applied, and zoning is only added or changed if there is a reason for this from geology. If not, a larger residual is accepted because it can also be that the underlying model still has conceptual shortcomings. In this project we applied a methodology that benefits from both approaches.

Within the Dutch part of the IBRAHYM v2 model the transmissivity values have been optimized based on the geological distribution of permeability as mapped in REGIS v2.1. As this part has now been replaced by the geological distribution of H3O-ROERDAL and H3O-ROSE projects, with average permeability values per model layers the optimized transmissivity values of IBRAHYM v2 can no longer be used. This also applies to the German part in the current IBRAHYM-ROERDAL model where the optimized RWE transmissivity values were used in combination with a revised geological interpretation of the GD-NRW. Both optimized transmissivity values conflict with each other and more importantly they already reflect imperfections in the input data in their underlying models. For example, the optimized parameters in the IBRAHYM v2 model might correct for missing and incomplete data; and the optimized parameters from the RWE model in Germany are affected by the assumption that the Maas is a watershed. Therefore, the permeability values are revised on both the Dutch, Belgium and German side.

3.3 Pilot-Points

Instead of zoning, the adjustment of the permeability is done via so-called *pilot points* (Doherty, 2003) as implemented in iMOD (Vermeulen *et al.*, 2019). A pilot point is a representative point for which the permeability is estimated. A Kriging interpolation (Krige, 1951) is applied to fill in the area in between the pilot points. The use of Kriging avoids abrupt transitions in permeability values. A Kriging range of 10 kilometer has been applied to avoid severe modifications on a local scale. It is possible to place more or fewer pilot points so that more detail can be created where more measurements are present and/or more changes in geology are to be expected. Each pilot point is a single, random-parameter that needs to be optimized, this means that the calculation times of the optimization increases as more pilot points are defined. In this study, a pilot point is added for every 5 kilometers whenever there is a measurement within that distance as well. If not, the pilot point is added, but not changed during the optimization, see *Figure 3.1*.

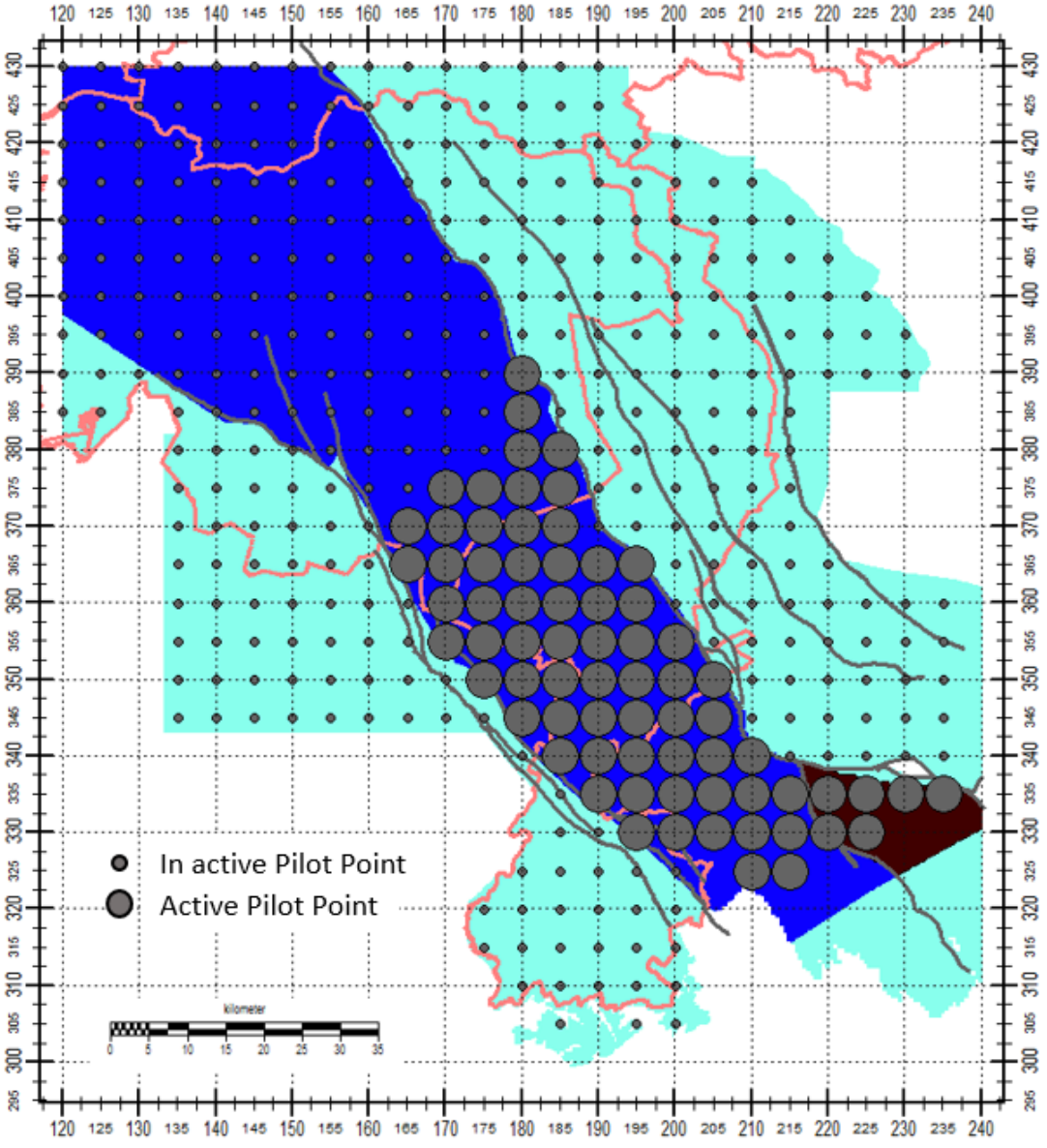

Figure 3.1 Position of the (in)active pilot points and separate zones for the Kriging interpolation.

Furthermore, pilot points are connected (grouped to a single pilot point) whenever they are vertically separated without any significant resistance. In this case a minimal resistance of 50 days is used. For example, the first aquifer in the model is represented by multiply model layers and it is

not realistic to assume that permeability is significantly different at the top- and bottom of the aquifer. To avoid this happening in the automatic parameter optimization, those pilot points within the same aquifer are joined together, see *Figure 3.2*.

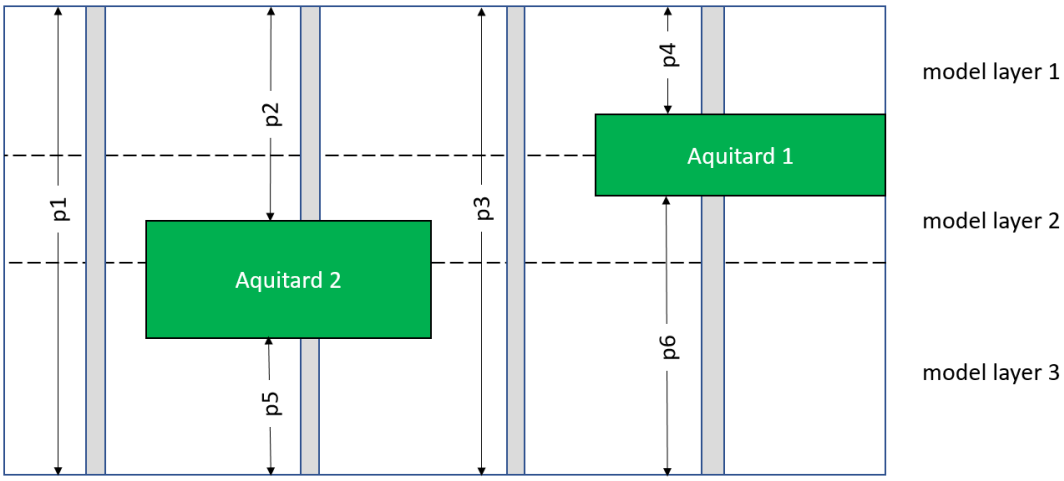

Figure 3.2 3-D image of the grouping of pilot points (p1 up to p6) in model layers divided by aquitard.

The location of the main faults (Peelrand- and Feldbiβ-fault) can lead to sharp transitions in permeability values per model layer. To facilitate that during the pilot point Kriging-interpolation, three zones have been created, see *Figure 3.1*. For the interpolation for each location, only values from the pilot points that are within the same zone as the current location are used.

3.4 Measurements

The measurements were received from Erftverband up to 1st of January 2016. No update was carried out to extend the series to the 1st of January 2018. The measurements of the Netherlands are up to 1st of January 2013 as they origin from the IBRAHYM v2 model. For the Belgian part of the Roer Valley Graben, 11 measurements are collected from the VMM (Flemish Environmental Organization; Mr. C. Slenter), they range to 31st of December 2017. The measurements vary in length and interval and are aggregated to yearly averaged values, see inset in *Figure 3.3*. The fluctuations of the yearly averaged values are significantly smaller than the fluctuations shown on a higher interval. This coincides also with the multiplication factors for the net recharge on *Figure 2.3*. The measurements are spatially and vertically well distributed, see *Figure 3.3*.

In total, 1,355 measurements are used in the parameter calibration. The vertical position of the measurement is initially based on the given depth of the filter screen. However, it was noticed that some of the filter depths do not coincide with the geology, simply because not all measurements are included in the definition of the geology. Normally, when less severe drawdowns are considered, the difference between aquifers is less significant. In the current context, however, with measured drawdowns of >10-20 meters in combination with very high resistances in between adjacent aquifers, the vertical position of the filter is essential. A vertical shift of a measurement of <5 meter can yield a significant change in computed hydraulic head and a very different fit with the measurement. For all measurements we examined the correctness of the vertical position in relation to the geologic model.

For each measurement the layer is determined for which the absolute median difference between computed and measured head is lowest (*lowest-error*). If this *lowest-error* is greater than 5 meters, the filter might be positioned incorrectly, and/or the measurement is unreliable. In that case the measurement is left unchanged, however a reduced weight value of 0.5 was assigned to the

measurement in the formulation of the objective function. All other measurements have a weight value of 1.0. For measurements that benefit from a change in layer, whereby the *lowest-error* became less than 1.0 meter, and the improvement is more than 1.0 meter, are moved toward the layer with the *lowest-error*. It is important to note that this is carried out on the pre-results of the calibrated model before the last optimization run was started. If it has been done on the misfit before calibration, observation might have been shifted for wrong reasons. The modifications are displayed in *Figure 3.3*.

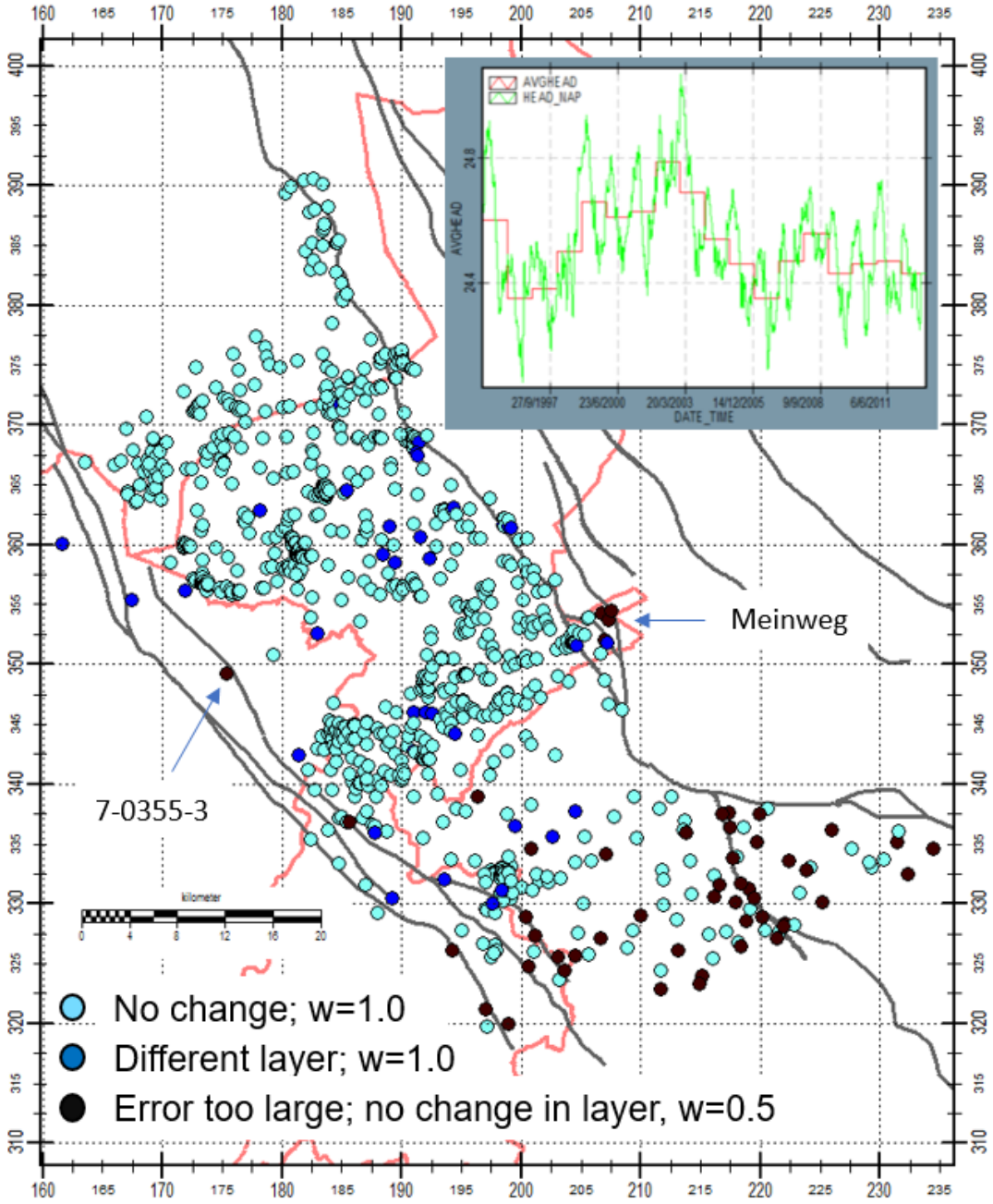

Figure 3.3 Overview of the location of measurements and their potential change in model layer. Inset: an example of the aggregation of the original measurement (green line) to yearly values (red line).

Three measurements in the Meinweg-area are remarkable as they show a *lowest-error* of >5 meter. A reason for this is that the calibration does not modify the permeability values in that region as it is outside the limits of the Roer Valley Graben. There is a single measurement 7-355-3

in Belgium, that appears to be wrong. After a close examination in combination with the location of the fault, it appeared that the measurement needed to be shifted laterally a few 100 meters to be on the right side of the fault. After that, it showed a perfect match for the model layer in which it initially wasassigned. In the eastern side of the Roer Valley Graben, in Germany, more measurements show a large *lowest-error*. However, as show in *Figure 3.3*, changing the model layers was not the solution here. The geology of the IBRAHYM-ROERDAL model shows fewer aquitards in the east than the more detailed geological model of the RWE model (RWE AG, 2013). This could be a reason for larger values for the *lowest-error*. Due to the reduced weighting value of 0.5 assigned to these measurements, they have less influence on the parameter optimization.

3.5 Set of Parameters

3.5.1 Horizontal Permeability

The initial horizontal permeability for each model layer (see *Table 2.1*) within the Roer Valley Graben is optimized via pilot points. Each model layer has a maximum of 71 pilot points, see *Figure 3.1*. The actual number of active pilot points depends on the active computational nodes for each layer, as the number of active nodes decreases with depth (layer number), and therefore so does the number of active pilot points. A total of 699 pilot points remains; this includes the vertical aggregation of pilot points, due to a lack of significant vertical resistance in between model layers (see section A.7).

3.5.2 Vertical Permeability

The initial vertical permeability of aquitards is optimized using zones, see *Table 2.1*. Each aquitard is modified with a single multiplication factor. Pilot points are not used for aquitards since a single sensitivity of a pilot point within an aquitard is very limited and therefore a local modification of an aquitard is not identifiable.

3.5.3 Storage Coefficient

The storage coefficient determines the amount of groundwater that can be stored temporarily in the subsoil without playing a role in the groundwater flow. A large value for the storage coefficient means that more water can be captured or is released by a change in groundwater level. A rise of the groundwater level forces groundwater to be captured by the storage capacity, a drop of groundwater levels releases this captured water again. In steady-state solution, the net storage is 0.0.

The storage coefficient is optimized using zones, just like the vertical permeability (see section 3.5.2). For model layer 1, the initial value is 0.15, which is an acceptable estimate for a phreatic storage coefficient in unconfined conditions. The remaining confined aquifers are a multiplication of 1×10^{-5} times the thickness of the aquifer. Thicker aquifers have a larger storage capacity that thinner aquifers. As the storage coefficient of the first model layer is 4-5 orders of magnitude larger than the deeper ones, this phreatic storage coefficient is most determinative for groundwater storage.

3.5.4 Faults

The lateral resistance of faults is difficult to determine. A major modification was made in the pre-calibration phase (i.e. all activities prior to the automatic calibration process as described in this section), in which the Peelrand Fault, Feldbiβ Fault and major faults in Germany were changed to match the drawn isohypses. The Feldbiβ Fault was cut into 4 different sections as depicted on *Figure 2.12*. These sections have an initial lateral resistance of 100,000 days and are subject to the model optimization in which their resistance is optimized.

3.6 Optimization results

3.6.1 Residuals

The parameter optimization was simulated on a model resolution of 250 x 250 meter. Each transient simulation took ~30 minutes to complete. The total sum of squared residuals (objective function) between measured and simulated groundwater heads is computed for the period from the 1st of January 2010 up to the 1st of January 2018 (this is head at the end of the last simulation period). An important reason not to include measurements before 2010, are the simulated boundary conditions from the RWE model (RWE AG, 2013). The run-up from 1970 (start of the open-pit Mining in Inden) towards 2010 is not reliable enough as mentioned by RWE. The computed groundwater head is interpolated to the location of the measurement. The computed residuals after the parameter estimation process are given in *Figure 3.4*.

The statistics of the model optimization are presented for 5,943 measurements for a set of 1,355 unique observation wells. The minimal and maximal errors are -52.67 meters and +60.4 meters which is quite severe. These are local measurements near the Hambach Open Pit in the Erft Scholle. In that area steep gradients emerge which can hardly be represented with this model on a resolution of 250 x 250 meter. The average error is nevertheless 0.05 meters and 80% of the errors are within -1.80 meters and 1.37 meters.

A measure for the performance (efficiency) of the model is the so-called *Goodness of Fit* and the *Nash Sutcliffe* errors; they are 0.981 and 0.962, respectively (Nash and Sutcliffe, 1970). Essentially, the closer the model efficiency is to 1, the more accurate the model is. Threshold values to indicate a model of sufficient quality have been suggested between 0.5 and 0.65. As both the Nash Sutcliffe and the Goodness of Fit are above this, the model can be objectively accepted to be accurate enough for representing the measurements.

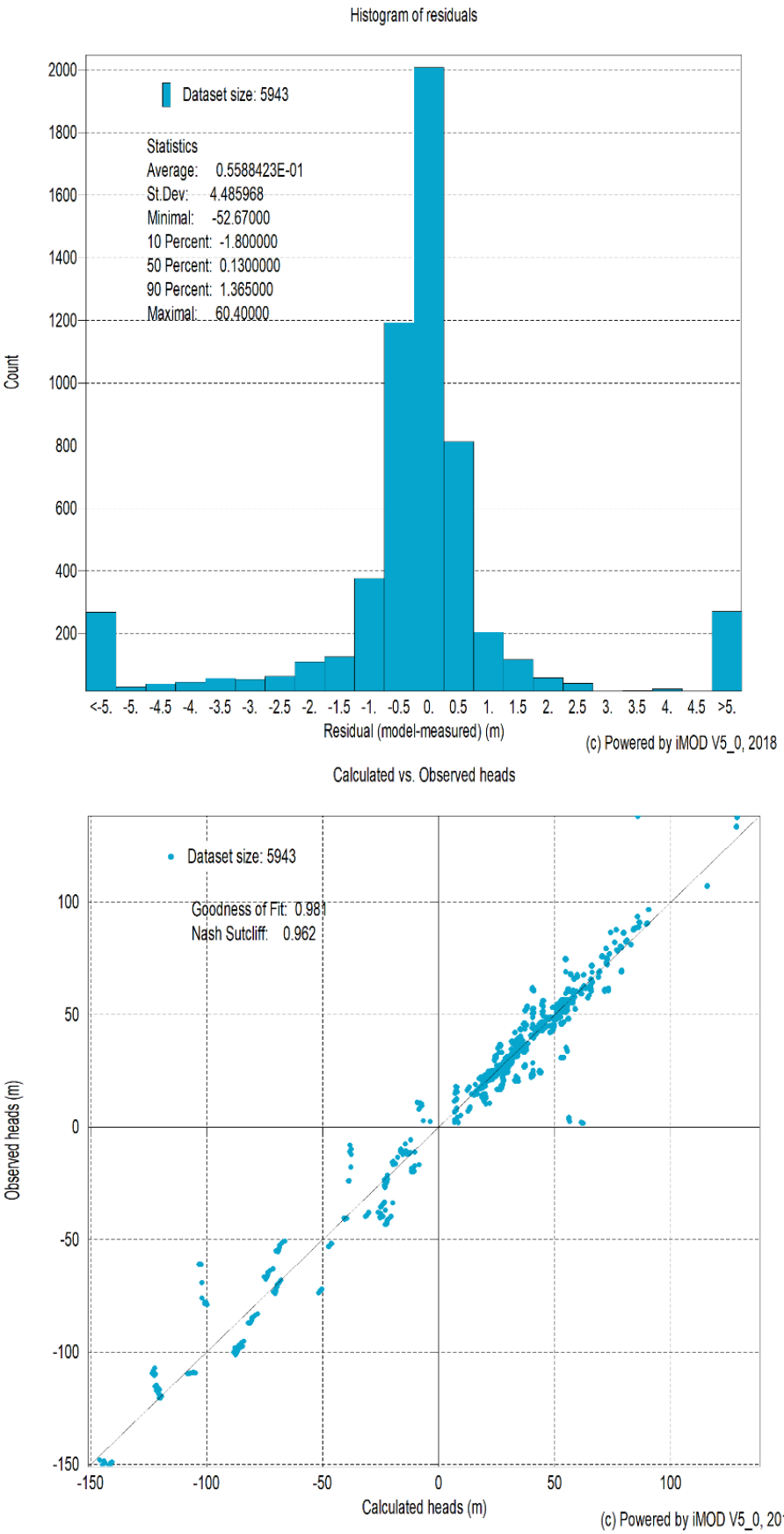

Figure 3.4 Computed residuals for yearly average measurement in the period 1st of January 2010 up to 1st of January 2018.

3.6.2 Estimated parameters

The horizontal permeability values for the aquifers are optimized using pilot points. Each pilot point can have a different value from which a 2-D spatial pattern is interpolated using Kriging interpolation. The estimated values for the parameters are given in *Table 3.1*.

Table 3.1 Posterior Parameters (horizontal- and vertical permeability and specific storage coefficients).

Model layer	NLD / GER	Formations	SAND	CLAY	AVERAGE	10%	90%	CLAY	SPEC. STORAGE	
			PRIOR		POSTERIOR				PRIOR	P.RIOR
1		BXZ1 / BEZ1	30	-	37	13	40	-	0.15	0.19
	NLD / GER	BXK1 / BXLMK1	-	0.002000	-	-	-	0.002230		-
2		BXZ2 / BEZ2	30	-	48	10	61	-	1.00E-05	1.42E-05
	NLD	BXK2 / BEK1 / STK1	-	0.002000	-	-	-	0.000488		-
3		BXZ2/ BEZ2	30	-	48	10	61	-	1.00E-05	1.85E-06
	NLD	BEK1 / BEK2 / BXLMK1 / STK1	-	0.002000	-	-	-	0.001940		-
4		BEZ1 / BEZ2 / BXZ2	30	-	48	10	61	-	1.00E-05	1.25E-05
	NDL / GER	STK1 BEK2 / JHK1	-	0.000300	-	-	-	0.000155		-
5		STZ1 / BEZ2	30	-	48	10	61	-	1.00E-05	4.70E-06
	NLD	STK1 / SYK1 / RUK1 / RUK2	-	0.000300	-	-	-	0.000281		-
6		STZ2 / SYZ1 / RUZ1	30	-	48	10	61	-	1.00E-05	4.75E-05
	NDL / GER	SYK1 / AHK2	-	0.000300	-	-	-	0.007500		-
7		SYZ1	15	-	25	6	32	-	1.00E-05	1.60E-04
	NLD	SYK2	-	0.000300	-	-	-	0.002500		-
8		SYZ3	15	-	25	6	32	-	1.00E-05	3.22E-05
	NDL / GER	SYK3 / WAK1 / AHK3	-	0.000300	-	-	-	0.000821		-
9		SYZ4 / WAZ2	30	-	51	18	44	-	1.00E-05	2.68E-06
	NLD	SYK3 / WAK2	-	0.000300	-	-	-	0.002090		-
10		SYZ4 / WAZ2	30	-	51	18	44	-	1.00E-05	4.82E-05
	NLD	WAK3	-	0.000300	-	-	-	0.000298		-
11		WAZ4	30	-	51	18	44	-	1.00E-05	1.04E-04
	NLD	MSK1	-	0.000300	-	-	-	0.000236		-
12		MSZ1	25	-	42	15	36	-	1.00E-05	4.35E-05
	NLD / GER	KIK1 / Reuver 11	-	0.000300	-	-	-	0.000280		-
13		KiZ1 / 10	25	-	30	20	31	-	1.00E-05	1.40E-05
	NLD / GER	KIK2 / Rotton 9C	-	0.000300	-	-	-	0.000442		-
14		Sands of Pey / 9B	25	-	30	13	36	-	1.00E-05	1.94E-06
	NLD / GER	KIK3 / Rotton 9A	-	0.000300	-	-	-	0.000217		-
15		Sands of Waubach / 8	10	-	11	5	15	-	1.00E-05	6.78E-06
	NLD	KIK4	-	0.000300	-	-	-	0.000370		-
16		Sands of Waubach / 8	10	-	11	5	15	-	1.00E-05	1.16E-06
	NLD / GER	IEK1 / 7F	-	0.000300	-	-	-	0.001040		-
17		Sands of Inden / 7E	5	-	5	3	6	-	1.00E-05	1.09E-06
	NLD / GER	IEK2 / 7D	-	0.000300	-	-	-	0.000014		-
18		Sands of Inden / 6D	5	-	6	3	9	-	1.00E-05	3.04E-05
	NLD / GER	ViB1 / Frimmersdorf / 6C	-	0.000009	-	-	-	0.000082		-
19		Heksenberg / 6B	2	-	3	1	2	-	1.00E-05	2.71E-06
	NLD / GER	ViB2 / Morken / 6A	-	0.000009	-	-	-	0.000124		-
20		BR-Lower (Heksenberg / Vib2 / 5)	2	-	3	1	2	-	1.00E-05	1.00E-07

The model optimization increased the average initial (prior) values of almost all model layers by a factor of ~1.5, which is reasonable. The value among those pilot points differ (bandwidth) and 80% of the bandwidth is represented by the 10% and 90% values of the posterior value (value after calibration) given in *Table 3.1*. Within each parameter, these 10% and 90% values represent values that can vary locally between 20% and 140% of the average estimated value. For model layer 15 (Waubach Sands), the posterior distribution of the permeability is illustrated in *Figure 6.4* (Appendix A.6). Here, it is clearly visible that the pilot point approach introduces local modifications and patterns. When those patterns show irregularities, which cannot be explained, it might indicate misplaced measurements and/or conceptual errors in the model. The occurrence of the first potential cause is minimized by evaluating measurements to the model behavior (see section 3.4). The latter potential cause is always present, but the smoothness of the permeability field yields confidence that the level of conceptual errors remaining in the model is acceptable.

The vertical permeability is altered in the optimization per aquitard. Here, no pilot points are used as explained in section 3.3. A single permeability value is assigned to each aquitard per model

layer. The prior total average permeability for the aquitards is 0.0005 m/day, this is altered to a posterior value of 0.001 m/d.

The permeabilities of the shallow aquitards, up to model layer 5, are decreased and they introduce more vertical resistance in the model. However, not many shallow aquitards are present within the area of interest. This also holds for the middle deep aquitards, which show an increase of permeability (model layers 6 up to 9). The Kiezelooliet formation (which appears within the area of interest) is changed limited, as the IEk2 is decreased from $3.0E^{-4}$ m/d to $1.4E^{-5}$ m/d.

Especially the Frimmersdorf and Morken aquitards have been increased from $8.6E^{-6}$ m/d to $8.2E^{-5}$ m/d and $1.24E^{-4}$ m/d, respectively. The total vertical resistance of both aquitards decreased from ~4 million days to 400,000 days. The extent of both aquitards is uncertain in the model and an increase of permeability through the model calibration may correct for an overestimation for the extent and thickness of those layers in The Netherlands.

Finally, the specific storage coefficients have been modified. The phreatic unconfined storage coefficient is altered from the prior estimated value of 0.15 to 0.19 which falls within an acceptable bandwidth. The confined and deeper specific storage coefficients changed with factors of 0.01 up to 15. This is significant; however, those specific storage coefficients are still considerable acceptable. Remarkable, but defendable nonetheless due to the great depth of this aquifer, is the decrease of the specific storage coefficient from $1.0E^{-5}$ to $1.0E^{-7}$.

The lateral resistance of the Feldbiβ Fault was optimized for four segments, see *Figure 2.12*. Any modification of the resistances for these faults yielded extremely low sensitivities, especially compared to other parameters. It was not possible to adjust the resistances from their prior estimated values with this model and set of observations.

Overall, the conclusion is that the minor adjustments of the parameters yielded a significantly improved model. The posterior total transmissivity value is presented in *Figure 3.5* and the posterior vertical resistance per model layer in *Figure 6.5*. On average, the total transmissivity in the Roer Valley Graben is 2,000-7,500 m^2/day. The total vertical resistance varies between 300,000 days up to 1.5 million days.

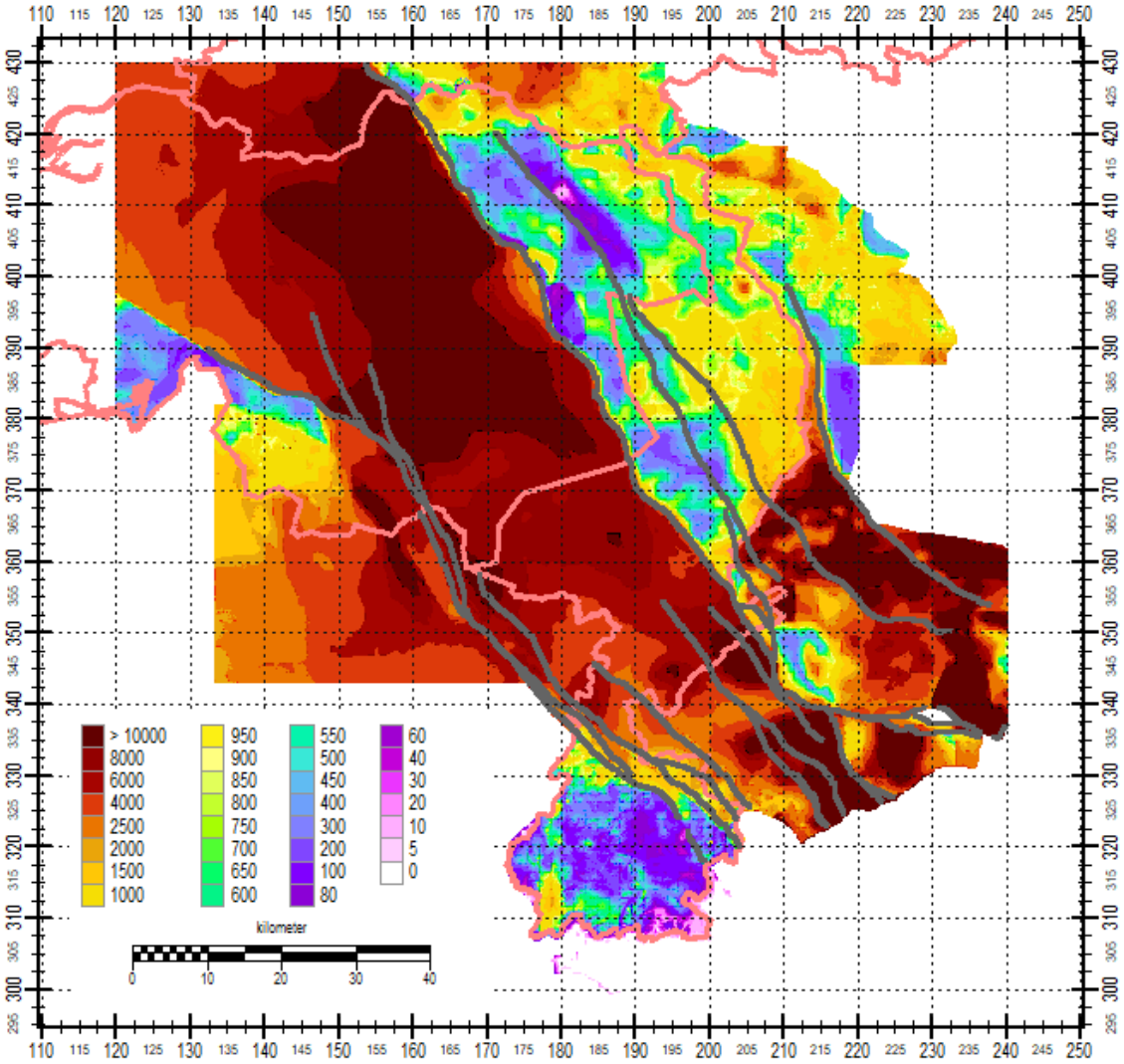

Figure 3.5 Posterior total transmissivity in m^2/day.

3.6.3 Spatial pattern of groundwater levels

The spatial pattern of groundwater levels is depicted in *Figure 3.6* (top). Cleary visible is the effect of the major river Meuse that cuts through the Roer Valley Graben and generates a water shed east and west from the river. The Kempen Blok in Belgium at the south and the Peel Blok (see *Figure 1.1*) in the north form the south and north watershed, respectively. The obstructive effect on groundwater of the Peelrand fault is clearly seen, this is more distinctive than caused by the FeldbiB fault, as the resistance of the latter is less.

The hydraulic head of the deepest aquifer is presented in *Figure 3.6* (bottom). A watershed emerges east of the Meuse, from which groundwater flows to the north-west and south-east towards the open pit Inden mine. The effect of the Feldbiβ- and Peelrand fault are both clearly visible as well as a few major faults in Germany – especially the fault between the Rur-Scholle and Erft Scholle. The drawdown, caused by the open pit Inden- and Hambach, shows values below sea level, up to values of 100 m-MSL in the Erft Scholle.

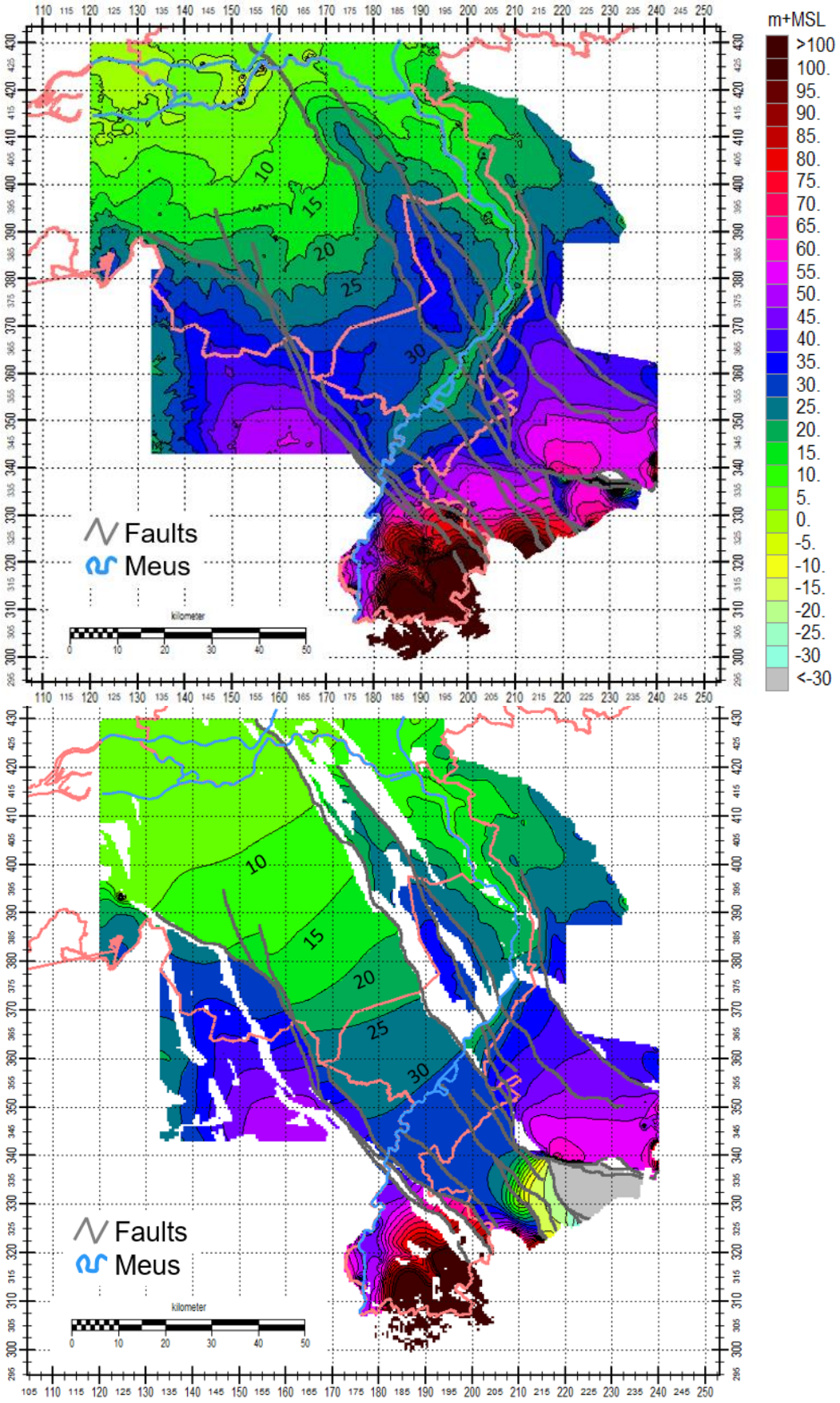

Figure 3.6 Computed (top) phreatic level in m+MSL and (bottom) the pressure heads in the deepest aquifer, model layer 20 for the 1st of January 2018.

3.6.4 Temporal pattern of groundwater-pressure heads

A list of measurements was predefined by the client to present the results; these are given in *Table 3.2* and spatially presented in *Figure 3.7*. As an example, for some of the observations the measured and computed heads are presented as an inset figure in *Figure 3.7* as well. All other measurements are listed in Appendix A.8.

Table 3.2 List of preselected observations in Noord-Brabant (red), Limburg (orange), Germany (blue) and Belgium (green).

Observation	X	Y	Observation	X*	Y*
B45G0166	160598	403978	7-0357	171901	356190
B51E0181	160775	394145	7-0186	181384	342399
B51H0137	177675	386793	7-0355	175385	349251
B51H0164	175936	379421	21867336 (5)	198793	342794
B60B0106	339556	365089	21960431 (9B)	199417	336534
B60A2742	187825	338950	21864302 (10)	216122	332431
B58A0089	180358	368999			

The initial position of observation 7-0355 was on the left side of the Feldbiβ Fault. The measurement showed a clear evidence that it measured the pressure heads in the Roer Valley Graben. Therefore, it has been shifted 500 meters to the east, such that it is on the east side of the Feldbiβ Fault and matches the observation accurately. Probably, the modelled location of the Feldbiβ is inaccurate at that location.

Some measurements show a remarkable drop and/or jump, such as B51H0164-001 and B45G0166-008, which is not represented by the model. These might need some more investigation, although the remaining part of the timeseries is represented quite well with the model. The observation B58A0089 shows a good match for the shallow pressure heads. The middle-deep filter, however, shows that the computed head is ~3 meters lower than the measurement. This area is characterized by a complex geology with many aquitards that thin-out and/or interchange with others, see appendix A.4. Any local distortion, which is not represented correctly in this model on a resolution of 250x250 meter, might affect the hydraulic head significantly.

The overall performance of the computed heads at the preselected observations is acceptable and even above prior expectation. It seems that the prediction of the model improves with depth. This is caused by the fact that the resolution of the model is coarse which effects an accurate representation of the phreatic groundwater level at the location of a measurement. Stream locations are represented less accurately at that scale. At greater depths, the pressure heads are more regional determined, more smoothened and effected mostly by extractions.

Important to note is that the behavior of the model, compared to the measurements is comparable. The drawdown in time, including a short-term upcoming, is represented by the model quite well. The fact that the model can reproduce those deeper heads, benefits the application of the model.

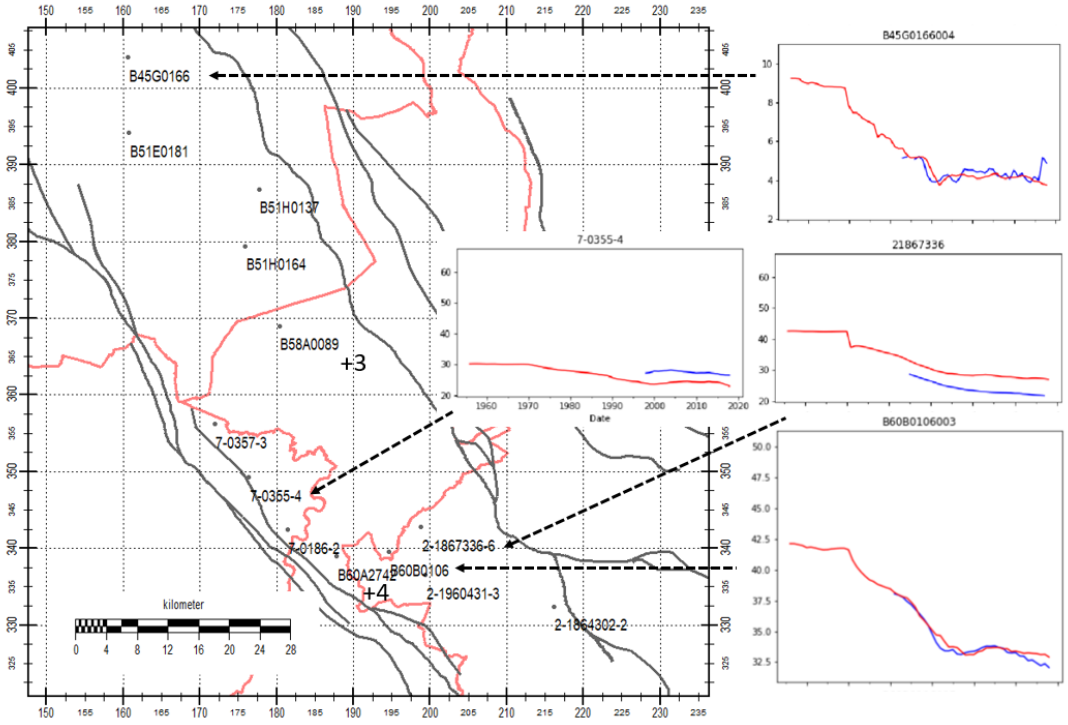

Figure 3.7 Overview of the location of measurements for the evaluation of the model and the scenarios, inset figures are some examples of measured and observed pressure heads.

3.6.5 Water balance

An important aspect of the water balance is the amount of water that flows over the Peelrand Fault. On the one hand there is a net inflow of 13.1 million m^3/year, mostly due to the infiltration near the Meinweg area as compensation for the extracted groundwater for the open pit mines. On the other hand, there is a significant outflow of 28.4 million m^3/year towards the Erft Scholle to the Hambach open pit mine. If those values are compared with the results from the RWE Model (RWE AG, 2013), the IBRAHYM Roer Valley Graben model yields similar volumes.

An amount of 24.2 million m^3/year groundwater flows from the eastern boundary of the model towards the Inden open pit mine. The Inden open pit mine extracts most of the groundwater from the deep aquifers (below the brown-coal formations Frimmersdorf (ViB1) and Morken (ViB2)), the flow volumes are here largest. The total net volume, as extracted, is in the order of 100 million m^3/year. The difference with the model is caused by the fact that the model computes the flow from the west only and does not include any flow from other directions towards the pit.

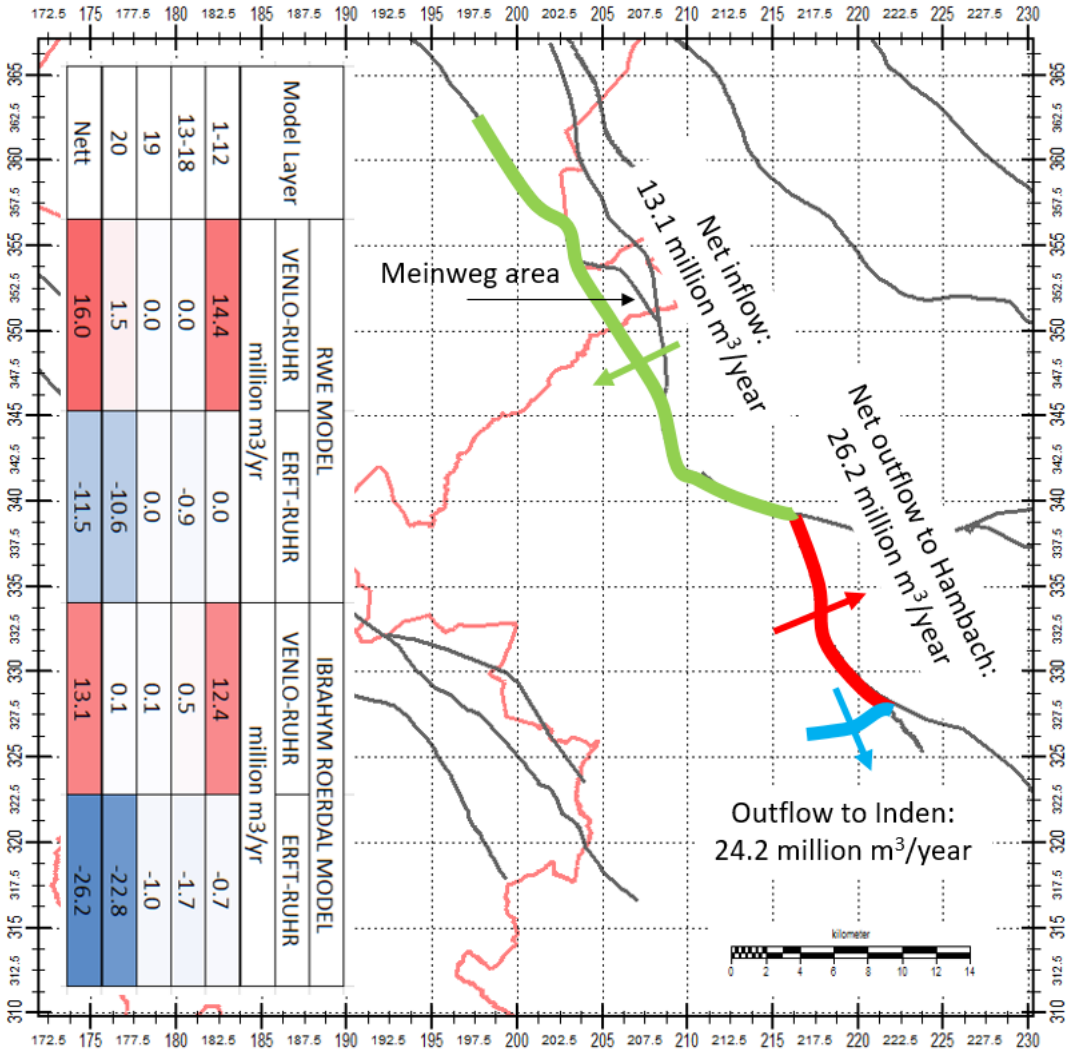

Figure 3.8 Computed fluxes (2018) over the Peelrand Fault compared to the results of the RWE Model; and the flux to and from the Open Pit Mine Inden and Hambach.

A complete water balance of the Roer Valley Graben is given in *Figure 3.9*. The Roer Valley Graben is mostly fed by recharge (41%; 484 million m^3/year), the Meuse (20%; net 12% and 135 million m^3/year) and from the sides of the Roer Valley Graben (26%; net 17% and 199 million m^3/year). Most of this inflow is coming from the south of the Roer Valley Graben (94.3 million m^3/year), which is represented by a significant aquifer of a thickness of ~400 meter in which aquitards are outcropping. The inflow from the north-east (crossing the Peelrand Fault) is ~45 million m^3/year, whereas the inflow from the south-west (crossing the Feldbiβ Fault) is ~75 million m^3/year. On the north-west of the Roer Valley Graben, ~11 million m^3/year is flowing further northwards. A total volume of 1.170 billion m^3/year is flowing through the Roer Valley Graben.

Interesting, furthermore, is that ~47% of all this groundwater is net extracted by surface water, 71% is infiltrated (8+33+30) and 25% (20+5+0) is extracted (again). The extraction wells in the Roer Valley Graben extract ~172 million m^3/year, which is 15% of the total computed water balance. A flow from the Rur-Scholle towards the open pit mines in Germany is equal to a computed volume of 50 million m^3/year, which is 5% of the total computed water balance for the Rur-Scholle as defined in the model.

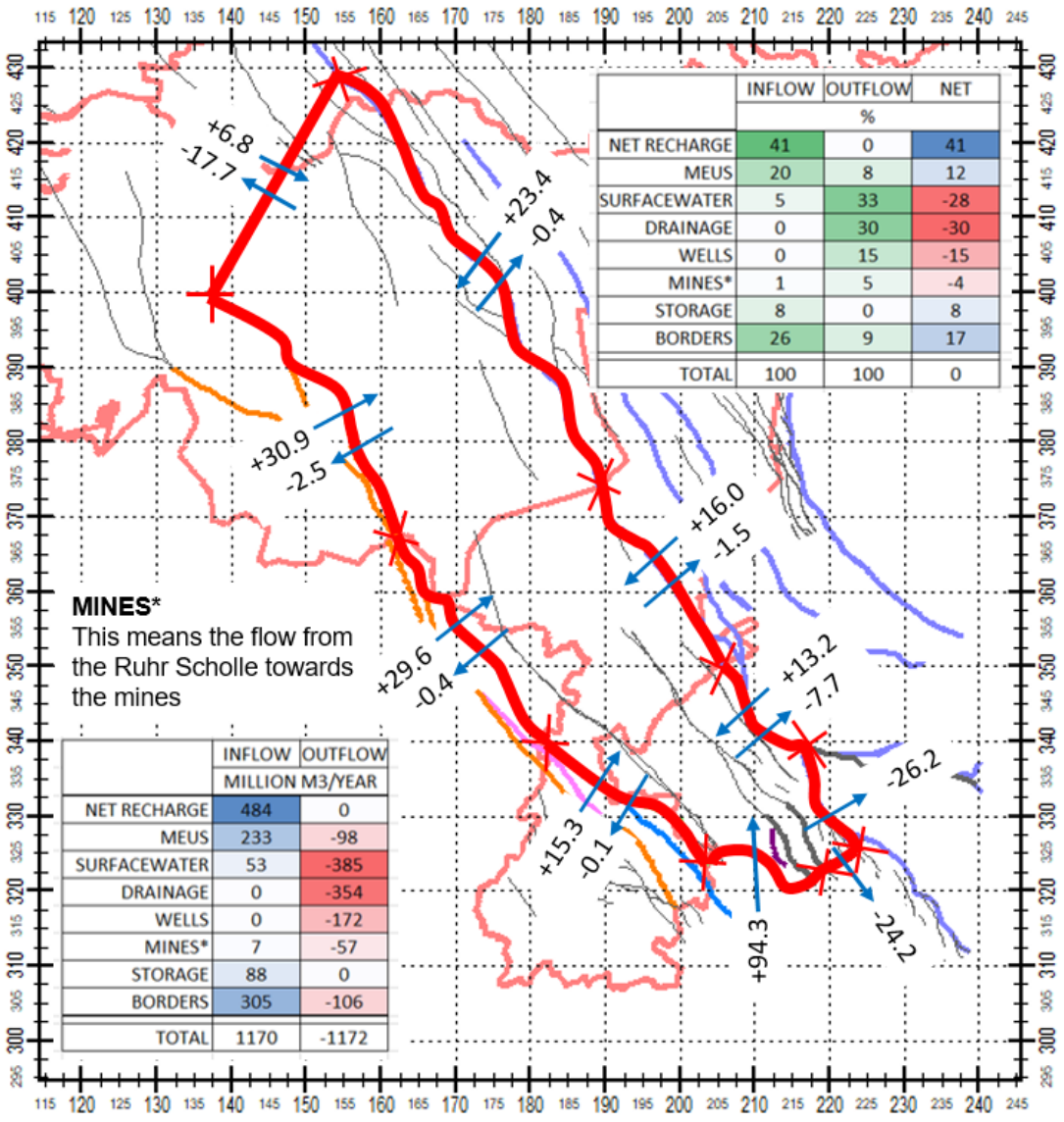

	INFLOW	OUTFLOW	NET
	%		
NET RECHARGE	41	0	41
MEUS	20	8	12
SURFACEWATER	5	33	-28
DRAINAGE	0	30	-30
WELLS	0	15	-15
MINES*	1	5	-4
STORAGE	8	0	8
BORDERS	26	9	17
TOTAL	100	100	0

	INFLOW	OUTFLOW
	MILLION M3/YEAR	
NET RECHARGE	484	0
MEUS	233	-98
SURFACEWATER	53	-385
DRAINAGE	0	-354
WELLS	0	-172
MINES*	7	-57
STORAGE	88	0
BORDERS	305	-106
TOTAL	1170	-1172

Figure 3.9 Computed water balance for the Roer Valley Graben for 1st of January 2018. In two inset figures, the different components of the water balance are presented in actual yearly volumes for 2018 (top-right) and in percentages (bottom-left).

4 Scenarios

4.1 Introduction

The calibrated model is used to simulate the effects of withholding extractions per category as listed in *Table 4.1*. The reference situation is the calibrated model, each scenario is a small modification to that model. Scenario 2, where the influence of the open pit mining is diminished, is modelled by reusing the open model boundaries (see section 2.1.2.2) from 1955 for the entire simulation. The other scenarios turn off all appropriate extractions that belong to that category.

Table 4.1 Overview of the categories used for the scenarios.

Number	RWE-Power	Erfverband	Limburg	N.-Brabant	Belgium	Remark
1	X	X	X	X	X	Reference situation
2		X	X	X	X	No influence of the open pit mining Inden and Hambach
3	X		X	X	X	No extraction of Erftverband
4	X	X		X	X	No extraction of Limburg (WML and Province)
5	X	X	X		X	No extraction of N.-Brabant (Brabant Water and Province)
6	X	X	X	X		No extraction of Belgium
7	X	X			X	No extraction of The Netherlands
8						No extraction at all

The results are presented in 2-D maps, time series and water balances. They will be briefly described in the coming sections and listed in the corresponding appendices.

4.2 Local Effect at the Rode- and Saeffelerbach

It is unknown whether the development of Rode- (NL) and Saeffelerbach (GER) is influenced by groundwater effects of drinking water extraction in the Netherlands and withdrawals from brown coal mining in Germany.

4.2.1 Spatial Effects

The effect of all groundwater extractions on the phreatic level and the pressure heads in the 1st and 2nd aquifer is given in A.13. From these it can be concluded that the total drawdown at the 31st of December 2018, along to the Rode Beek are significant in the order of magnitude of ~1-2 meter. At the river itself, the effect is limited, and this stream keeps draining groundwater. For the upper-stream of the Saeffelerbach the drawdown is significantly more in the order of magnitude of ~3-5 meter. Within the area in between the Rode Beek and the Saeffelerbach, the drawdown varies between 0 and ~5 meters. In the deeper aquifers, this drawdown is even ~10 meters.

4.2.2 Water Balance Effect

As the deeper aquifers show a larger drawdown than the shallow ones, the upcoming flux is reduced which effect the draining capacity of both streams; consequently, the Rode Beek and Saeffelerbach discharge both less. This has been computed and depicted in Figure 4.1. It has been found that the model simulates a maximal discharge of groundwater for the Rode Beek of ~24000 m^3/d up to the 70^s, for the stretch of the Rode Beek as given on *Figure 1.1*. At the 31st of

December 2018, this is reduced with 65% to 15800 m^3/d. The total discharge of the Saeffelerbach reduces in that timeframe from 8500 m^3/d to 2500 m^3/d, which is a reduction of 52%.

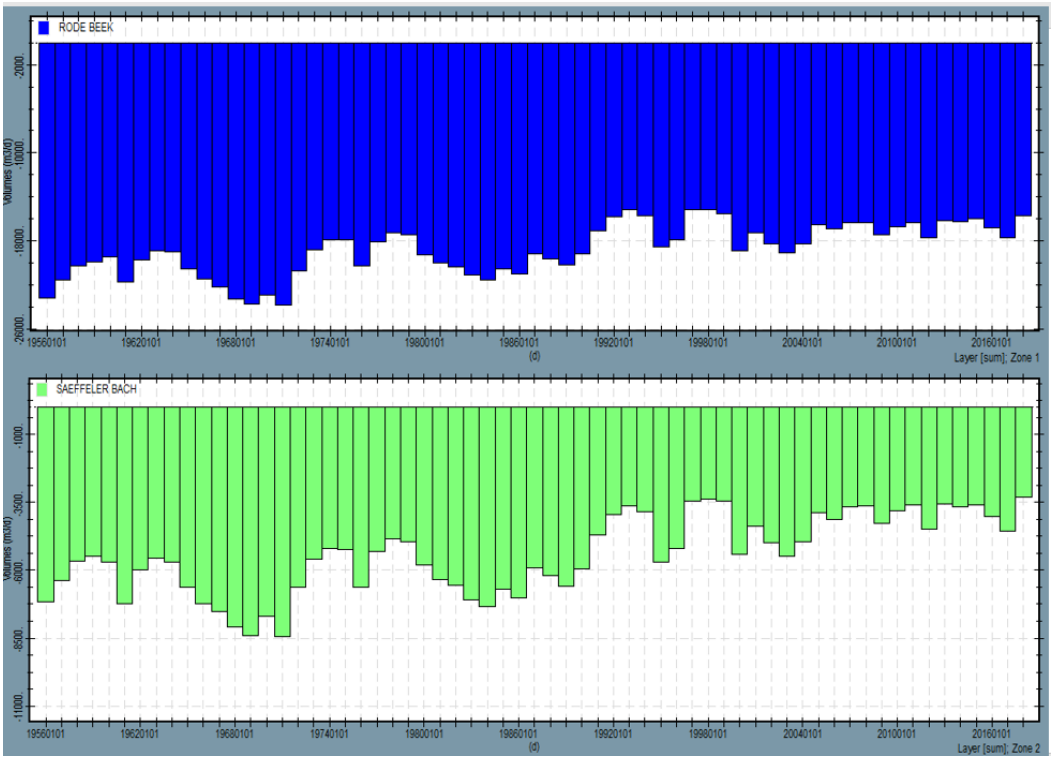

Figure 4.1 Computed discharge of (top) the Rode Beek and (bottom) the Saeffelerbach, both in m^3/d.

4.2.3 Most important Influencer

At the location of the Saeffelerbach and the Rode Beek, the most important influencer seems to be twofold. For the downstream and south section of the Rode Beek it seems to be that the extractions of Limburg are mainly responsible. For the upstream section, the groundwater level is most influenced by the open pit mines, see *Figure 4.2*.

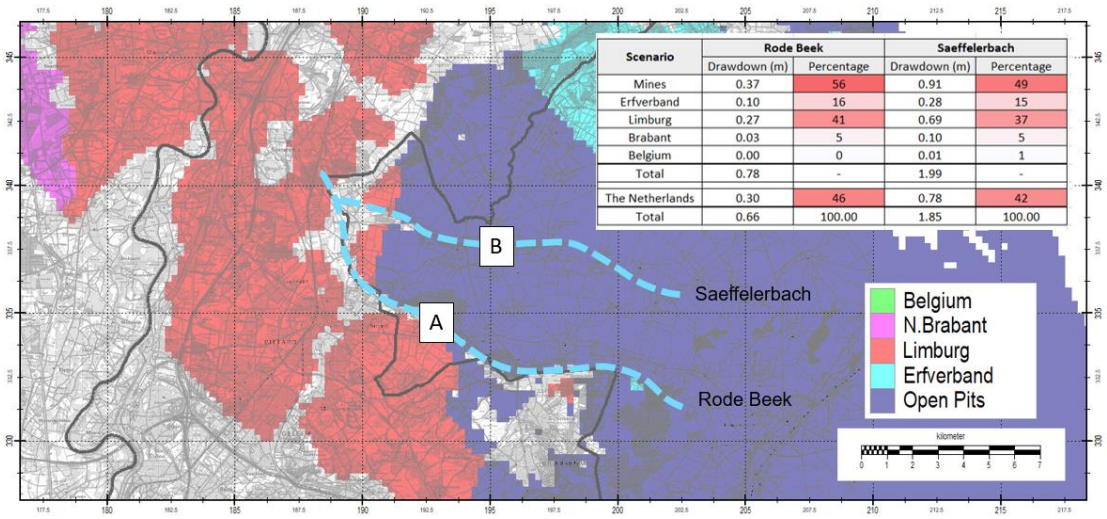

Figure 4.2 Computed most important influencer of the groundwater level near the Saeffelerbach and Rode Beek, A and B refer to locations that are used for a more detailed overview of drawdown as presented in the inset figure.

The Saeffelerbach is for a larger stretch mostly influenced by the open-pit mines. For two random locations (A and B), the total effect is listed per category (inset figure on *Figure 4.2*). While the open-pit mines influence majorly (~50%), the extractions in Limburg still account for ~40%. While the extractions of Erfverband account for ~15%, even the extraction in North Brabant still account for ~5%.

4.3 Regional Effects

4.3.1 Spatial Effects

The spatial effects of the different scenarios are presented for the 1st, 2nd, 3rd and 4th aquifer for the 31st of December 2018 and are listed in Appendix A.9. The 1st aquifer is model layer 1, the 2nd aquifer is represented by model layer 14 (Sands of Pey), the 3rd aquifer is model layer 15 (Sands of Waubach). It should be noticed that even this IBRAHYM-ROERDAL model is not large enough to accurately compute the influence of the extractions in the Roer Valley Graben; this is especially the case for the extraction in North-Brabant, for this the model should extent more to the west. However, due to the closed-boundary condition (see section 2.1.2.1) it over-estimates the drawdown in the northern-region of the model and therefor represents a worst-case.

4.3.2 Temporal Effects

Time Series are constructed for the specific set of observations from *Table 3.2*. These are listed in Appendix A.10 (Effect superposed on the observation) and Appendix A.11 (Net effect on the observation).

4.3.3 Water Balance Effect

For each scenario the amount of net groundwater is computed that flows over the Dutch border into the Roer Valley Graben, see *Figure 4.3*. For the reference situation, ~60,000 m^3/day (22 million m^3/year) flows over the Dutch border into the Roer Valley Graben, whereas ~20,000 m^3/day (7 million m^3/year) flow from Belgium. Whenever the open pit mines in Germany were absent during the simulation, the net inflow from Germany to The Netherlands would be ~36 million m^3/year. For scenario 4 and 7 (no extractions in Limburg or in The Netherlands) even less groundwater flows into The Netherlands. In that latter case, there is even a net outflow towards Belgium instead of an inflow. This is also the case when there was no extraction in the entire model. In that “natural” state, there is a net outflow to Belgium.

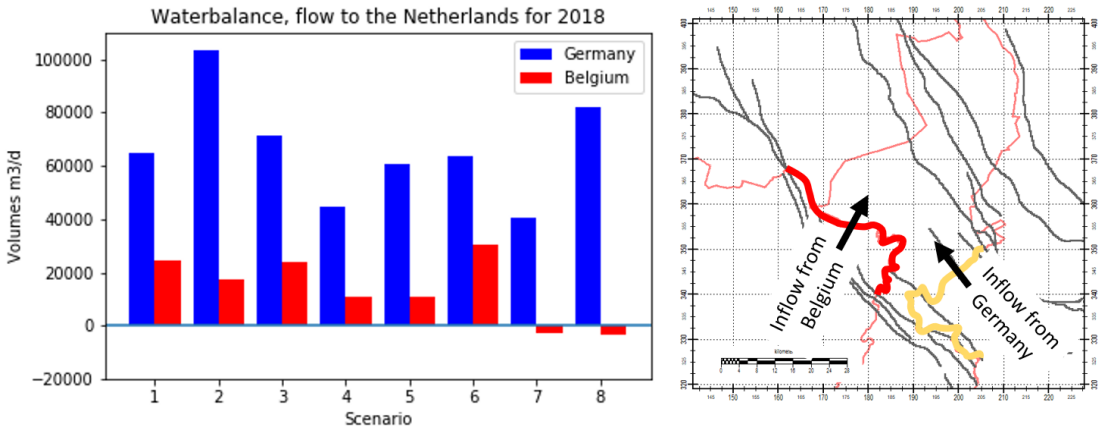

Figure 4.3 Computed groundwater quantities over the Dutch border into the Roer Valley Graben in 2018.

The absolute and percentage differences in the water balance across the Dutch border are given in *Figure 4.4*. Most sensitive to the Dutch inflow from Germany are the open pit mines, their

presence decreases the net inflow for ~50%. On the other hand, the Dutch extractions yielded an increased inflow from Germany of ~25% (scenario 7).

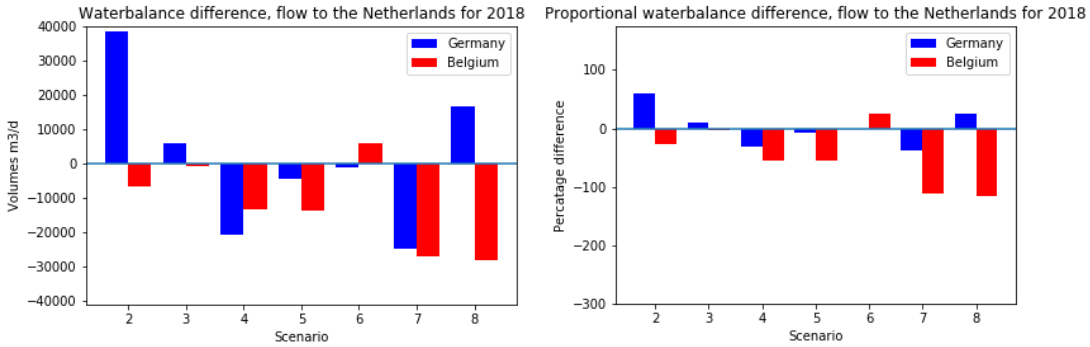

Figure 4.4 Computed absolute (left) and percentage (right) changes of the net in- of outflow across the Dutch border in the Roer Valley Graben.

4.3.4 Most Important Influencer

The most important influencer is computed per location (grid cell) as the category that affects the groundwater head in that cell the most. To avoid irrelevant influences, small effects of <0.10 meter are excluded, see *Figure 4.5*. It should be noted that at each location only one influencer can be largest. Although the open-pit mines are extracting groundwater since 50^{s}, the most important influencer in Limburg and Brabant are still excluding the open pit mines. The reason for that is that, although the mines are active since the 50^{s}, they are represented in the model since the 70^{s} as described in section 2.1.2.2.

The fraction for each influencer is presented in A.12. Here it is clearly seen that extractions from The Netherlands, Belgium and Germany effect the groundwater level of their neighboring country. The influence of the open pit mines in Germany can influence the total drawdown of the groundwater level for percentages of 40% and 25% in Limburg and Noord Brabant, respectively. On the other hand, Limburg effects the drawdown locally in Germany up to ~30% as it influences the drawdown in Noord Brabant less, ~25%. Noord Brabant, determines for almost half of Limburg most of the draw down with percentages of maximal 80%, it even influences the total drawdown in Germany for ~5-10%. The extractions of Erfverband and Belgium influence significant less of their neighboring countries.

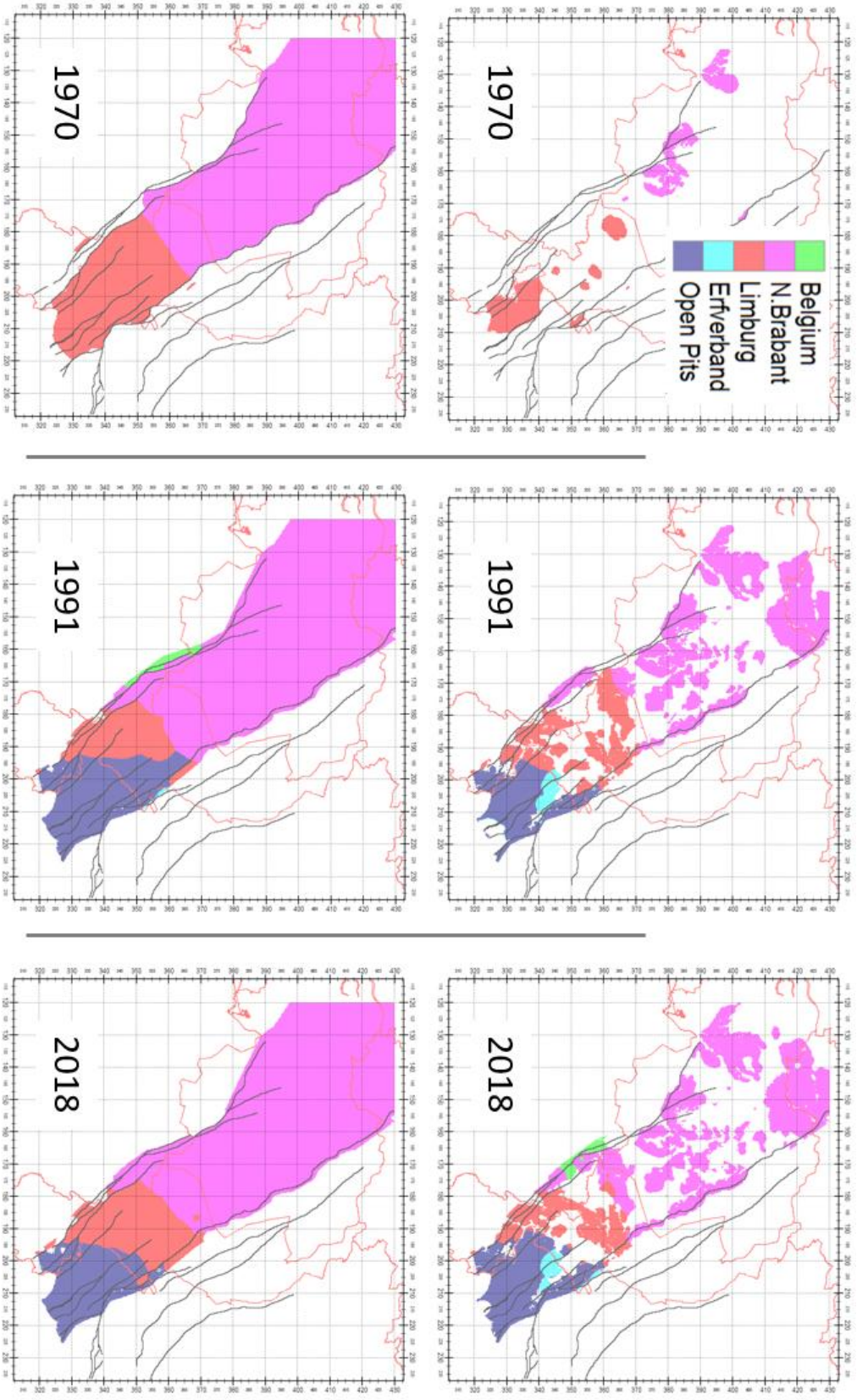

Figure 4.5 Computed most determining influencer of (right images) the phreatic level and (left images) pressure heads in 2nd aquifer (Sands of Waubach) for different periods of time.

5 Conclusions and discussion

5.1 Local Effects at the Rode- and Saeffelerbach

The effect on drawdown of all extractions on the groundwater level is significant along both rivers of the Rode Beek and the Saeffelerbach. Along the Rode Beek, a total drawdown of ~1-2 meter is expected as for the upper-stream of the Saeffelerbach this is can be significantly more in the order of magnitude of ~3-5 meter. The area in between the Rode Beek and the Saeffelerbach, the drawdown varies between 0 and ~5 meters. In the deeper aquifers, this drawdown is even ~10 meters. As the deeper aquifers show a larger drawdown than the shallow ones, the upcoming flux would be reduced as well as both streams tend to drain groundwater. Is has been found that the drainage capacity of the Rode Beek and Saeffelerbach are reduced with 65% and 52% since the 70^{s}. The most important influencer for both streams seems to be twofold. For the downstream and south section of the Rode Beek it seems to be that the extractions of Limburg are mainly responsible as for the further upstream section the groundwater level is most influenced by the open pit mines. The Saeffelerbach is for a larger stretch mostly influenced by the open-pit mines.

5.2 Regional Effects

From the numerical simulations it appeared that some areas near the Dutch border are affected mostly by the Inden open-pit pumping. Areas more inland are influenced for a smaller percentage – however – effects of the mining activities of several meters are commonly found in The Netherlands. The influence of the open pit mines in Germany can influence the total drawdown of the groundwater level for percentages of 40% and 25% in Limburg and Noord Brabant, respectively. On the other hand, Limburg effects the drawdown locally in Germany up to ~30% as it influences the drawdown in Noord Brabant less, ~25%. Noord Brabant, determines for almost half of Limburg most of the draw down with percentages of maximal 80%, it even influences the total drawdown in Germany for ~5-10%. Belgium and the extraction of Erfverband influence significant less of their neighboring countries. Due to the enormous resistances in the aquitards the effect of extractions underneath those aquitard reaches 10-100 kilometers.

5.3 Consequences of the Applied Superposition of the Scenarios

It should be noted that the total drawdown near location “A” and “B” is 0.66 meter and 1.85 meter, respectively. The sum of the individual drawdown is slightly more, 0.78 meter and 1.99 meter. This is caused by the non-linearities in the model. The reference model includes all extractions; therefore, the groundwater table is minimal in the reference situation. In fact, the individual scenarios do not compute the drawdown but the upraise caused by them individually. When multiple scenarios are simulated separately, the groundwater table rises accordingly. In some scenarios and locations, the groundwater table is not raised enough to reach the basis of the drainage systems. A rise in groundwater table is therefore not influenced by the drainage system. When all extractions are deactivated simultaneously, the combined effect results in higher groundwater tables that reach the basis of the drainage system. The combined effect is therefore affected by the drainage system.

5.4 Recommendation

The IBRAHYM-ROERDAL model proved to be able to compute a reliable and plausible estimate for the effects of the groundwater extractions in the Roer Valley Graben. The accuracy of the transient model, compared to measurements and to water balances from the RWE-AG model, is statistically sound.

The model is capable to explore measures to reduce the drawdown caused by extractions. The computed mutual effects for the scenario depends on the other scenarios as well, this is due to non linearities. This is acceptable for the explorative character of the scenarios; however, it is advised to compute total drawdown as a function of measures instead of the superposition of measures.

6 Literature

- Doherty, J., *Ground Water Model Calibration Using Pilot Points and Regularization*. Groundwater, Volume 41, issue 2, 2003, pp 170-177.
- Harbaugh, A.W. 2005. MODFLOW-2005, the U.S. Geological Survey modular ground-water model. The ground-water flow process: U.S. Geological Survey Techniques and Methods 6–A16, variously paged. http://pubs.er.usgs.gov/publication/tm6A16
- Helmbold, F.: Funktioneller Zusammenhang von Durchlässigkeit und entwässerbarem Porenraum in Sanden des Mitteldeutschen Braunkohlereviers. Unveröffentlichte Notiz, 2 S., 1988.
- Jef, D., Vernes, R. , W. Dabekaussen, M. Den Dulk, H. Doornenbal, M. Dusar ,J. Hummelman, J. Matthijs, A. Menkovic, R. Reindersma, J. Walstra, W. Westerhoff en N. Witmans, Geologisch en hydrogeologisch 3D model van het Cenozoïcum van de Roerdalslenk in ZuidoostNederland en Vlaanderen (H3O – Roerdalslenk), https://www.dinoloket.nl/sites/default/files/file/dinoloket_h3odownloads_20140724_eindrapport_h3o_23_07_2014.pdf, 2014.
- Krige, D.G, A statistical approach to some mine valuations and allied problems at the Witwatersrand, Master's thesis of the University of Witwatersrand, 1951.
- Nash, J. E. and J. V. Sutcliffe (1970), River flow forecasting through conceptual models part I -A discussion of principles, Journal of Hydrology, 10 (3), 282-290.
- RWE Power AG, Bericht Grundwassermodell für das Rheinische Braunkohlenrevier, Sammelbescheid zur Neugestaltung bzw. Optimierung des wasserwirtschaftlichen Berichtswesens im Rheinischen Braunkohlenrevier vom 16.10.2003 [86.42.63-2000-1], Bericht 5.5: Fortschreibung der Grundwassermodelle, Cologne, 31. October 2013.
- Vermeulen, Cross-boundary Groundwater Management Phase V, Rode Beek en Saeffeler Bach, Powerpoint presentative + iMOD-model, Deltares, 23 february 2018,
- Vermeulen, P.T.M, F.J. Roelofsen, B. Minnema, L.M.T. Burgering, J. Verkaik and A.D. Rakotonirina, 2018. *iMOD User Manual*. Version 4.4, 2019. Deltares, The Netherlands. (http://oss.deltares.nl/web/iMOD).
- Vermeulen, P.T.M., Linden van der W., Veldhuizen, Massop, H., Vermulst, H. and W. Swierstra, *IBRAHYM Grondwater Modelinstrumentarium Limburg*. TNO-rapport 2007-U-R0193/B, 2007.
- Vermeulen, P.T.M., Roelofsen, F.J. and A. Veldhuizen, Actualisatie en Kalibratie IBRAHYM, Beschrijving van activiteiten t.b.v. IBRAHYM v2.0, Deltares, maart 2015, 1206858-000-BGS-0022.
- Walsum, van P.E.V., Veldhuizen, A.A. and P. Groenendijk, Theory and model implementation 7.1.0, Alterra-report 913.1, 2010.

A Appendices

A.1 Wells Provence of Limburg

Some of the entries of the set of wells did not have any indication for upper- and lower elevation of the well screen, these are excluded, see *Table 6.1*.

Table 6.1 WML and Limburg wells that had '0' as top and bottom filter

id	x	y
699	199750	356818
376	176460	314480
720	176428	361312
938	191268	320920

A.2 Conversion of Stockwerk to Horizont to model layer

The *Horizont* values are used to give specific model layer numbers for each well, see *Table 6.2*. The layer numbers are then used to put specific top- and bottom-elevation from the model layers to each extraction wells. *Table 6.3* shows the conversion from *Horizont*, to model layer number, to the model layers which are used to determine the upper- and the lower elevation of the well screen.

Table 6.2 Conversion from given Stockwerk to Horizont and model layer.

Stockwerk	Horizont	Model layer
1	16-12	1-12
2	10	13
3	9B	14
4	8,7A	15
5	6b,6A	16-18
6	5,4,2	19-20

Table 6.3 Conversion used from Horizont to model layer number, to model layers used to get to top and bottom.

Horizont	Model layer	Model layer for the upper elevation	Model layer for the bottom elevation
11D,11,11D_8,11D_11B,11B_8, 16_8_6D,12,13,14,16,16_,14,18,19, 19A,16-14,18_6B,11D-16	1	L1	L12
10,18,8	2	L13	L13
9B	3	L14	L14
7A,8_6D,8	4	L15	L18
6A,6B	5	L19	L19
2,4,5	6	L20	L20

A.3 Geohydrological Sequence in Germany

On *Figure 6.1* the geohydrological sequence is presented for the geology in the Ruhr-, Erft, Venlo Scholle.

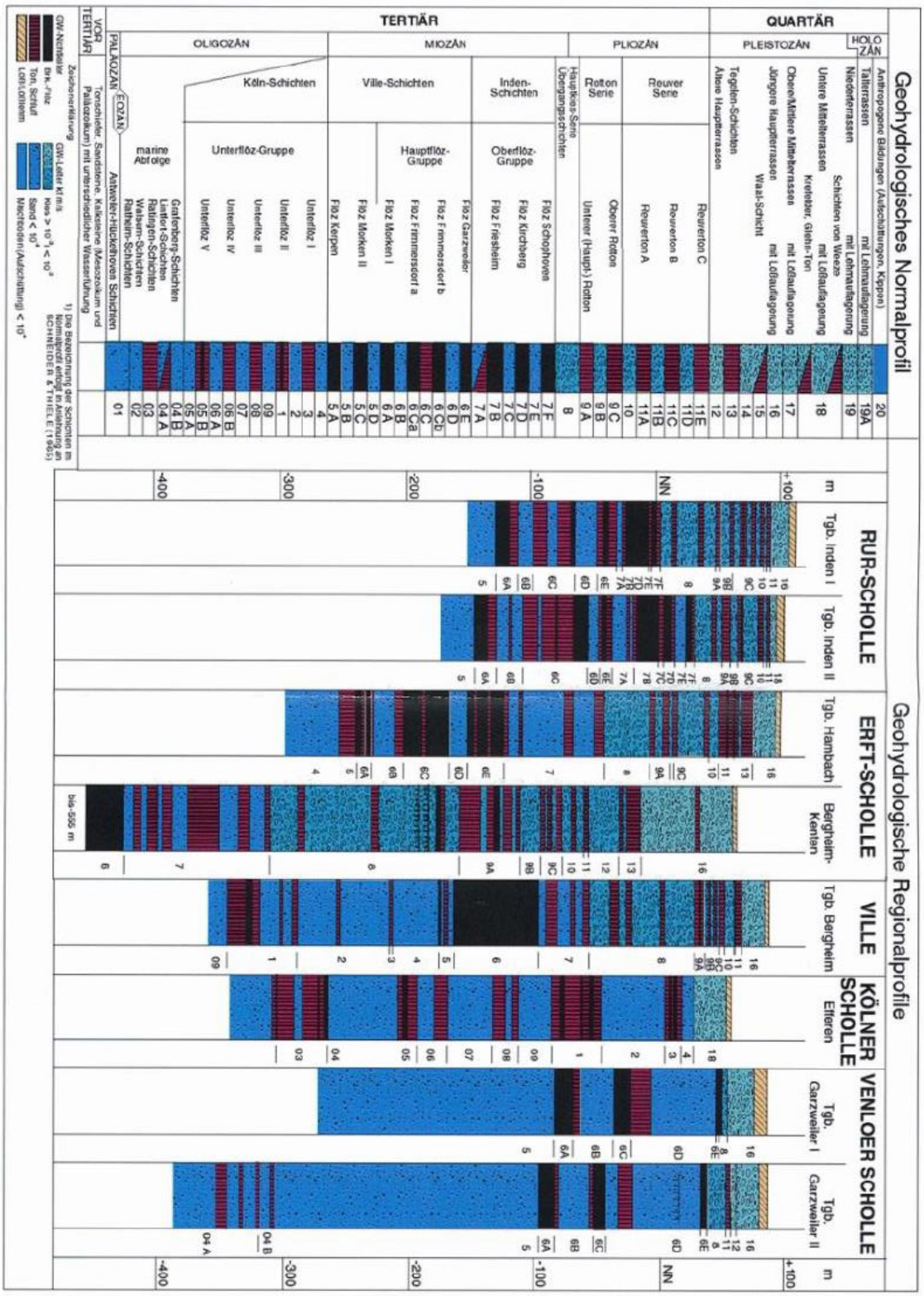

Figure 6.1 Overview of the geohydrological formation in the Erft, Ruhr and Venlo Scholle.

A.4 H3O-Rose Conceptual longitudinal cross-section

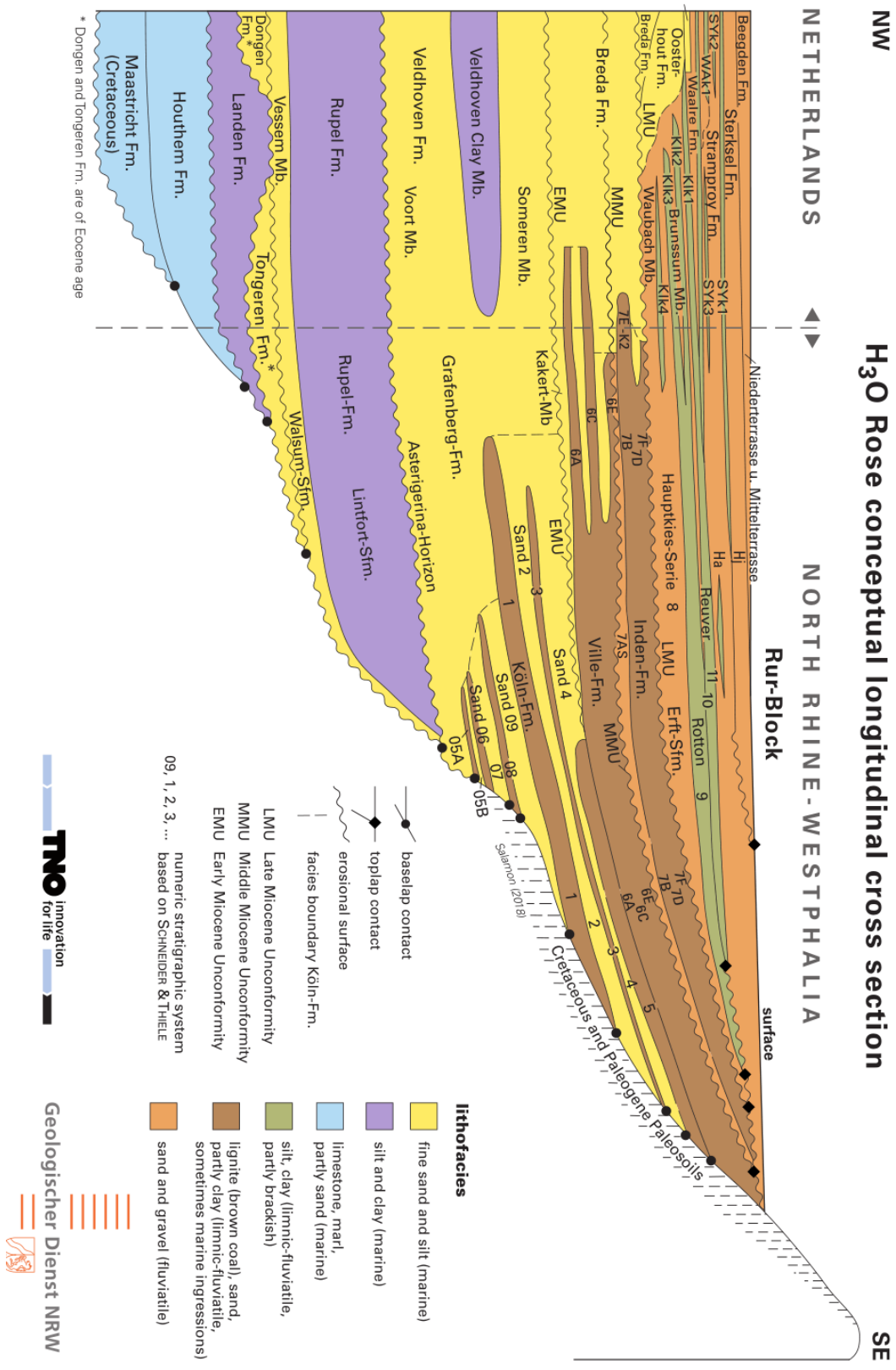

Figure 6.2 H3O-ROSE conceptual longitudinal cross-section.

A.5 H3O-Rose Conceptual Stratigraphy

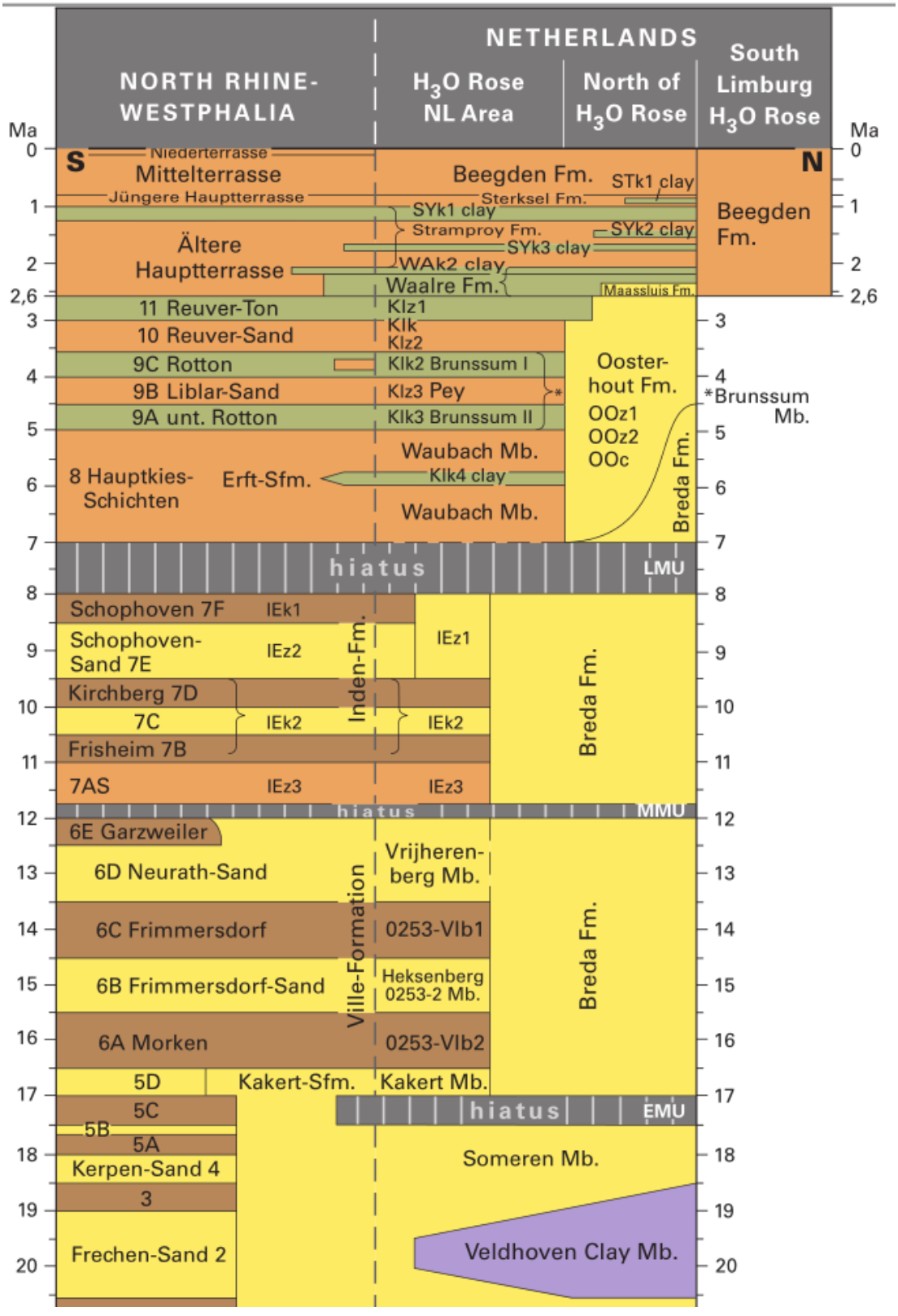

Figure 6.3 H3O-ROSE conceptual stratigraphy

A.6 Posterior estimated permeability

The posterior permeability of model layer 15 (Waubach Sands) is given in *Figure 6.4*. This is an example to demonstrate the smoothness of the parameter adjustments due to the pilot point approach.

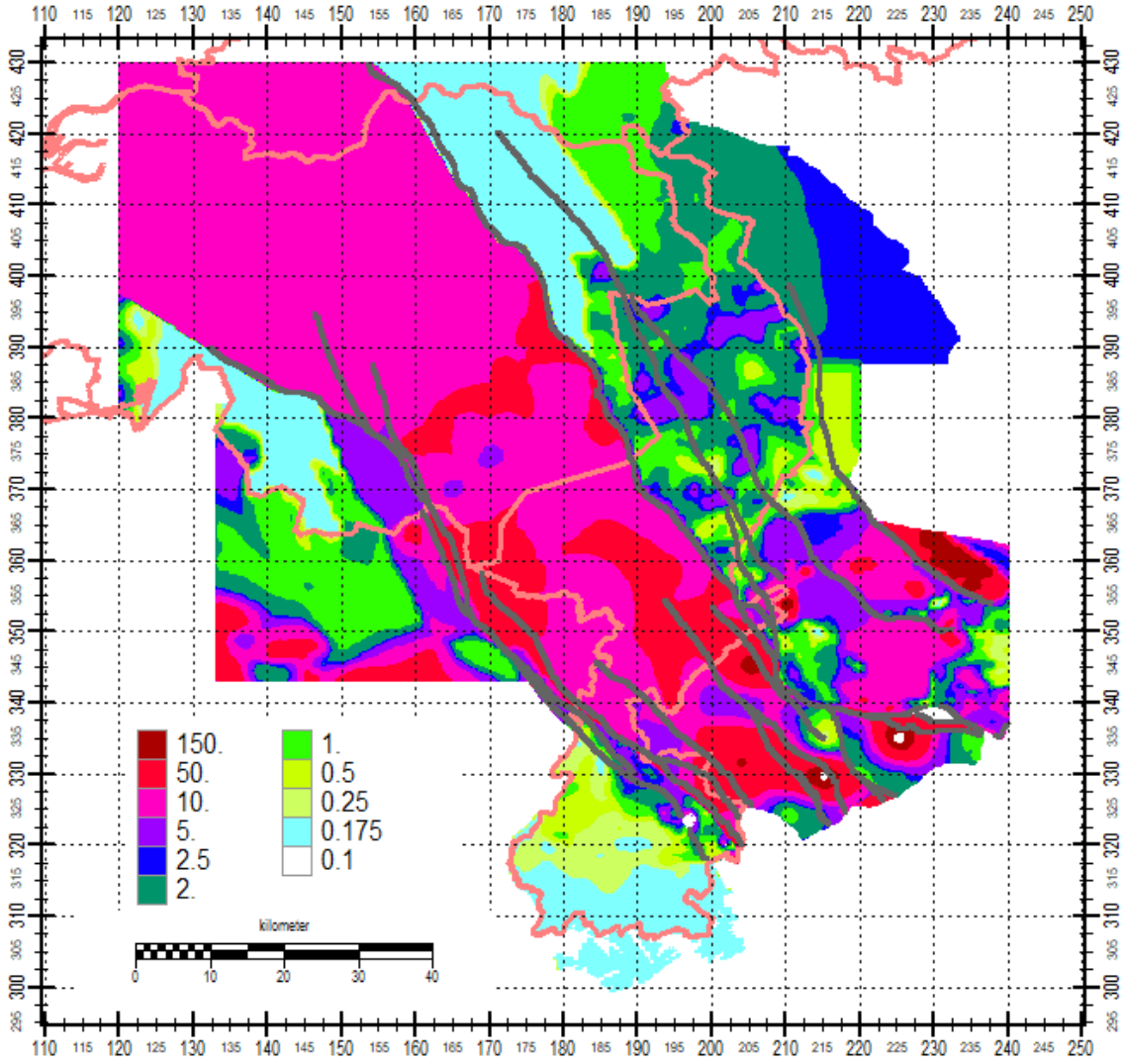

Figure 6.4 Computed Permeability (m/d) values after the calibration for model layer 15 (Sands of Waubach).

A.7 Vertical resistances

Here the posterior vertical resistances are presented in *Figure 6.5*.

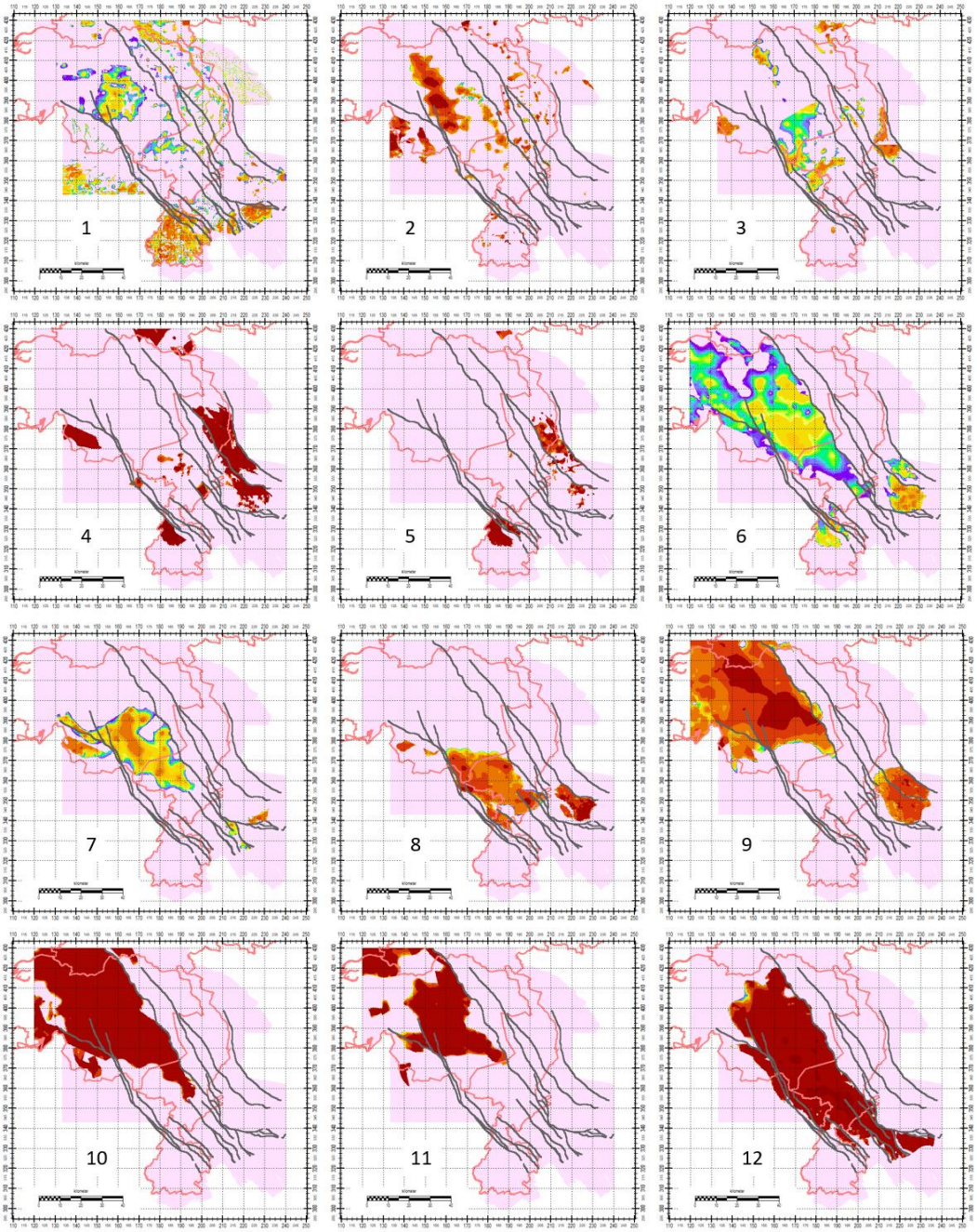

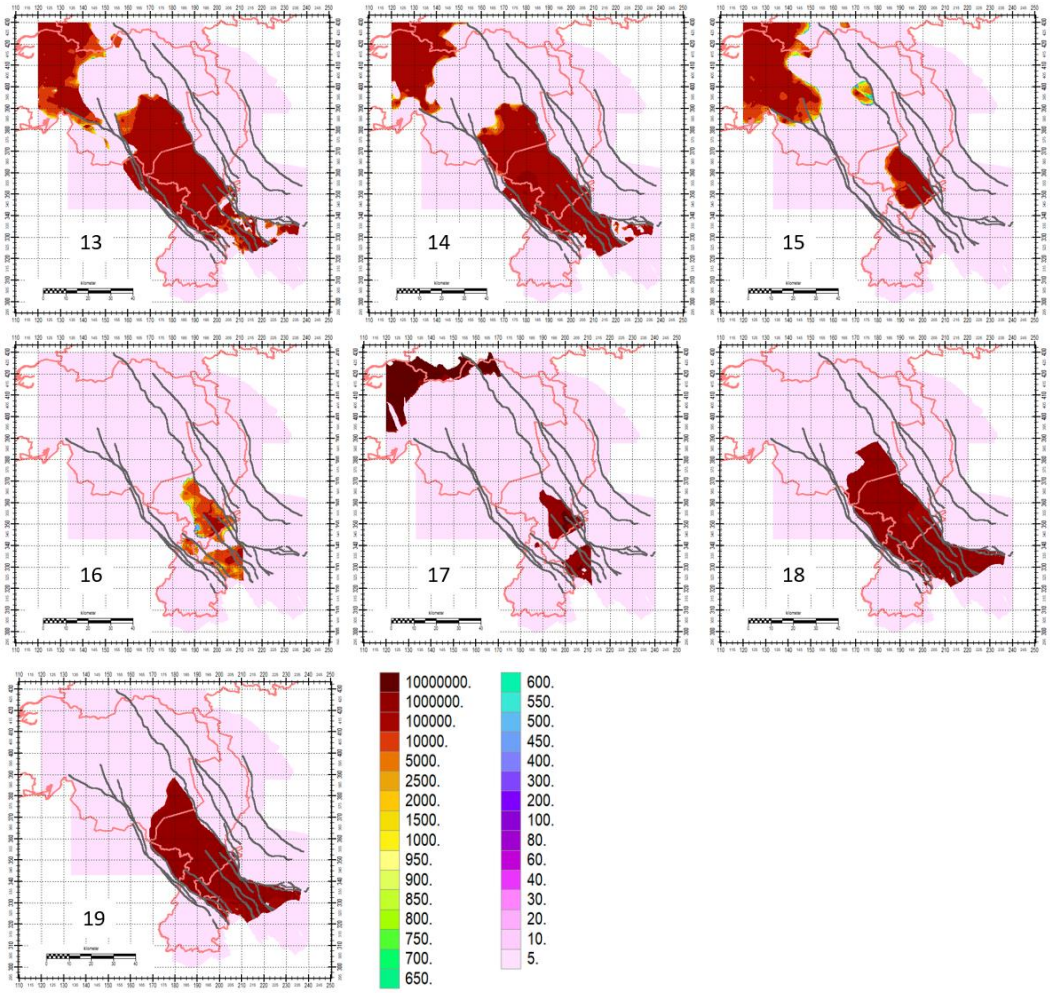

Figure 6.5 Posterior vertical resistance per model layer in days.

A.8 Computed and measured timeseries

The measured and computed hydraulic heads are presented on the following figures for the selected set of observations as specified beforehand.

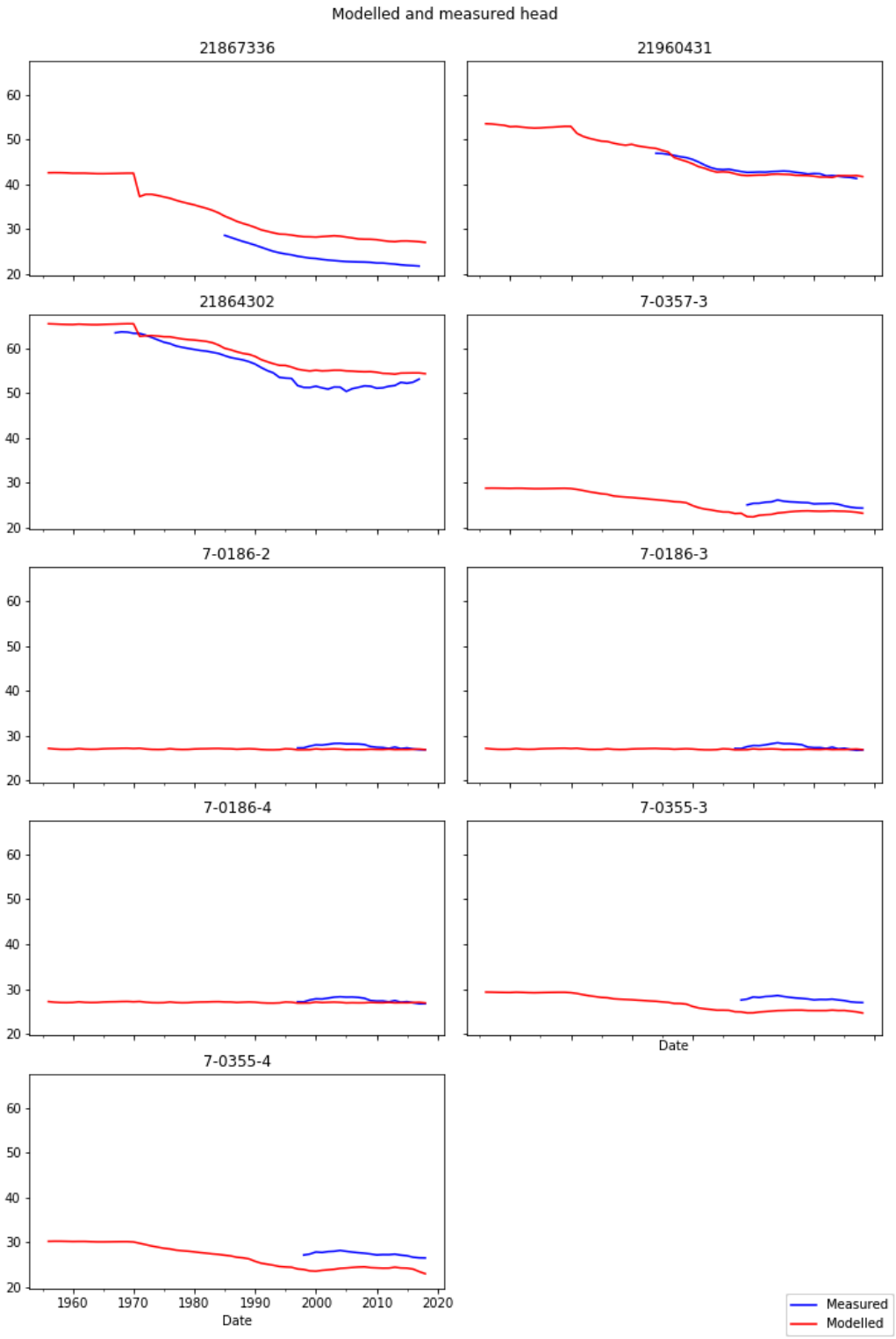

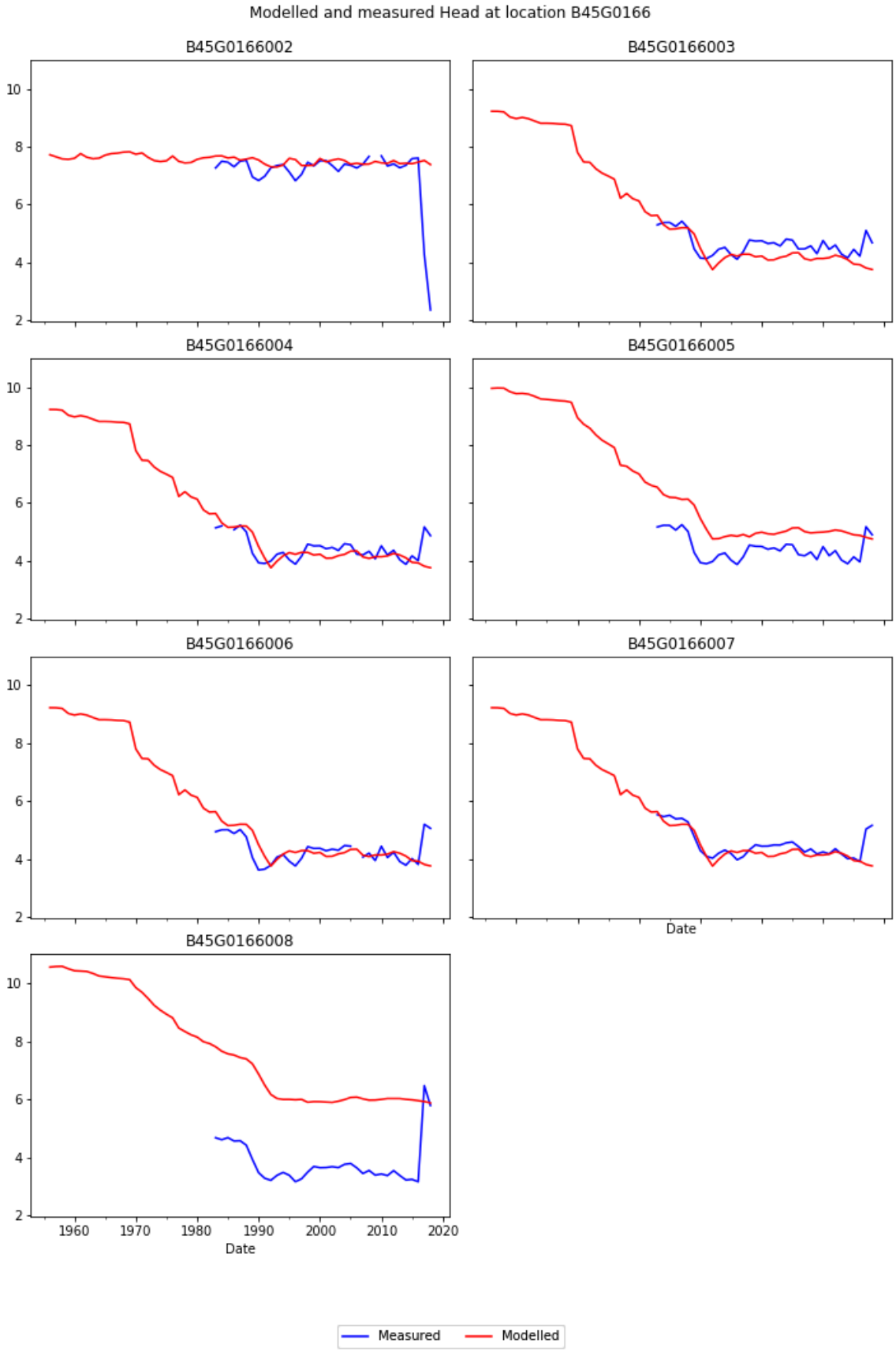
Modelled and measured Head at location B45G0166
B45G0166002
B45G0166003
B45G0166004
B45G0166005
B45G0166006
B45G0166007
B45G0166008
10
8
6
4
2
1960
1970
1980
1990
2000
2010
2020
Date
Measured
Modelled

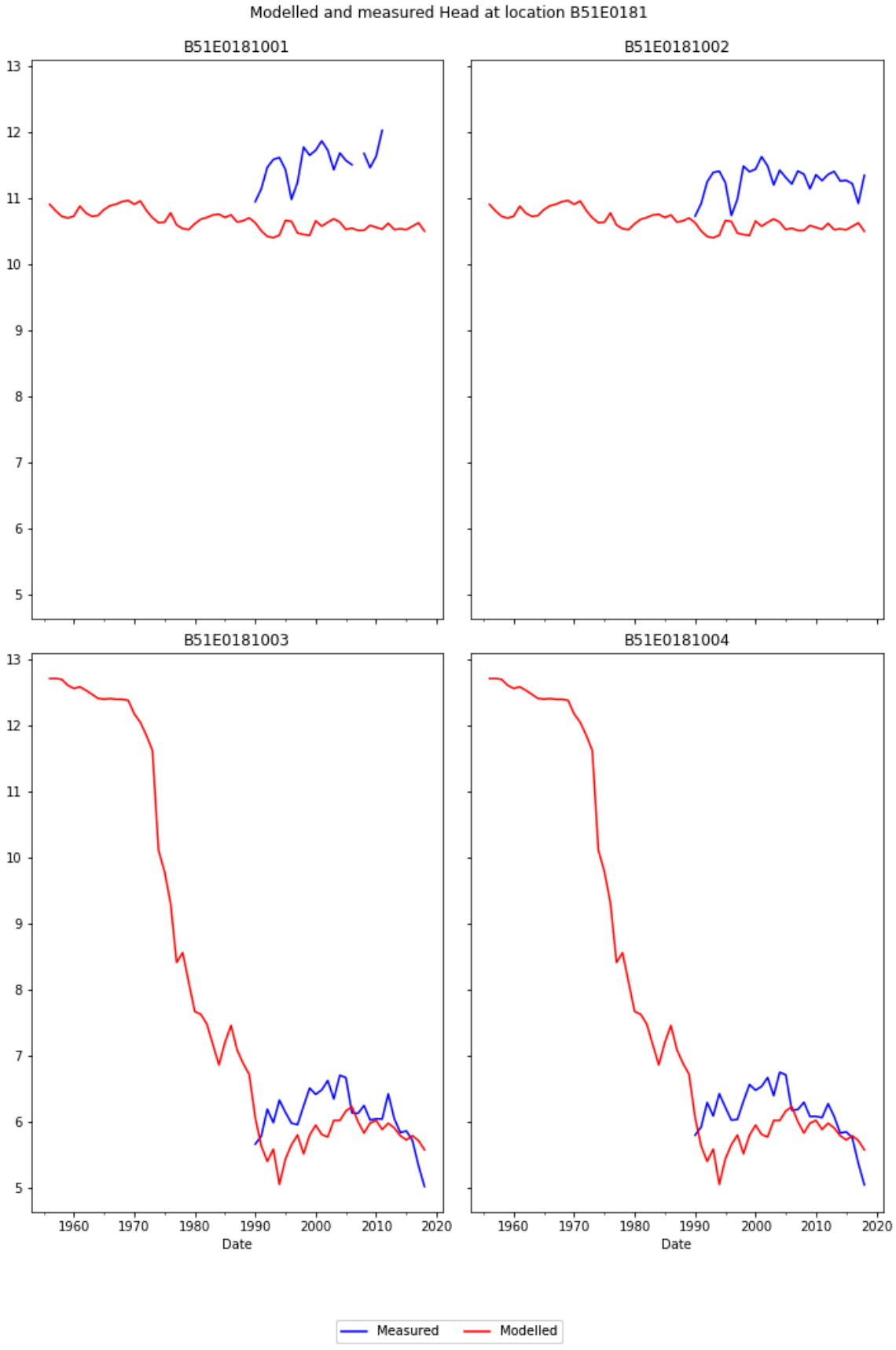
Modelled and measured Head at location B51E0181
B51E0181001
B51E0181002
B51E0181003
B51E0181004
13
12
11
10
9
8
7
6
5
1960
1970
1980
1990
2000
2010
2020
Date
Measured
Modelled

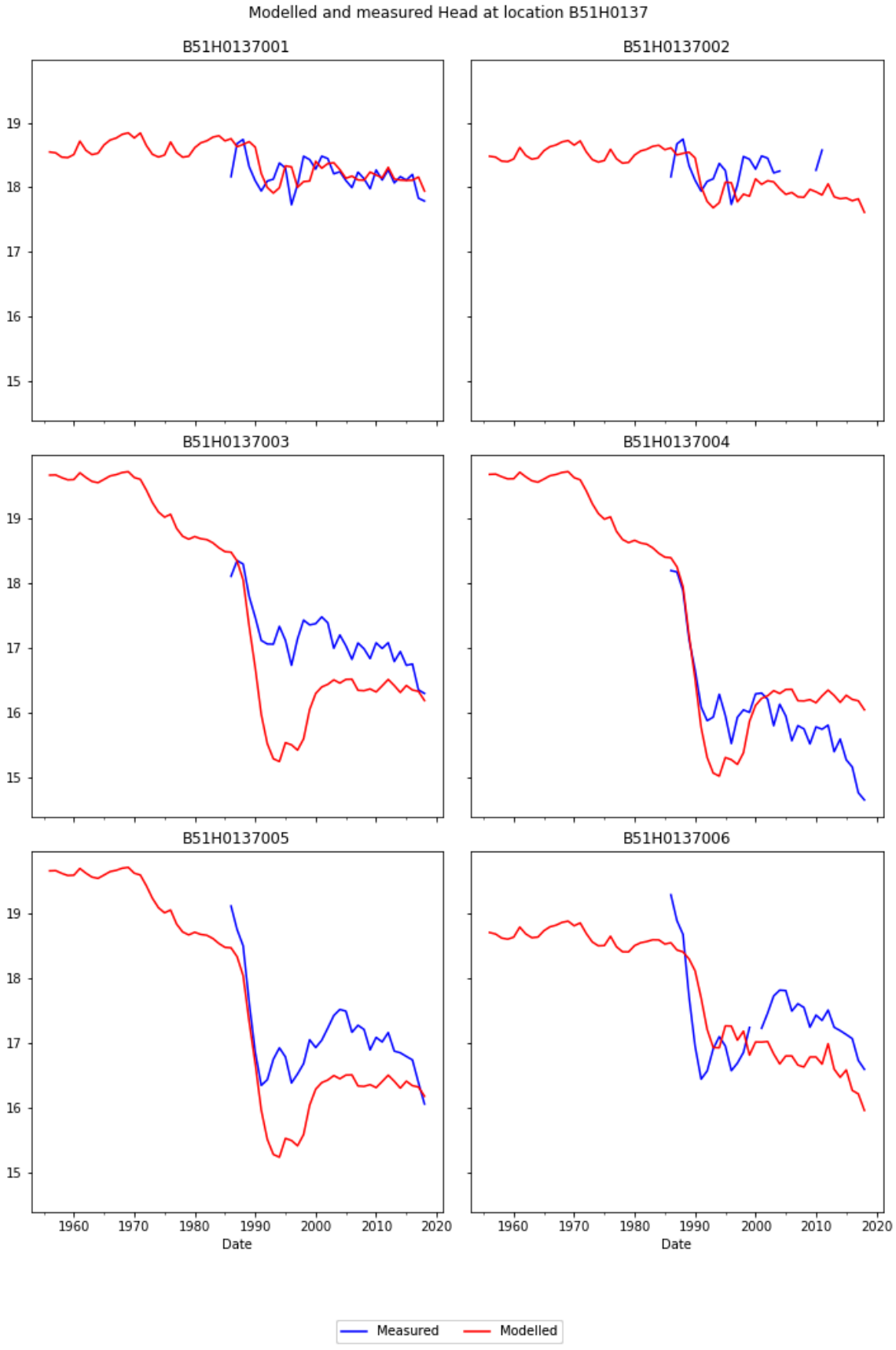
Modelled and measured Head at location B51H0137
B51H0137001
B51H0137002
B51H0137003
B51H0137004
B51H0137005
B51H0137006
19
18
17
16
15
1960
1970
1980
1990
2000
2010
2020
Date
Measured
Modelled

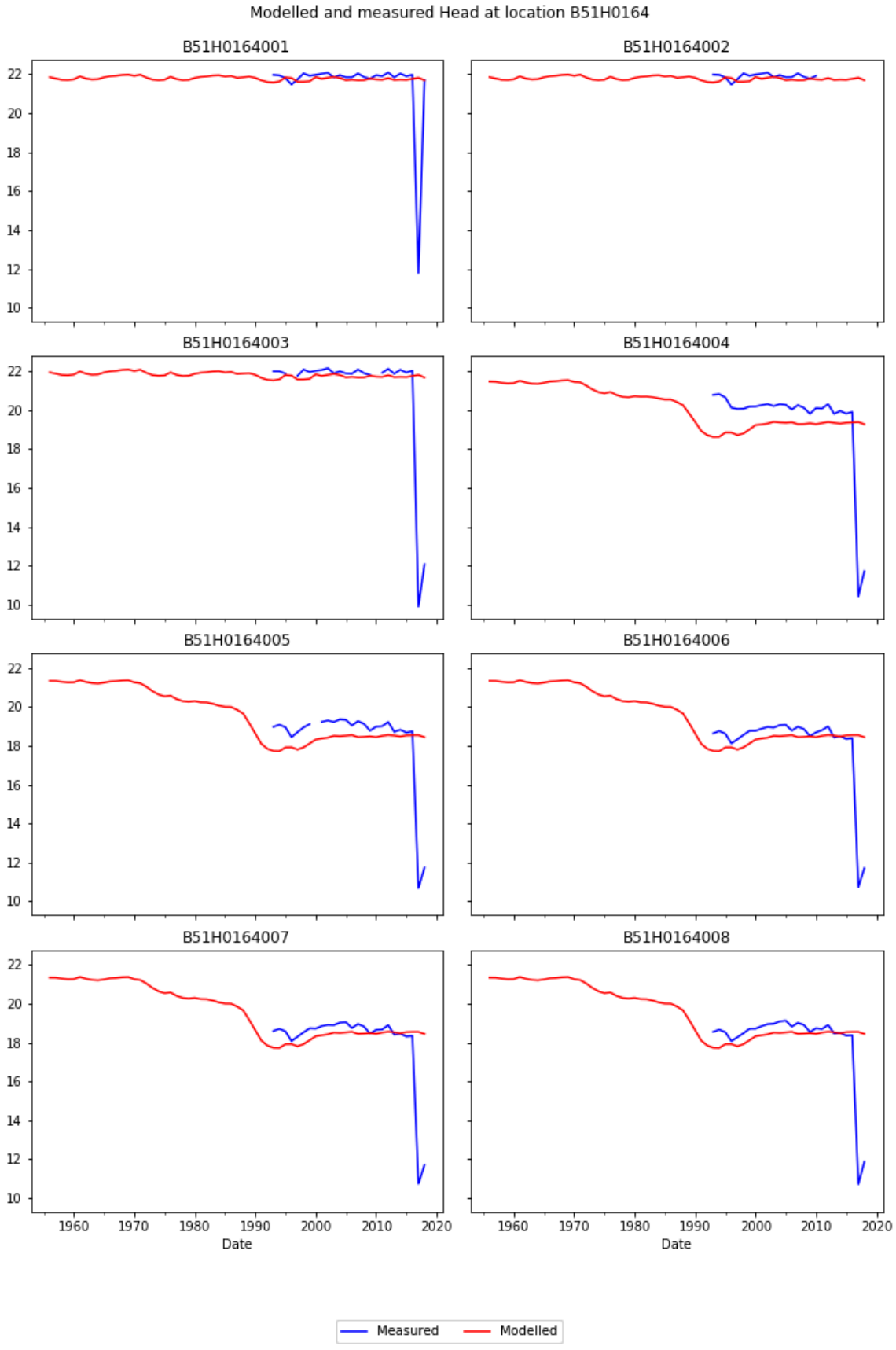
Modelled and measured Head at location B51H0164
B51H0164001
B51H0164002
B51H0164003
B51H0164004
B51H0164005
B51H0164006
B51H0164007
B51H0164008
22
20
18
16
14
12
10
1960
1970
1980
1990
2000
2010
2020
Date
Measured
Modelled

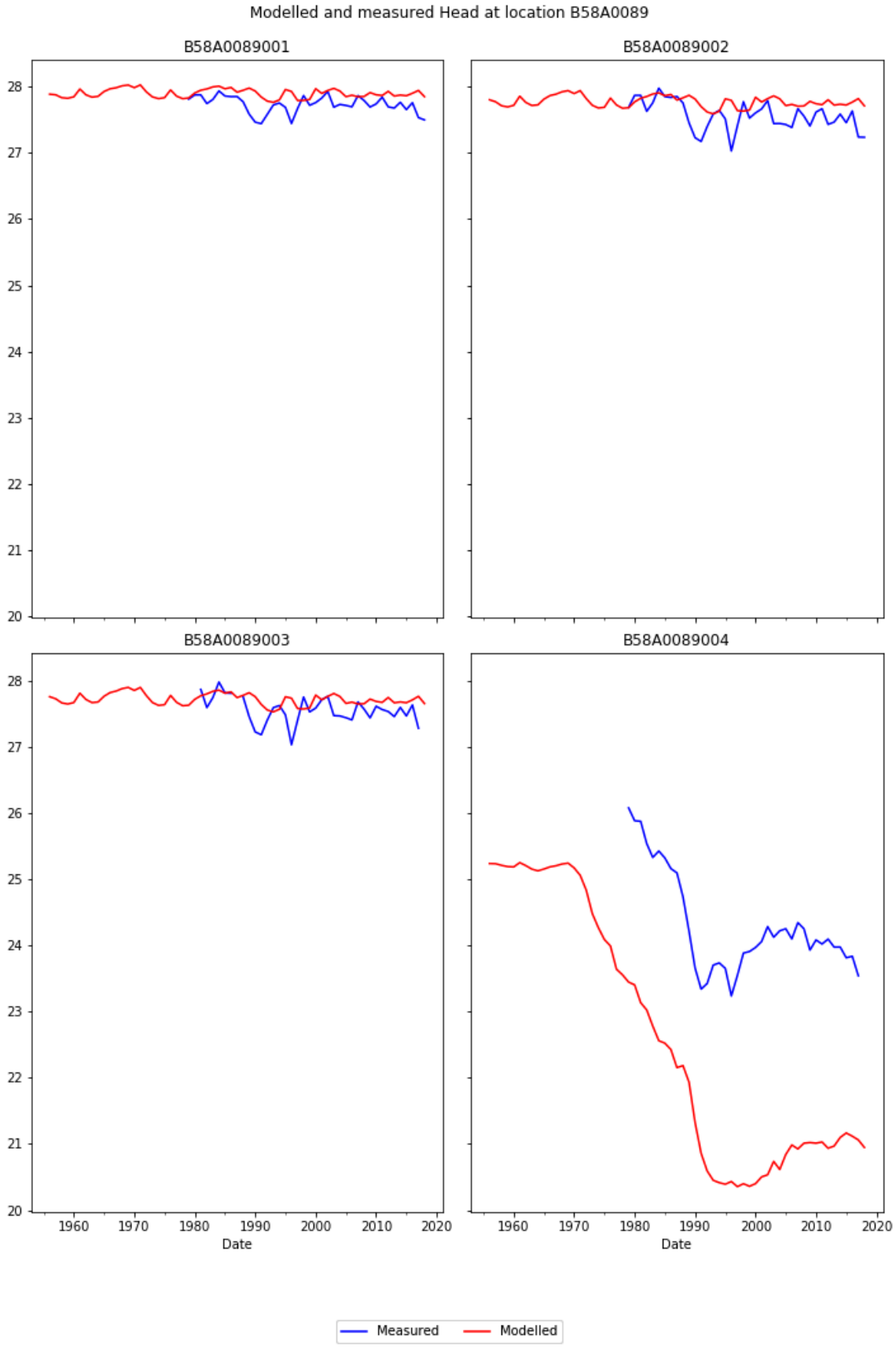
Modelled and measured Head at location B58A0089
B58A0089001
B58A0089002
B58A0089003
B58A0089004
28
27
26
25
24
23
22
21
20
1960
1970
1980
1990
2000
2010
2020
Date
Measured
Modelled

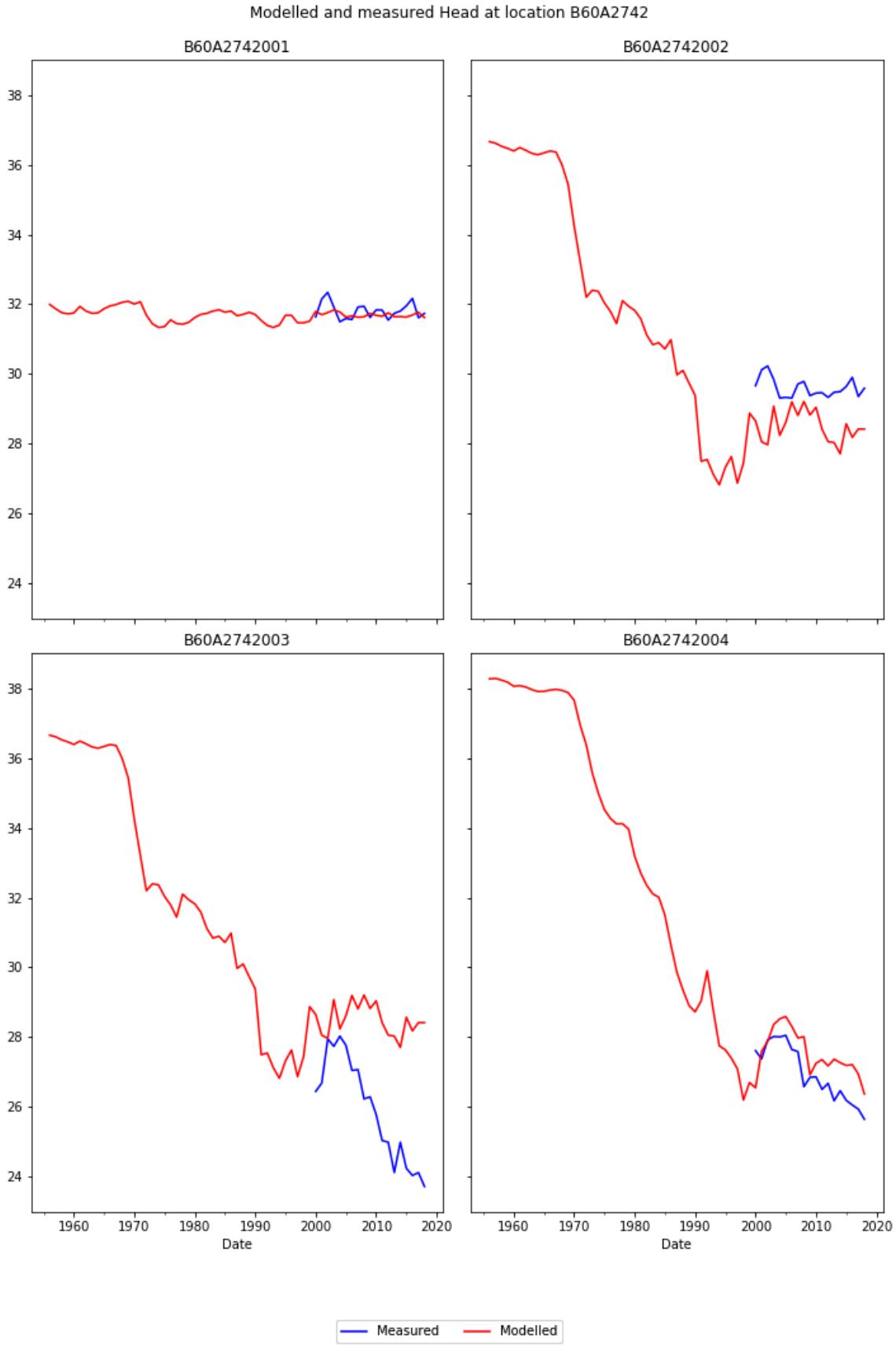
Modelled and measured Head at location B60A2742
B60A2742001
B60A2742002
B60A2742003
B60A2742004
38
36
34
32
30
28
26
24
1960
1970
1980
1990
2000
2010
2020
Date
Measured
Modelled

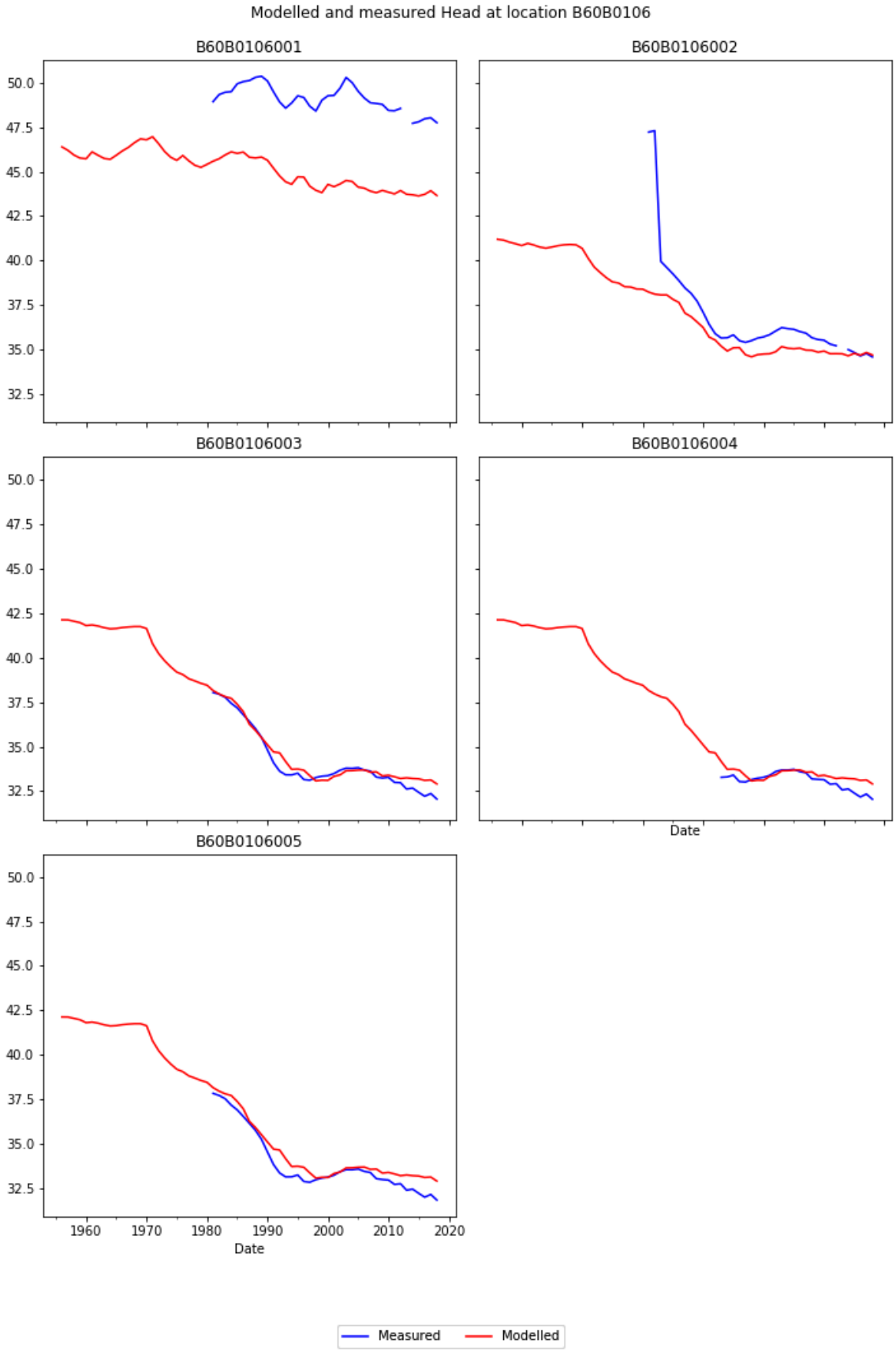
Modelled and measured Head at location B60B0106
B60B0106001
B60B0106002
B60B0106003
B60B0106004
B60B0106005
50.0
47.5
45.0
42.5
40.0
37.5
35.0
32.5
1960
1970
1980
1990
2000
2010
2020
Date
Measured
Modelled

A.9 Computed Effect for the Scenarios

The computed effect (meters) for the different scenarios on the hydraulic heads is presented on the following figures.

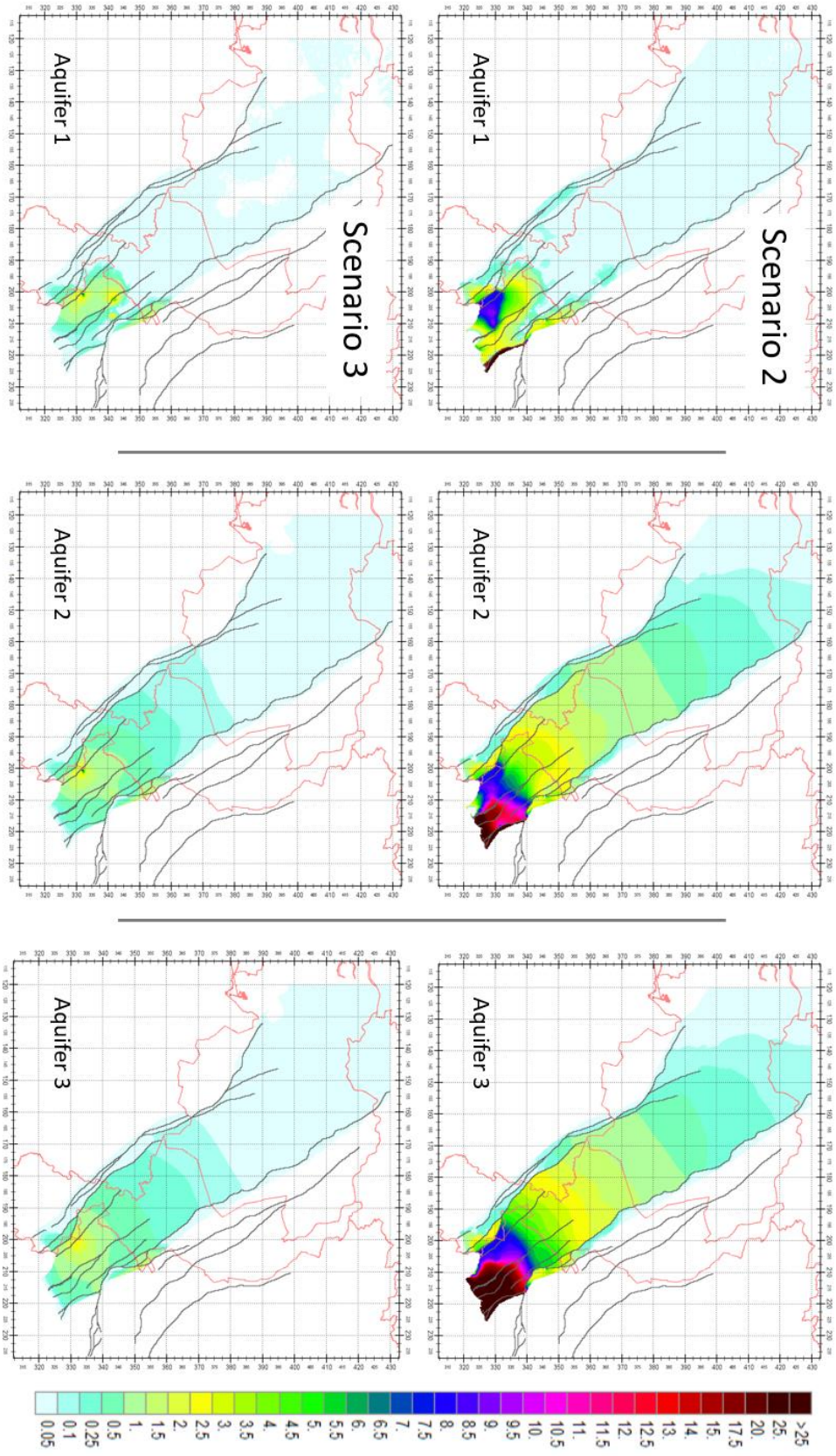

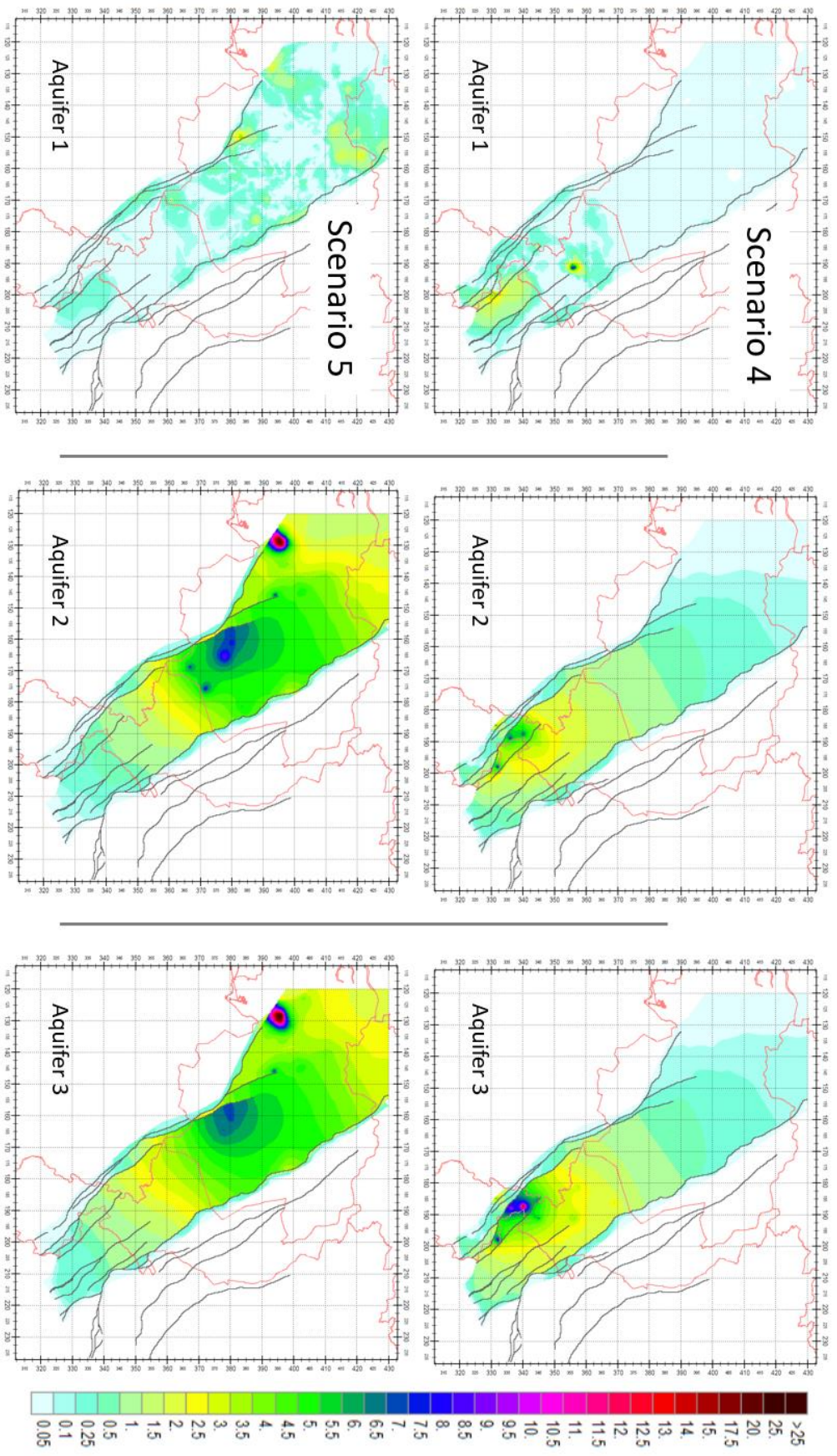
Scenario 4
Aquifer 1
Scenario 5
Aquifer 1
Aquifer 2
Aquifer 2
Aquifer 3
Aquifer 3
0.05
0.1
0.25
0.5
1.
1.5
2.
2.5
3.
3.5
4.
4.5
5.
5.5
6.
6.5
7.
7.5
8.
8.5
9.
9.5
10.
10.5
11.
11.5
12.
12.5
13.
14.
15.
17.5
20.
25.
>25

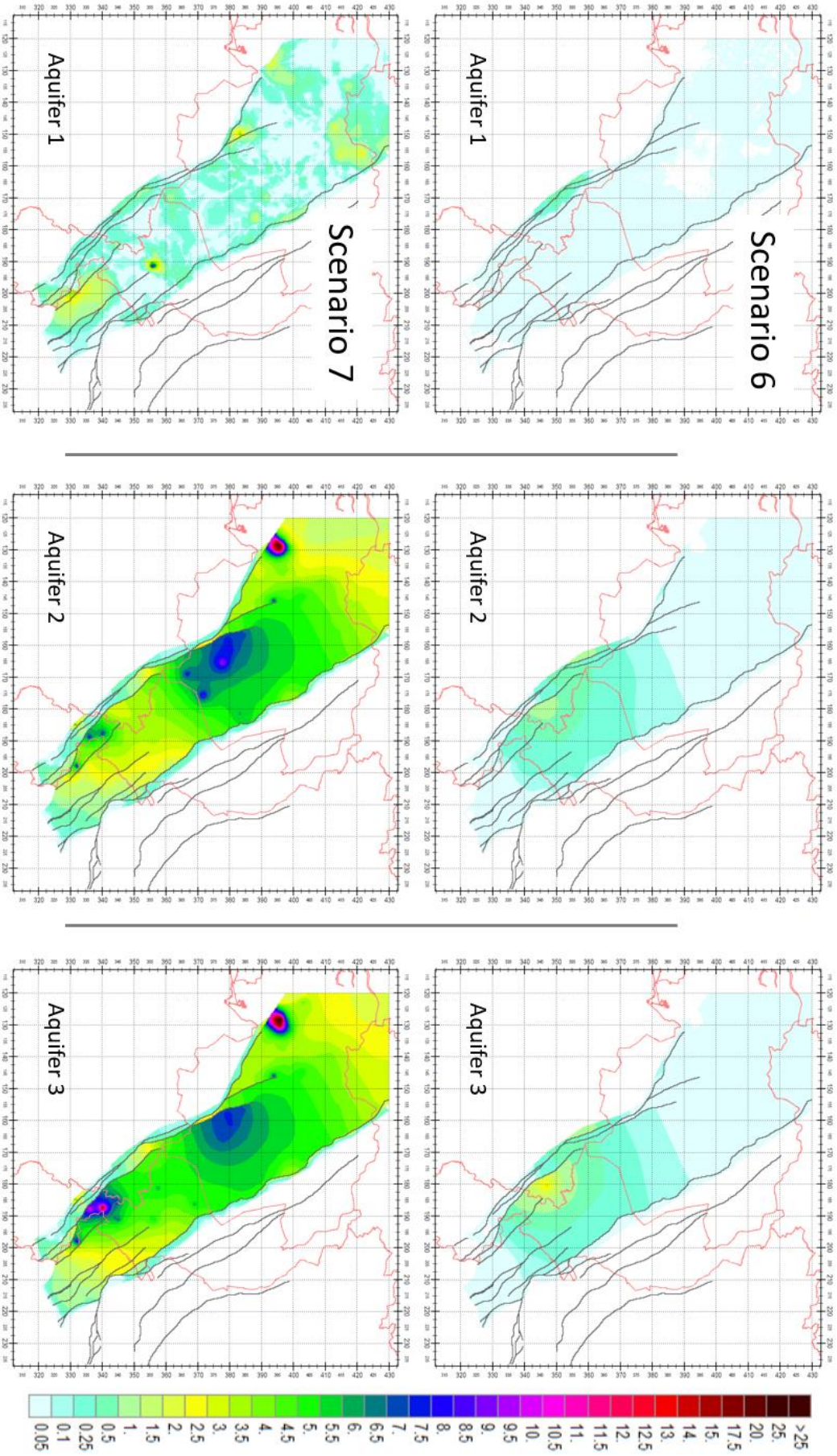
Aquifer 1
Scenario 6
Aquifer 1
Scenario 7
Aquifer 2
Aquifer 2
Aquifer 3
Aquifer 3
0.05
0.1
0.25
0.5
1.
1.5
2.
2.5
3.
3.5
4.
4.5
5.
5.5
6.
6.5
7.
7.5
8.
8.5
9.
9.5
10.
10.5
11.
11.5
12.
12.5
13.
14.
15.
17.5
20.
25.
>25

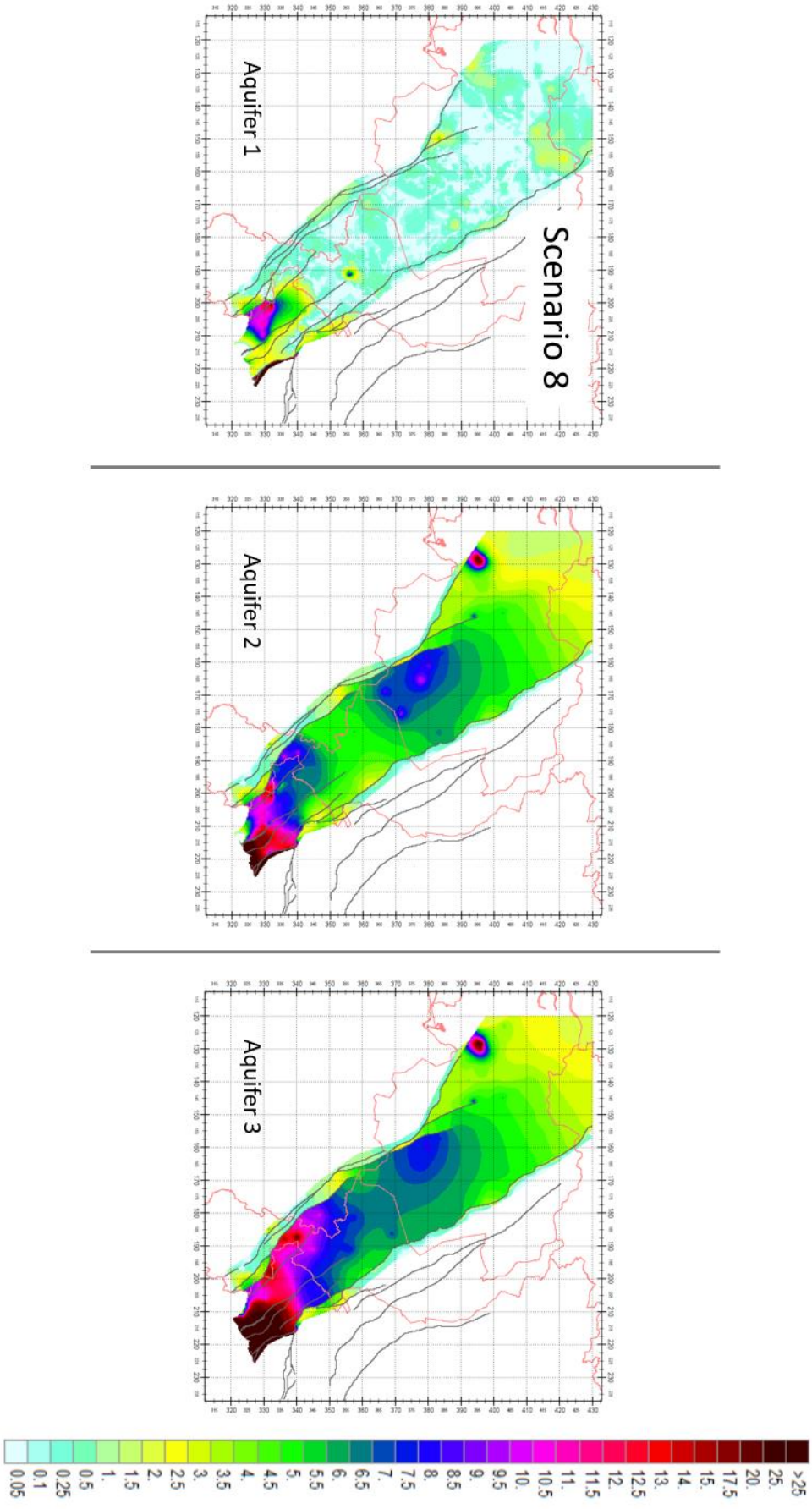
Aquifer 1
Scenario 8
Aquifer 2
Aquifer 3
0.05
0.1
0.25
0.5
1.
1.5
2.
2.5
3.
3.5
4.
4.5
5.
5.5
6.
6.5
7.
7.5
8.
8.5
9.
9.5
10.
10.5
11.
11.5
12.
12.5
13.
14.
15.
17.5
20.
25.
>25

A.10 Temporal Superposed Effects of the Scenarios

On the following figures the superposed effects of the scenarios are presented, here the “all pumping active” scenario is the baseline on which all individual effects are projected.

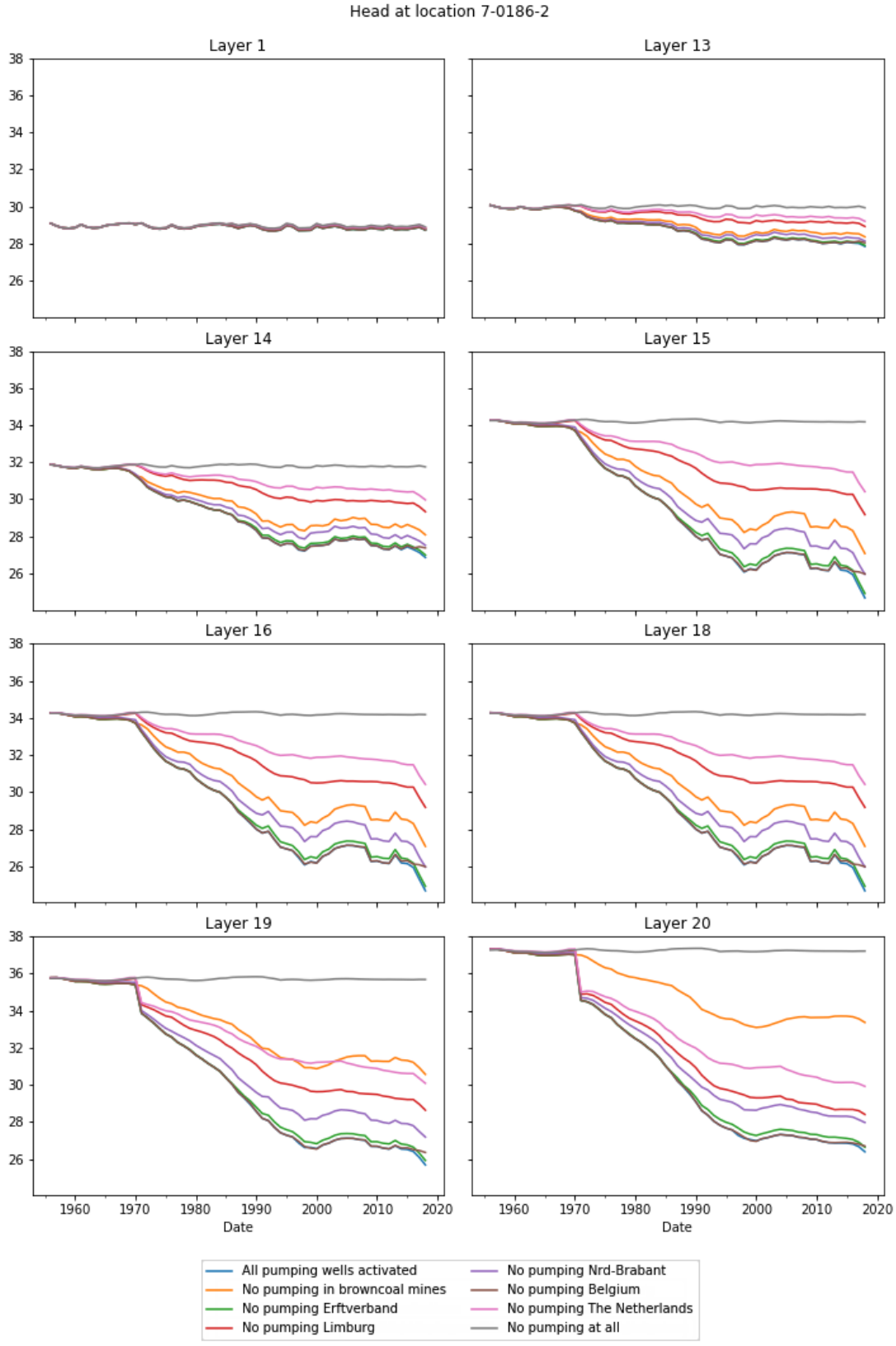

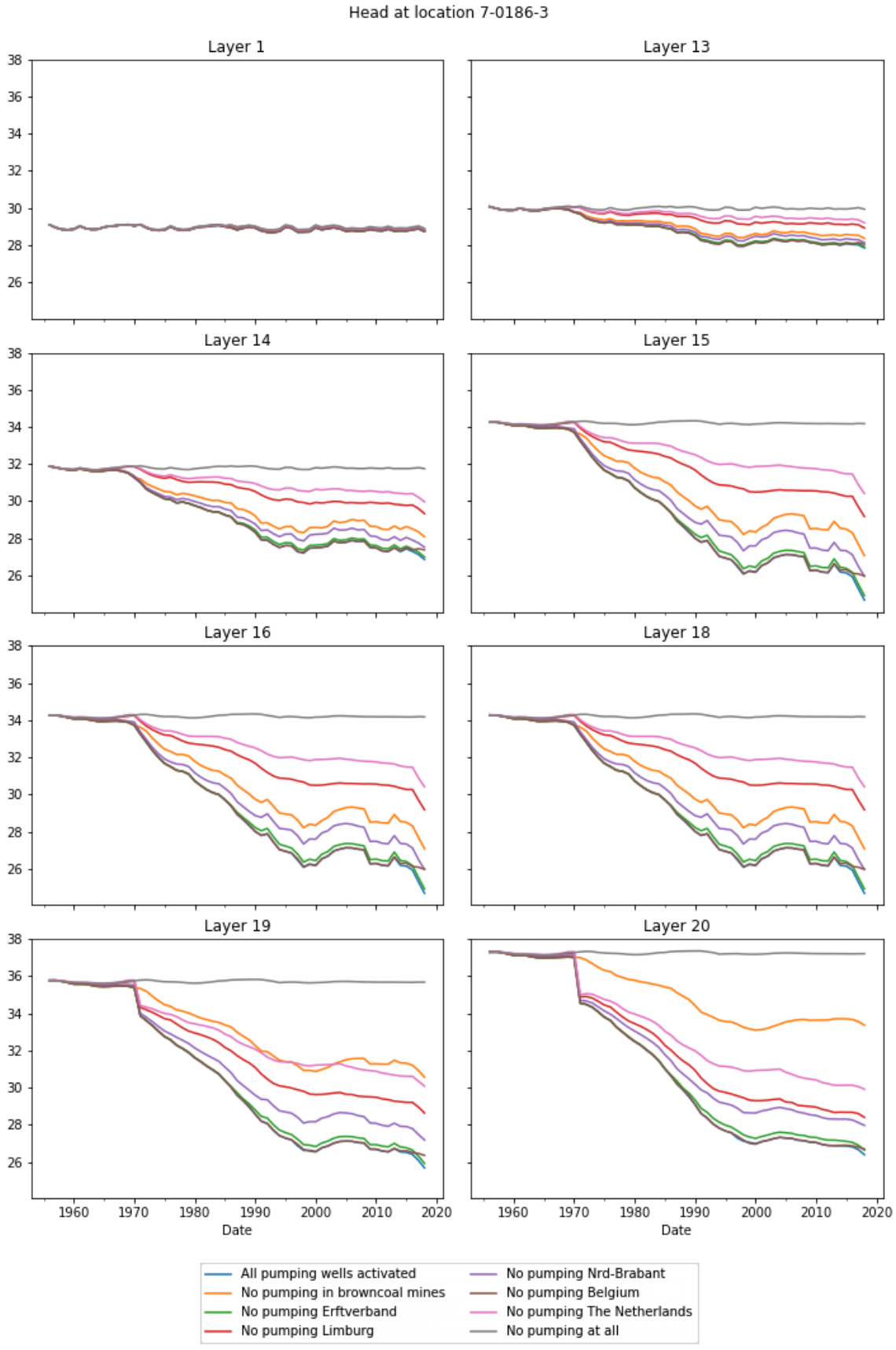
Head at location 7-0186-3
Layer 1
Layer 13
Layer 14
Layer 15
Layer 16
Layer 18
Layer 19
Layer 20
38
36
34
32
30
28
26
1960
1970
1980
1990
2000
2010
2020
Date
All pumping wells activated
No pumping in browncoal mines
No pumping Erftverband
No pumping Limburg
No pumping Nrd-Brabant
No pumping Belgium
No pumping The Netherlands
No pumping at all

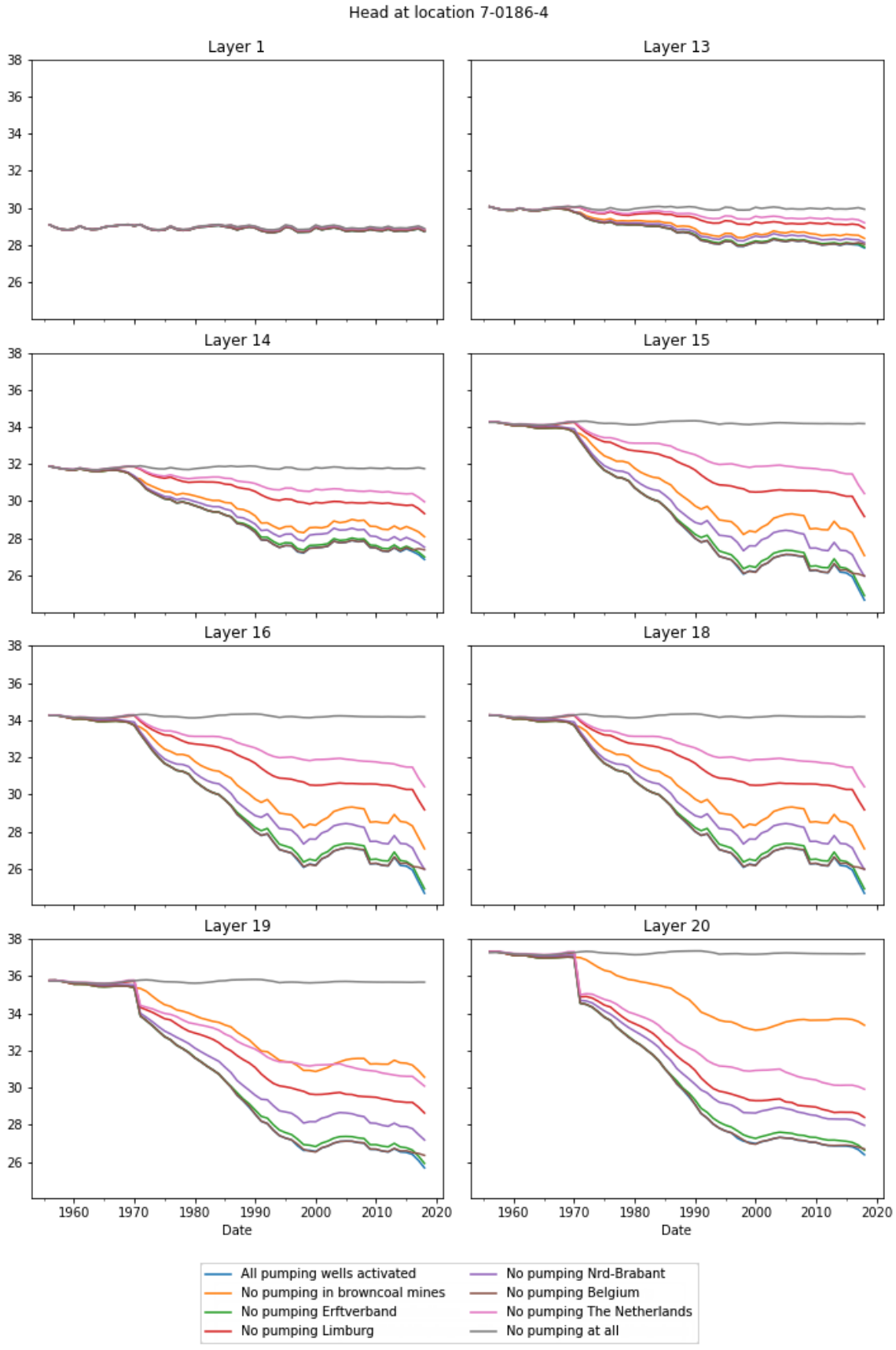
Head at location 7-0186-4
Layer 1
Layer 13
Layer 14
Layer 15
Layer 16
Layer 18
Layer 19
Layer 20
38
36
34
32
30
28
26
1960
1970
1980
1990
2000
2010
2020
Date
All pumping wells activated
No pumping in browncoal mines
No pumping Erftverband
No pumping Limburg
No pumping Nrd-Brabant
No pumping Belgium
No pumping The Netherlands
No pumping at all

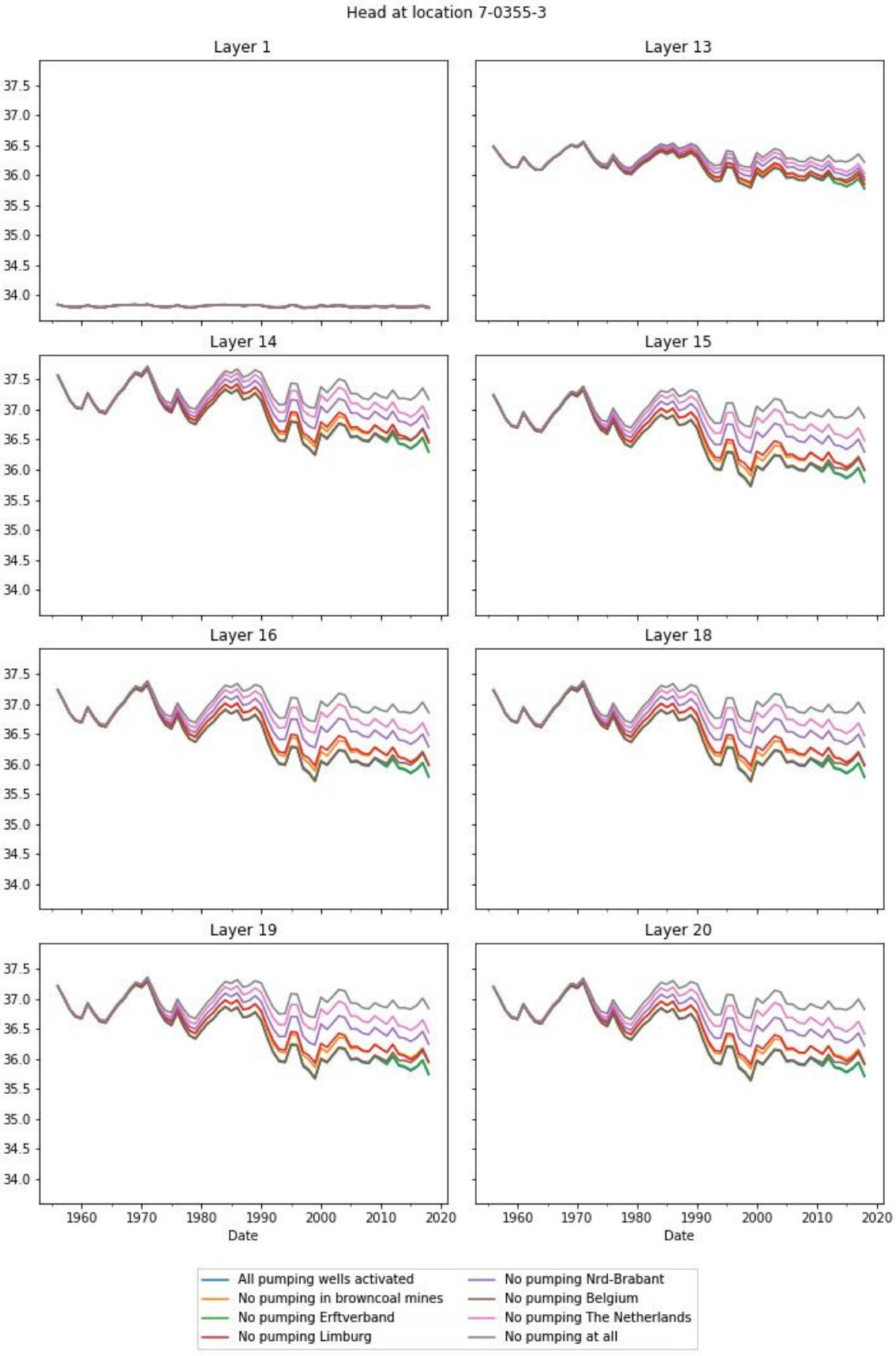
Head at location 7-0355-3
Layer 1
Layer 13
Layer 14
Layer 15
Layer 16
Layer 18
Layer 19
Layer 20
37.5
37.0
36.5
36.0
35.5
35.0
34.5
34.0
1960
1970
1980
1990
2000
2010
2020
Date
All pumping wells activated
No pumping in browncoal mines
No pumping Erftverband
No pumping Limburg
No pumping Nrd-Brabant
No pumping Belgium
No pumping The Netherlands
No pumping at all

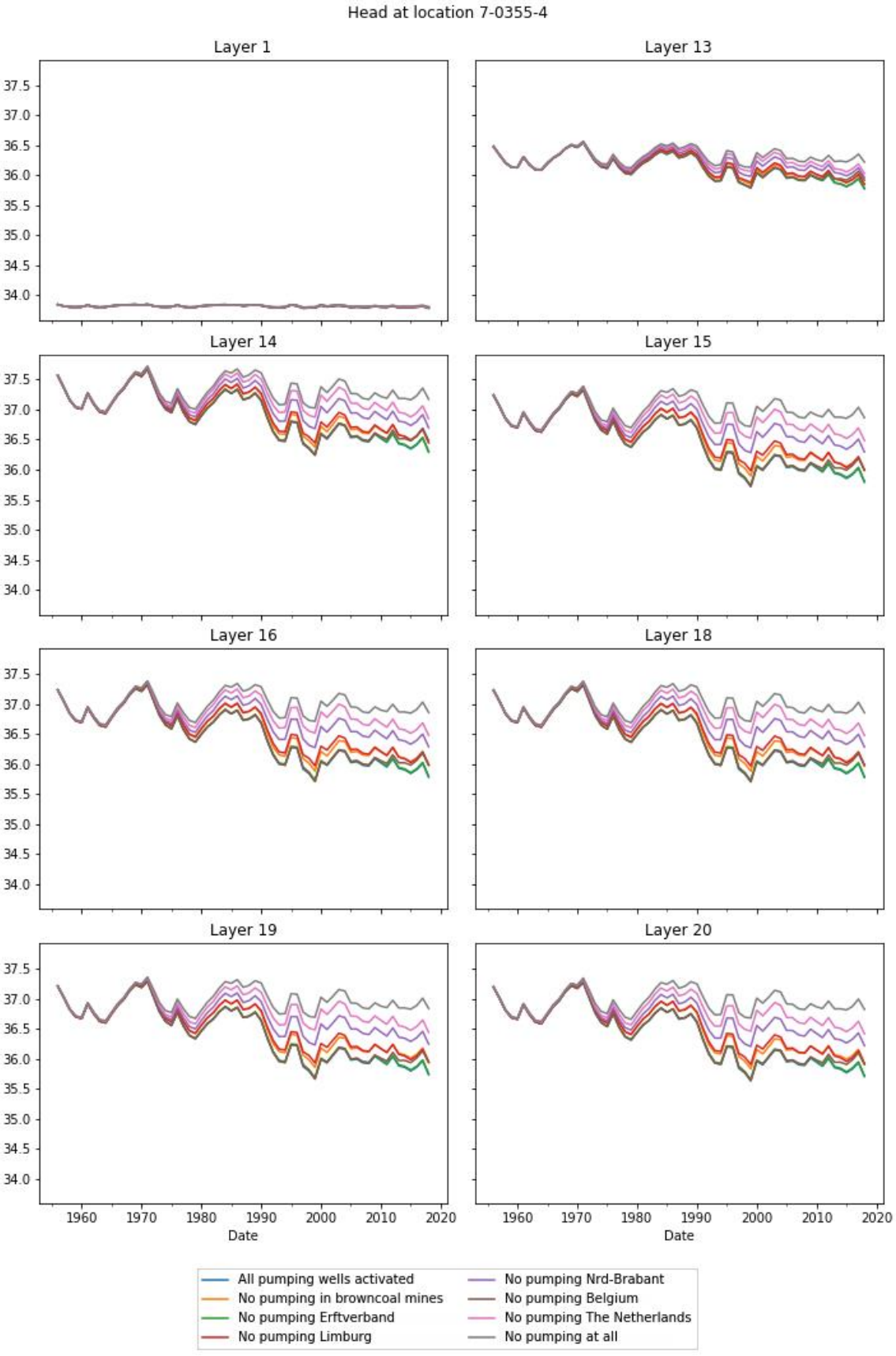
Head at location 7-0355-4
Layer 1
Layer 13
Layer 14
Layer 15
Layer 16
Layer 18
Layer 19
Layer 20
37.5
37.0
36.5
36.0
35.5
35.0
34.5
34.0
1960
1970
1980
1990
2000
2010
2020
Date
All pumping wells activated
No pumping in browncoal mines
No pumping Erftverband
No pumping Limburg
No pumping Nrd-Brabant
No pumping Belgium
No pumping The Netherlands
No pumping at all

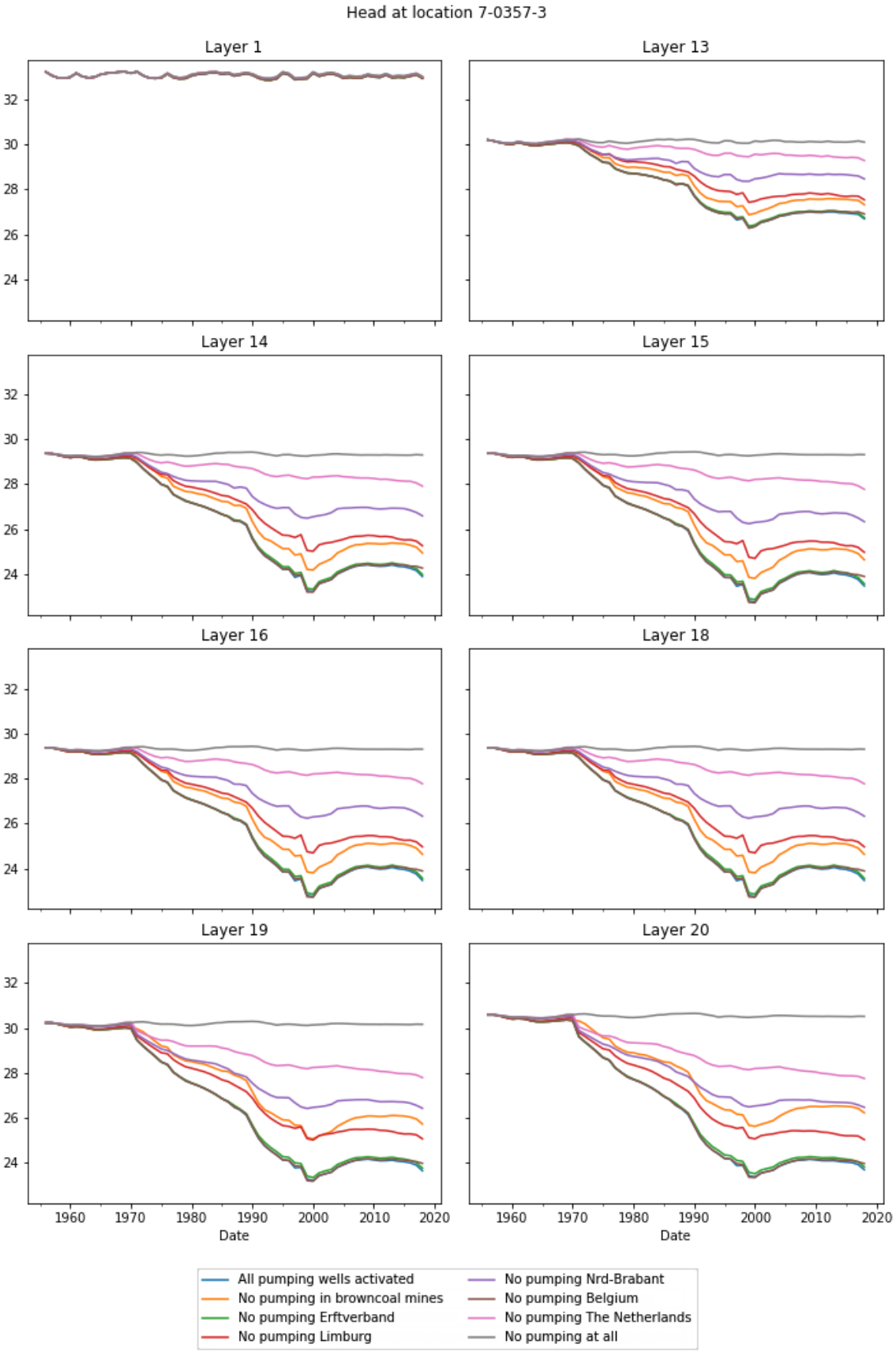
Head at location 7-0357-3
Layer 1
Layer 13
Layer 14
Layer 15
Layer 16
Layer 18
Layer 19
Layer 20
32
30
28
26
24
1960
1970
1980
1990
2000
2010
2020
Date
All pumping wells activated
No pumping in browncoal mines
No pumping Erftverband
No pumping Limburg
No pumping Nrd-Brabant
No pumping Belgium
No pumping The Netherlands
No pumping at all

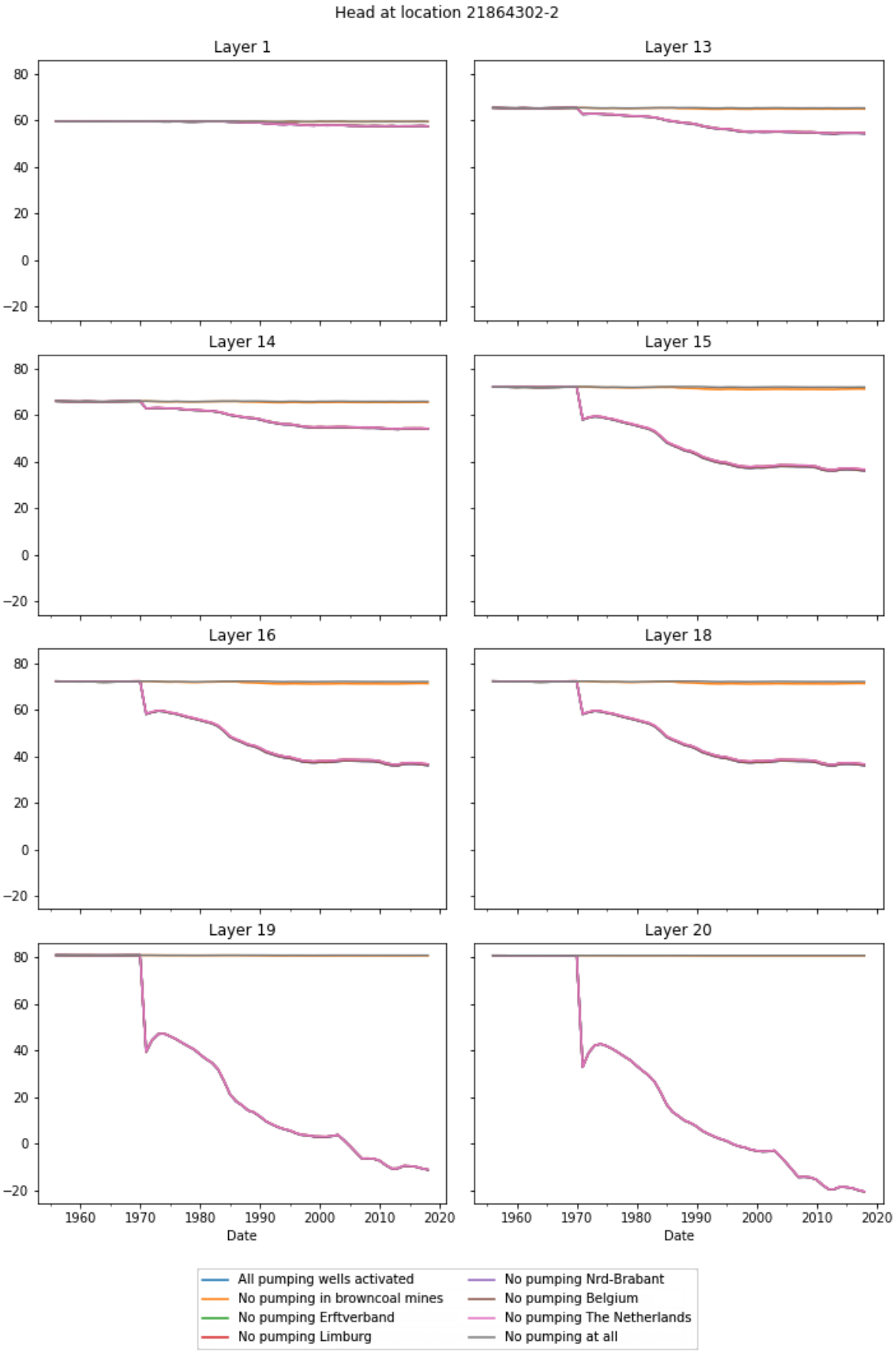
Head at location 21864302-2
Layer 1
Layer 13
Layer 14
Layer 15
Layer 16
Layer 18
Layer 19
Layer 20
80
60
40
20
0
−20
1960
1970
1980
1990
2000
2010
2020
Date
All pumping wells activated
No pumping in browncoal mines
No pumping Erftverband
No pumping Limburg
No pumping Nrd-Brabant
No pumping Belgium
No pumping The Netherlands
No pumping at all

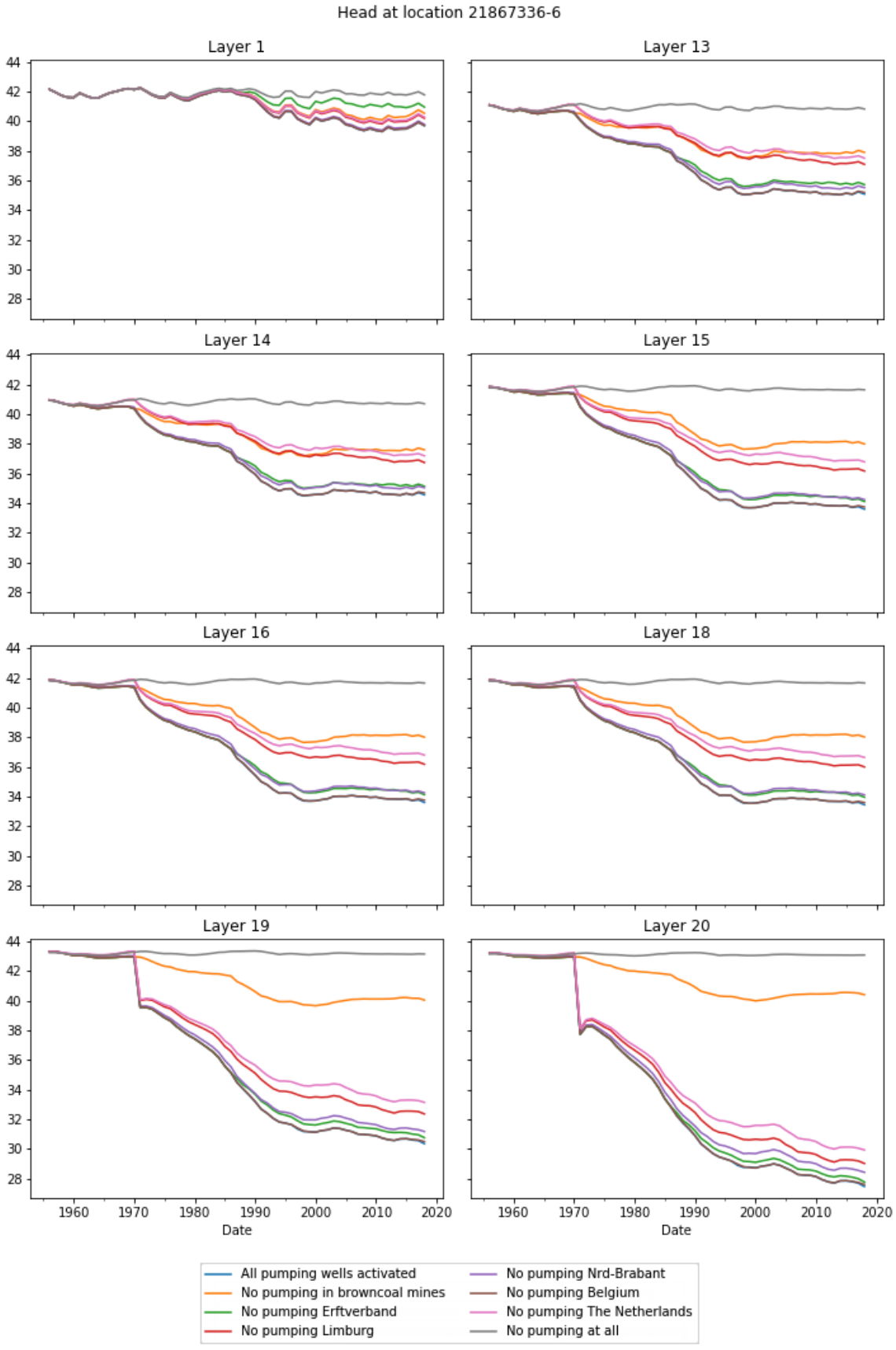
Head at location 21867336-6
Layer 1
Layer 13
Layer 14
Layer 15
Layer 16
Layer 18
Layer 19
Layer 20
44
42
40
38
36
34
32
30
28
1960
1970
1980
1990
2000
2010
2020
Date
All pumping wells activated
No pumping in browncoal mines
No pumping Erftverband
No pumping Limburg
No pumping Nrd-Brabant
No pumping Belgium
No pumping The Netherlands
No pumping at all

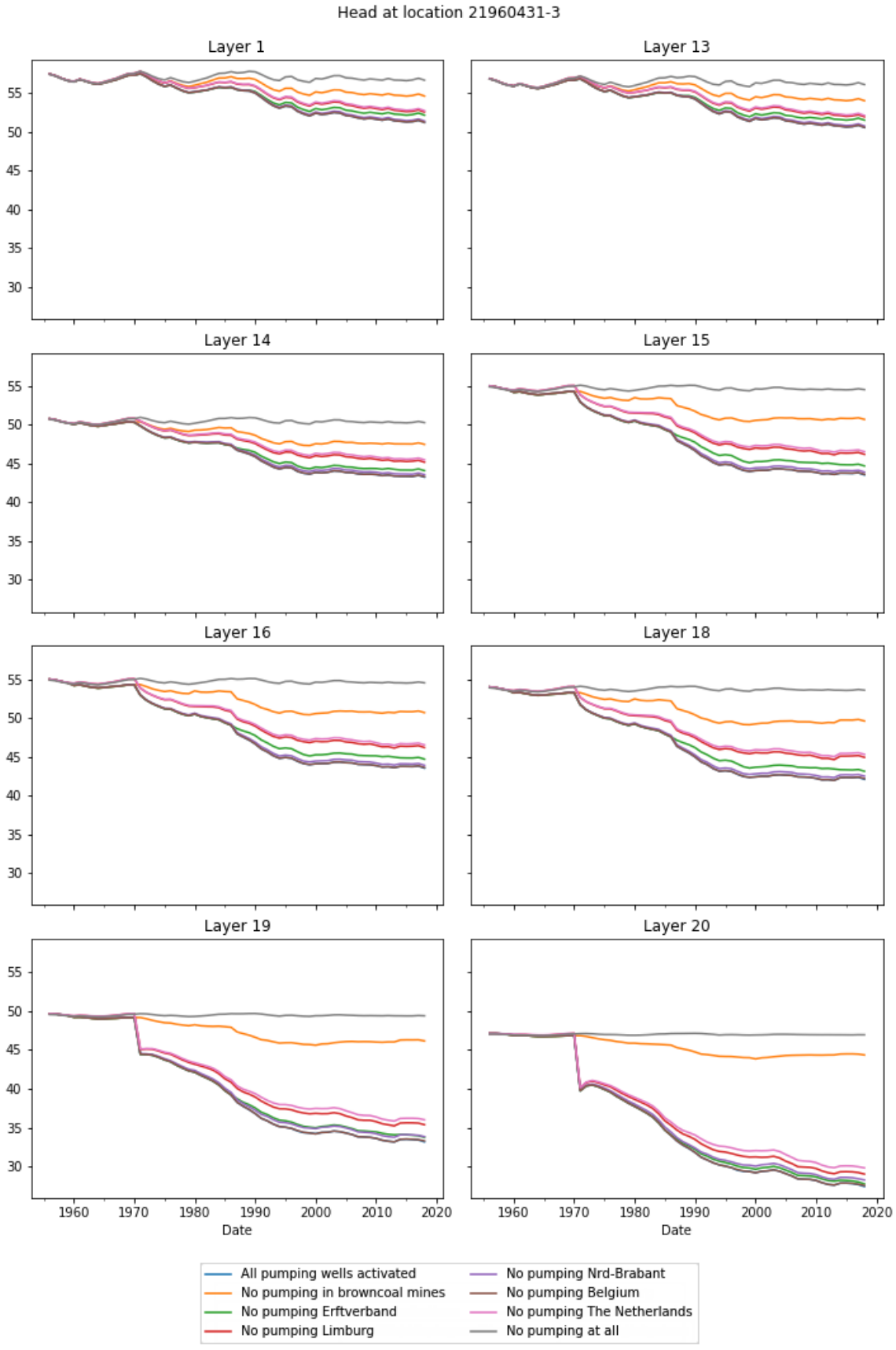
Head at location 21960431-3
Layer 1
Layer 13
Layer 14
Layer 15
Layer 16
Layer 18
Layer 19
Layer 20
55
50
45
40
35
30
1960
1970
1980
1990
2000
2010
2020
Date
All pumping wells activated
No pumping in browncoal mines
No pumping Erftverband
No pumping Limburg
No pumping Nrd-Brabant
No pumping Belgium
No pumping The Netherlands
No pumping at all

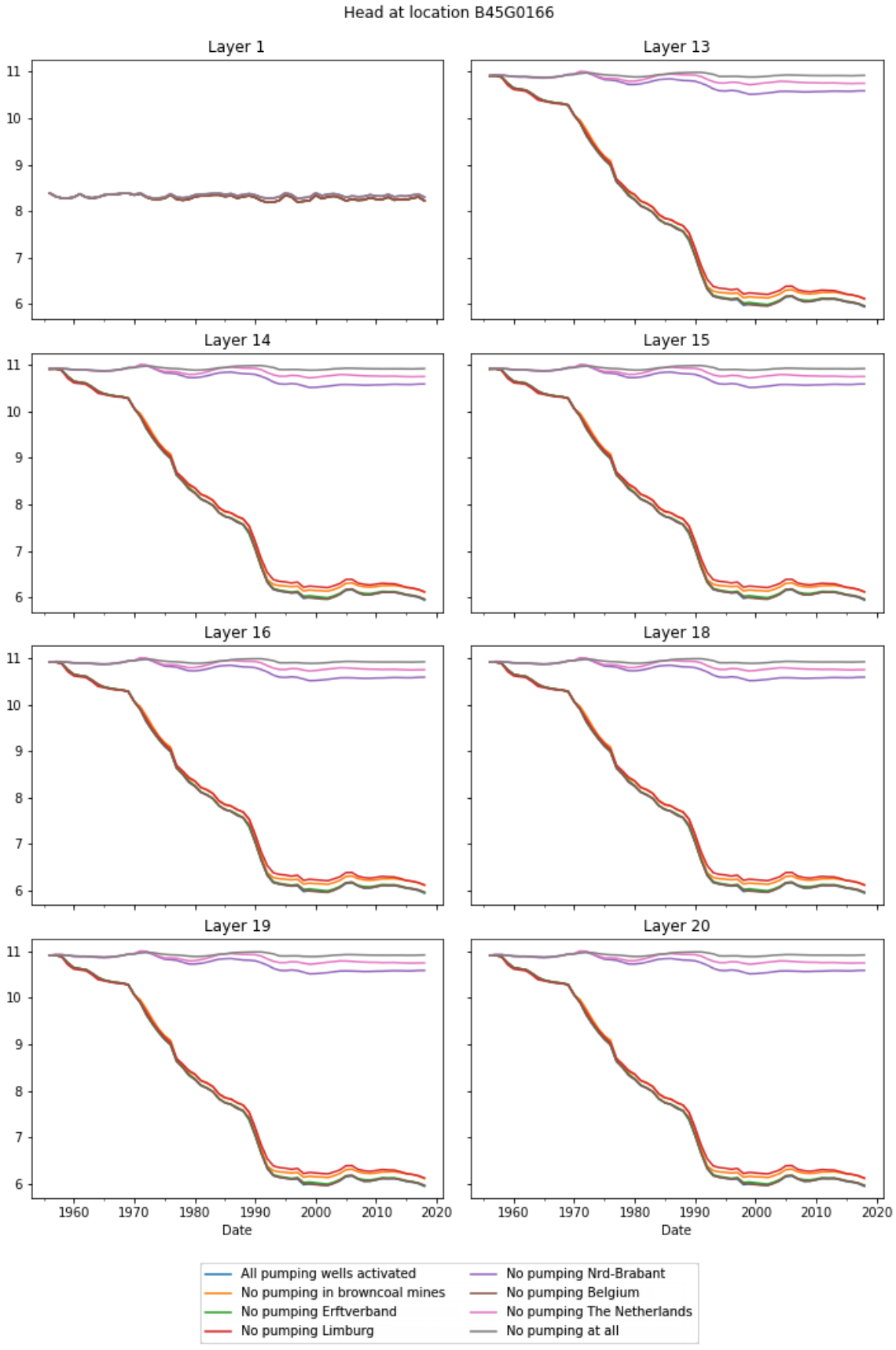
Head at location B45G0166
Layer 1
Layer 13
Layer 14
Layer 15
Layer 16
Layer 18
Layer 19
Layer 20
11
10
9
8
7
6
1960
1970
1980
1990
2000
2010
2020
Date
All pumping wells activated
No pumping in browncoal mines
No pumping Erftverband
No pumping Limburg
No pumping Nrd-Brabant
No pumping Belgium
No pumping The Netherlands
No pumping at all

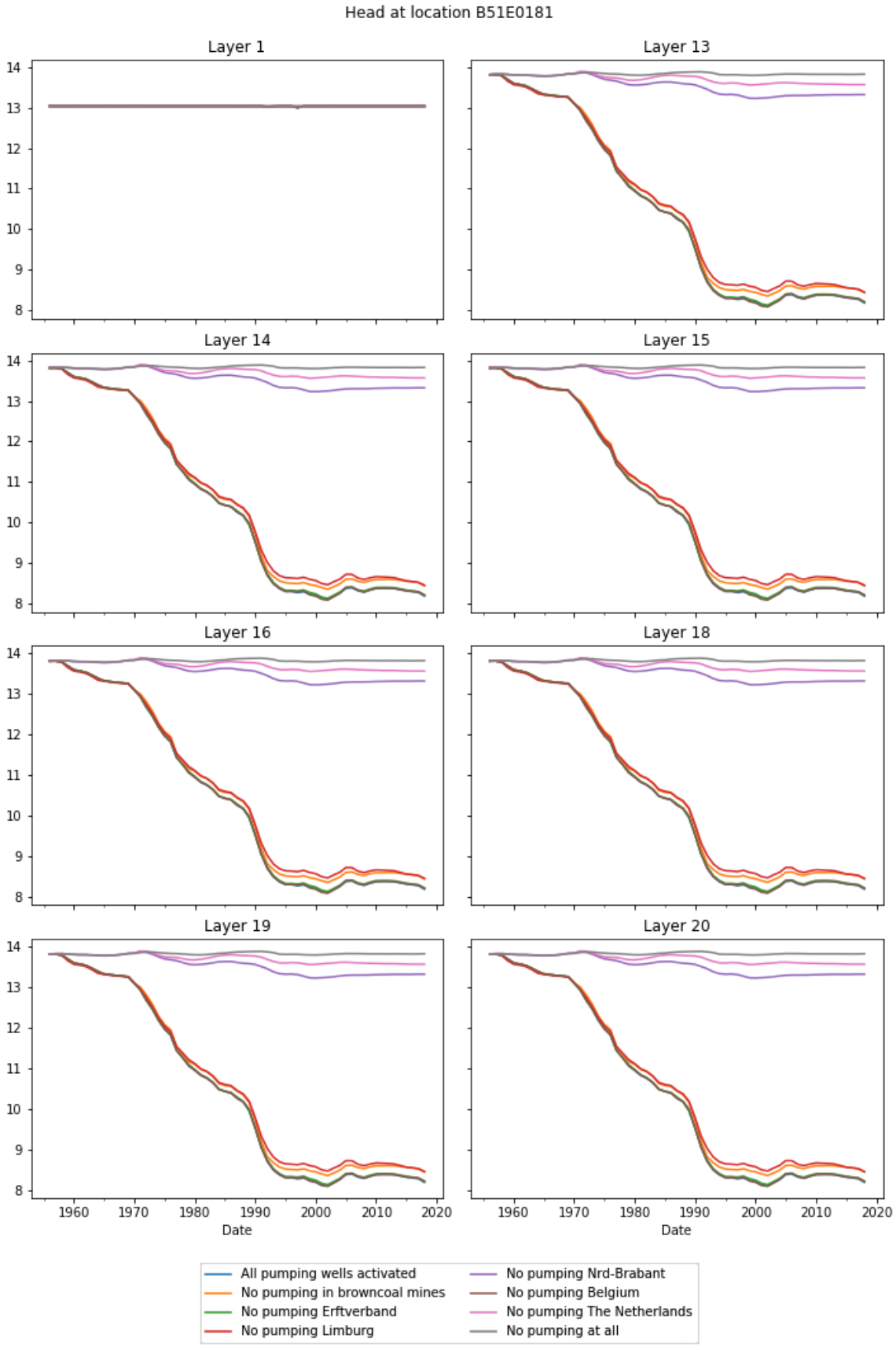
Head at location B51E0181
Layer 1
Layer 13
Layer 14
Layer 15
Layer 16
Layer 18
Layer 19
Layer 20
14
13
12
11
10
9
8
1960
1970
1980
1990
2000
2010
2020
Date
All pumping wells activated
No pumping in browncoal mines
No pumping Erftverband
No pumping Limburg
No pumping Nrd-Brabant
No pumping Belgium
No pumping The Netherlands
No pumping at all

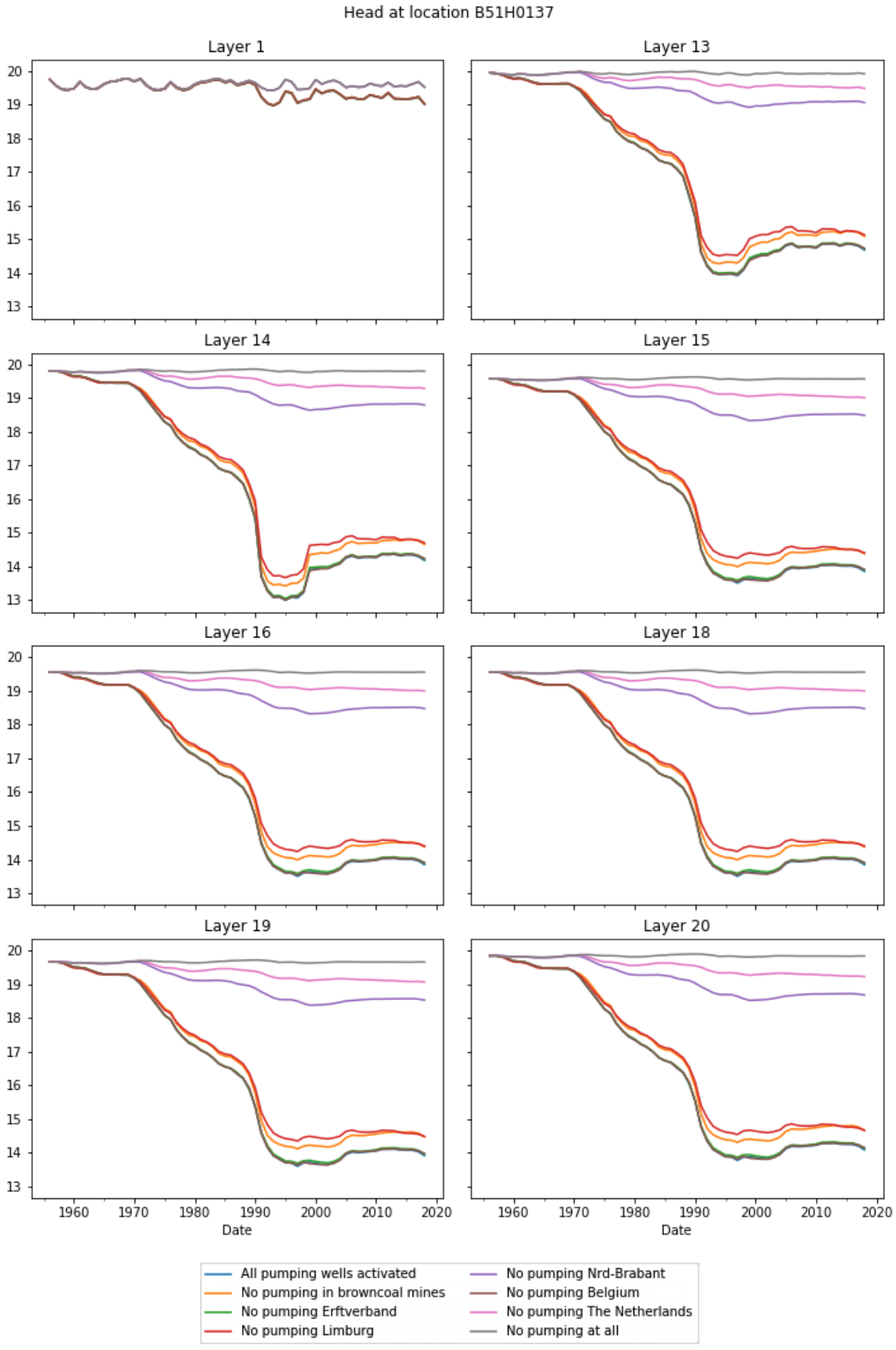
Head at location B51H0137
Layer 1
Layer 13
Layer 14
Layer 15
Layer 16
Layer 18
Layer 19
Layer 20
20
19
18
17
16
15
14
13
1960
1970
1980
1990
2000
2010
2020
Date
All pumping wells activated
No pumping in browncoal mines
No pumping Erftverband
No pumping Limburg
No pumping Nrd-Brabant
No pumping Belgium
No pumping The Netherlands
No pumping at all

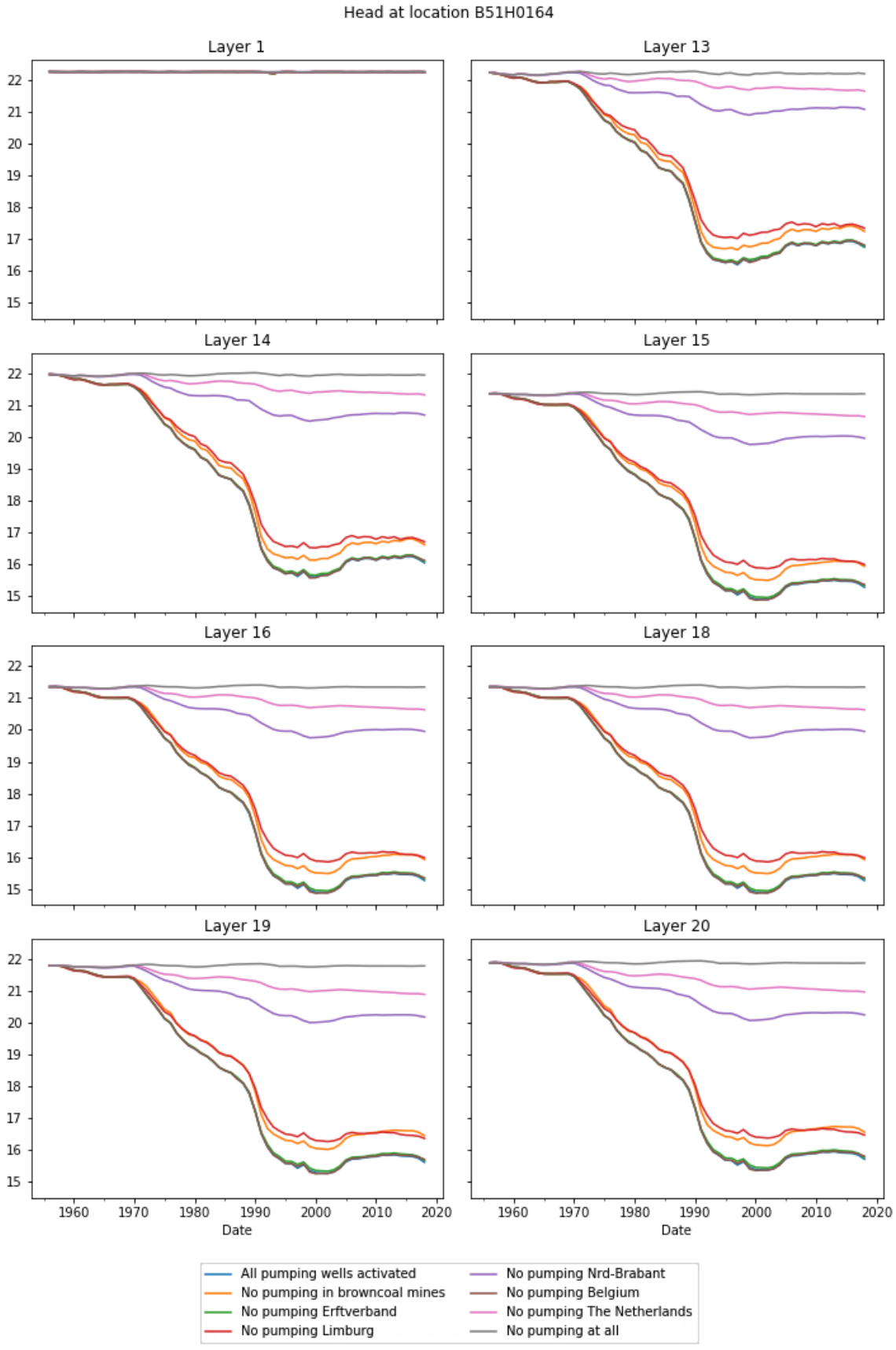
Head at location B51H0164
Layer 1
Layer 13
Layer 14
Layer 15
Layer 16
Layer 18
Layer 19
Layer 20
22
21
20
19
18
17
16
15
1960
1970
1980
1990
2000
2010
2020
Date
All pumping wells activated
No pumping in browncoal mines
No pumping Erftverband
No pumping Limburg
No pumping Nrd-Brabant
No pumping Belgium
No pumping The Netherlands
No pumping at all

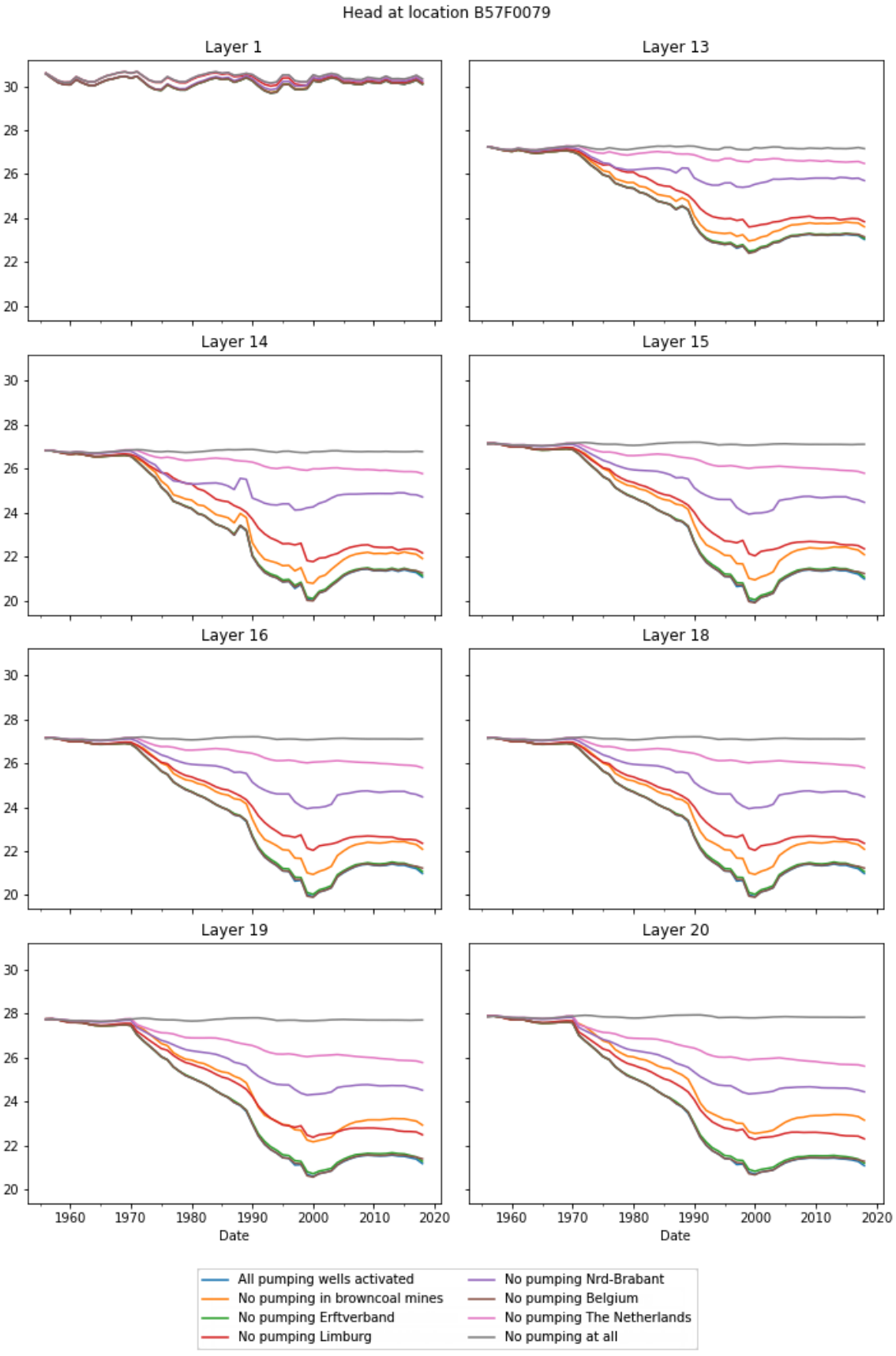
Head at location B57F0079
Layer 1
Layer 13
Layer 14
Layer 15
Layer 16
Layer 18
Layer 19
Layer 20
30
28
26
24
22
20
1960
1970
1980
1990
2000
2010
2020
Date
All pumping wells activated
No pumping in browncoal mines
No pumping Erftverband
No pumping Limburg
No pumping Nrd-Brabant
No pumping Belgium
No pumping The Netherlands
No pumping at all

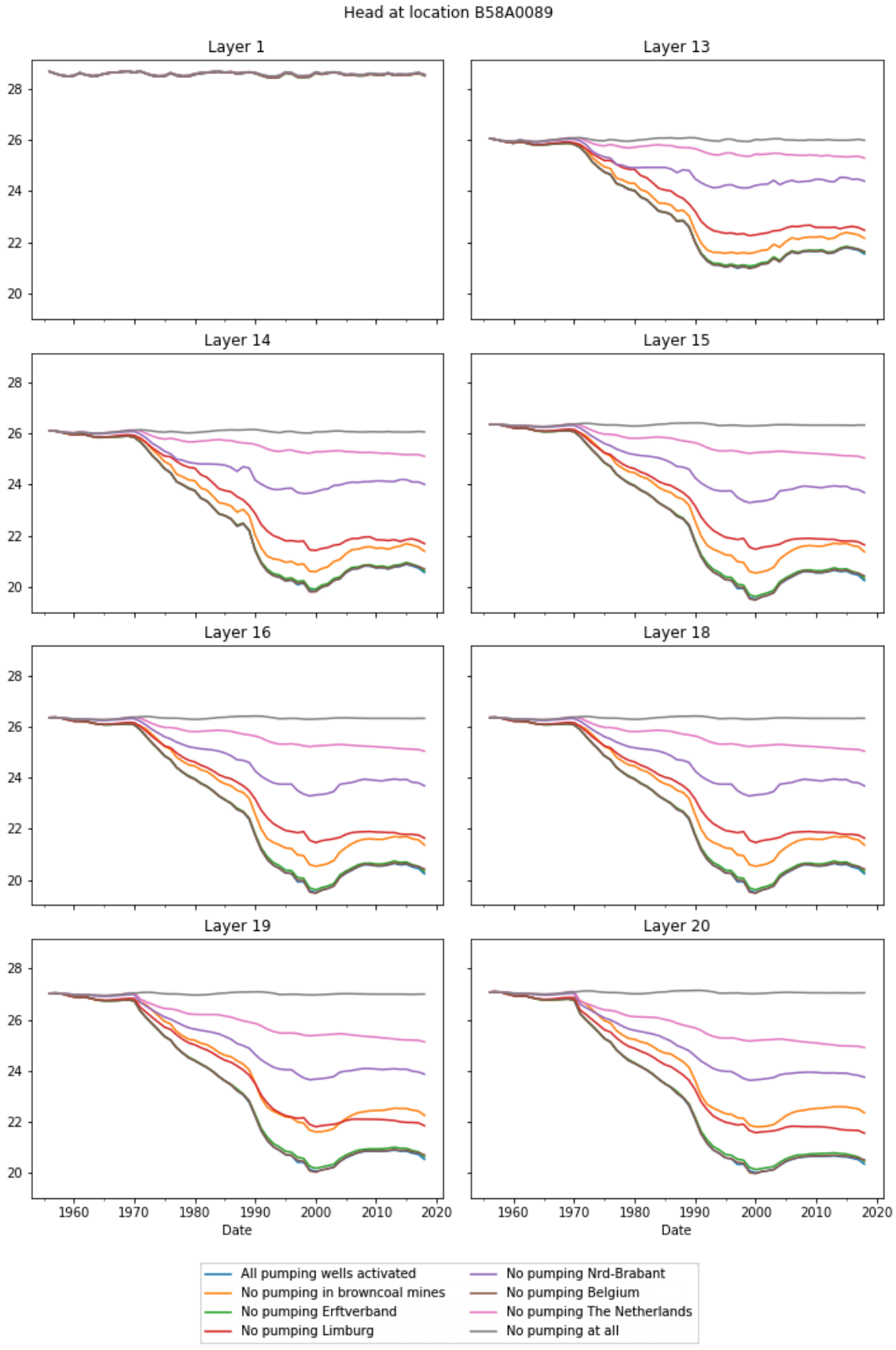
Head at location B58A0089
Layer 1
Layer 13
Layer 14
Layer 15
Layer 16
Layer 18
Layer 19
Layer 20
28
26
24
22
20
1960
1970
1980
1990
2000
2010
2020
Date
All pumping wells activated
No pumping in browncoal mines
No pumping Erftverband
No pumping Limburg
No pumping Nrd-Brabant
No pumping Belgium
No pumping The Netherlands
No pumping at all

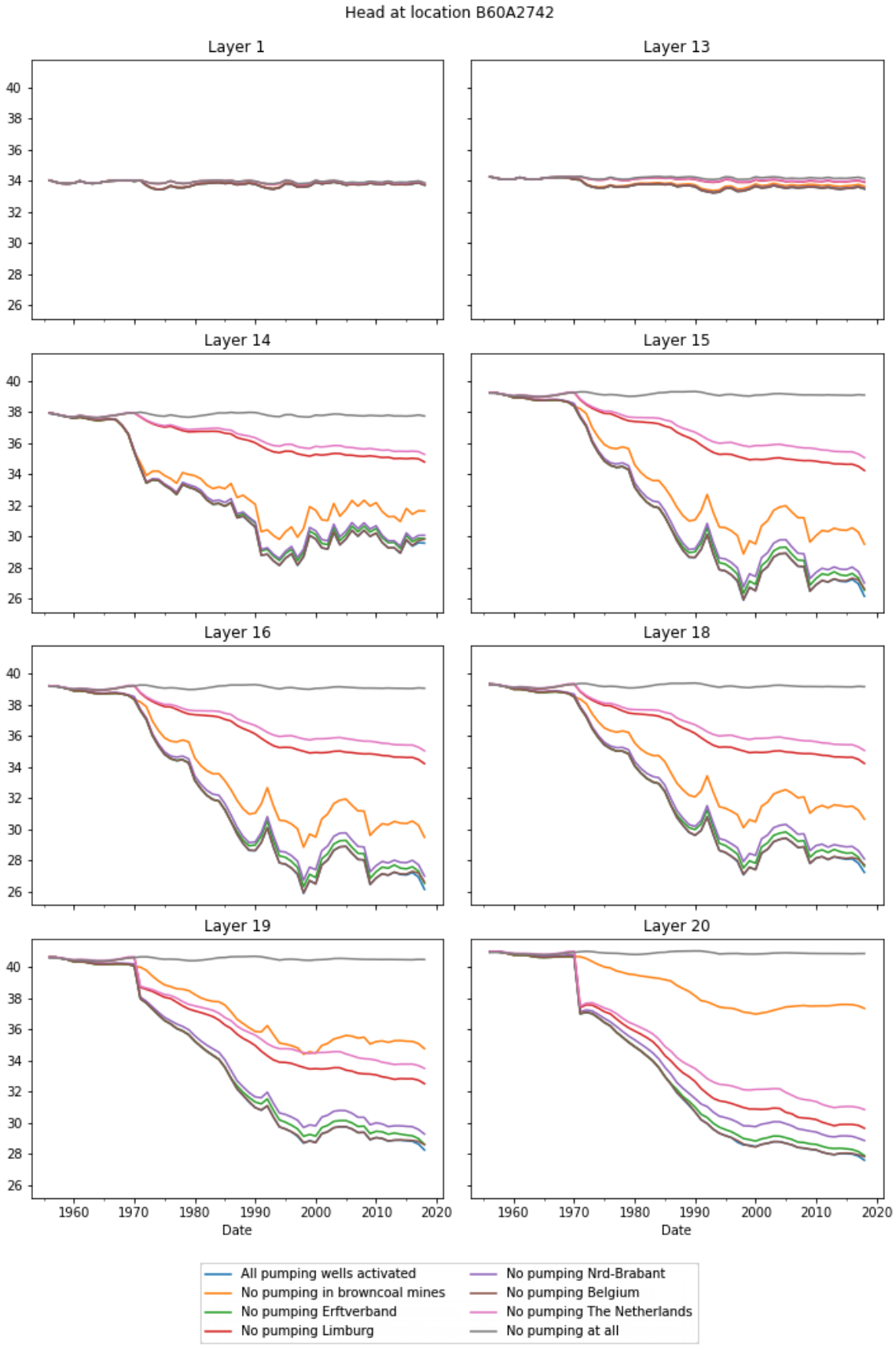
Head at location B60A2742
Layer 1
Layer 13
Layer 14
Layer 15
Layer 16
Layer 18
Layer 19
Layer 20
40
38
36
34
32
30
28
26
1960
1970
1980
1990
2000
2010
2020
Date
All pumping wells activated
No pumping in browncoal mines
No pumping Erftverband
No pumping Limburg
No pumping Nrd-Brabant
No pumping Belgium
No pumping The Netherlands
No pumping at all

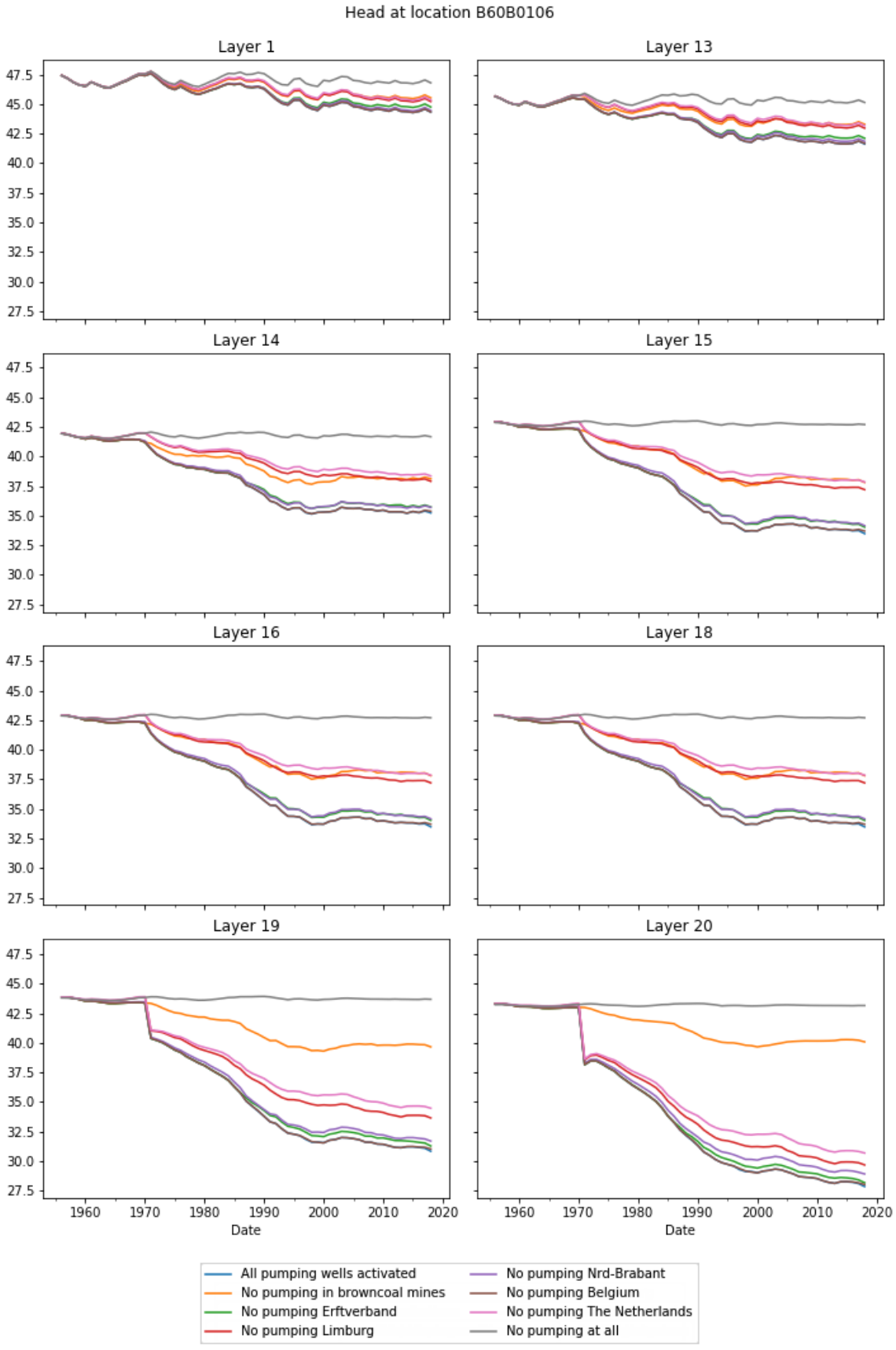
Head at location B60B0106
Layer 1
Layer 13
Layer 14
Layer 15
Layer 16
Layer 18
Layer 19
Layer 20
47.5
45.0
42.5
40.0
37.5
35.0
32.5
30.0
27.5
1960
1970
1980
1990
2000
2010
2020
Date
All pumping wells activated
No pumping in browncoal mines
No pumping Erftverband
No pumping Limburg
No pumping Nrd-Brabant
No pumping Belgium
No pumping The Netherlands
No pumping at all

A.11 Temporal Net Effects of the Scenarios

On the following figures the mutual effects of the scenarios are presented, here the “all pumping active” scenario is the baseline on which all individual effects are projected.

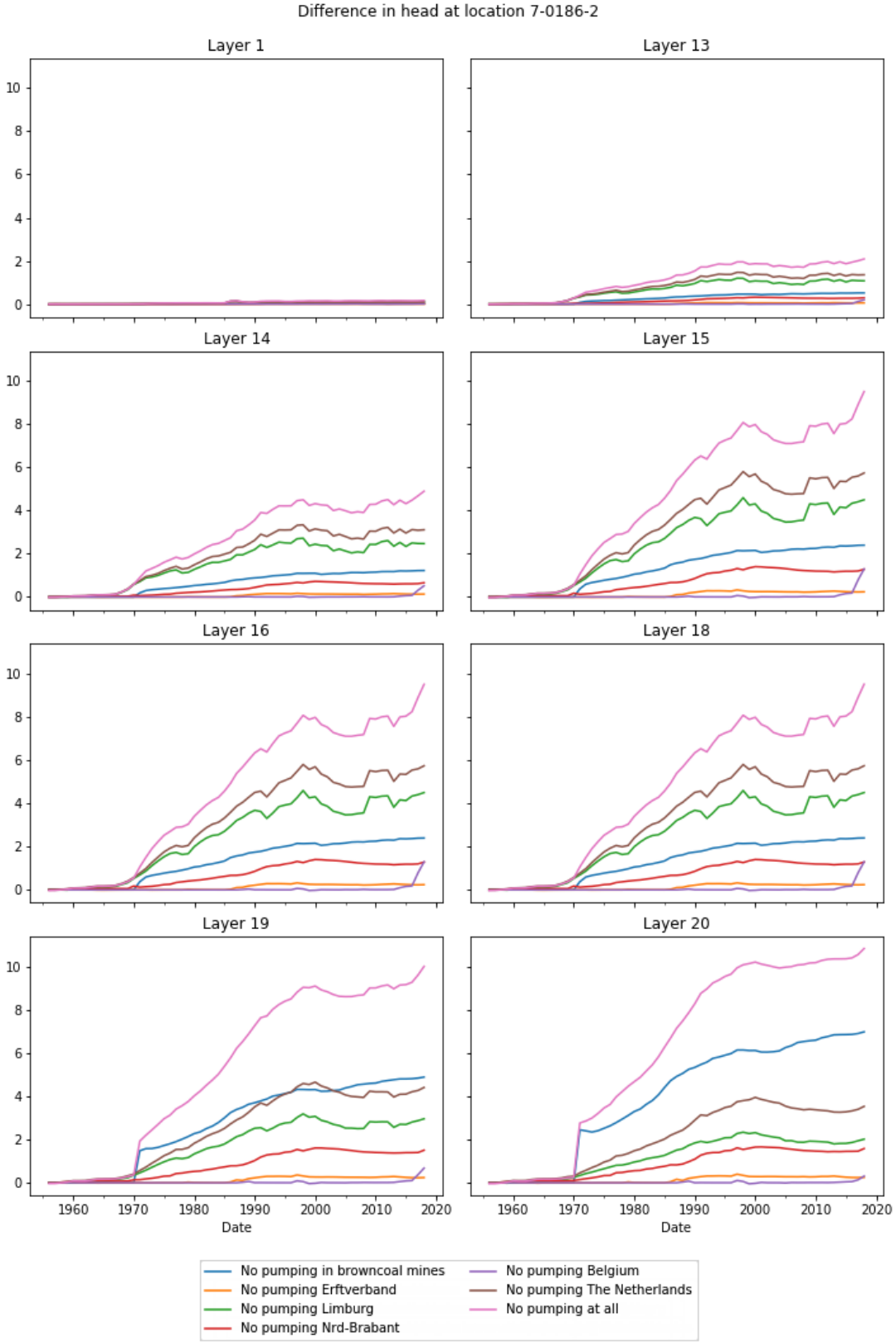

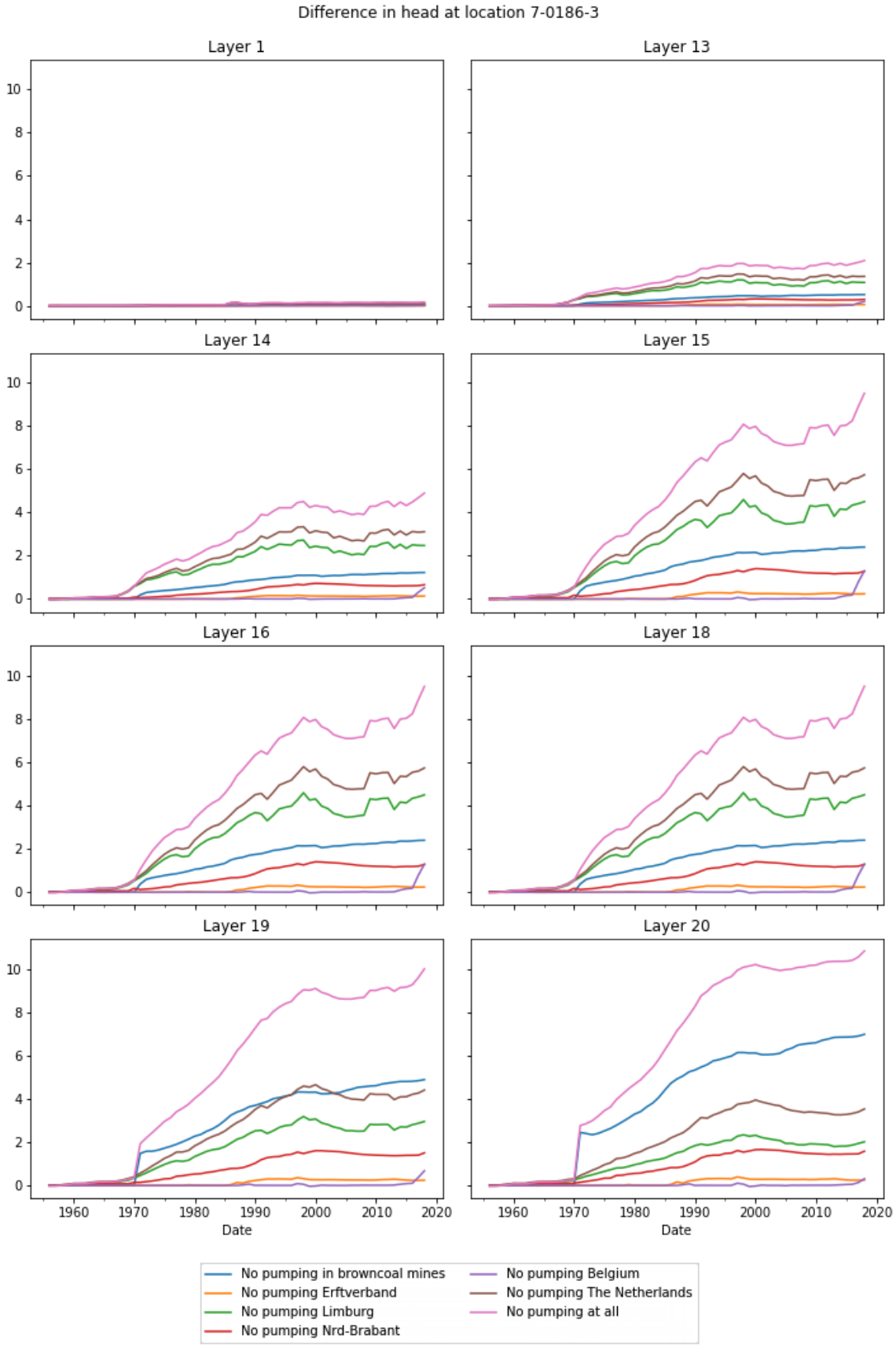
Difference in head at location 7-0186-3
Layer 1
Layer 13
Layer 14
Layer 15
Layer 16
Layer 18
Layer 19
Layer 20
0
2
4
6
8
10
1960
1970
1980
1990
2000
2010
2020
Date
No pumping in browncoal mines
No pumping Erftverband
No pumping Limburg
No pumping Nrd-Brabant
No pumping Belgium
No pumping The Netherlands
No pumping at all

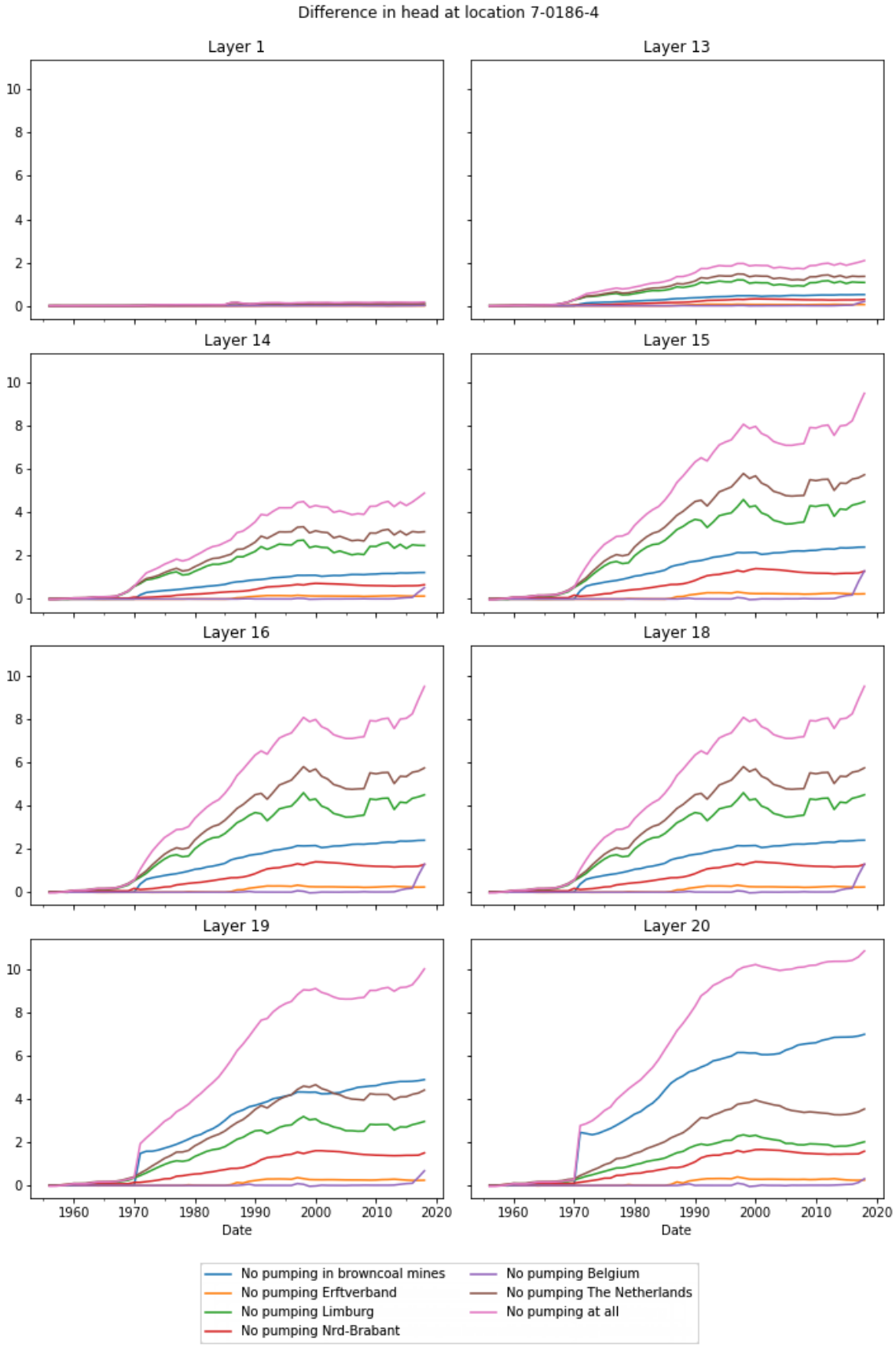
Difference in head at location 7-0186-4
Layer 1
Layer 13
Layer 14
Layer 15
Layer 16
Layer 18
Layer 19
Layer 20
0
2
4
6
8
10
1960
1970
1980
1990
2000
2010
2020
Date
No pumping in browncoal mines
No pumping Erftverband
No pumping Limburg
No pumping Nrd-Brabant
No pumping Belgium
No pumping The Netherlands
No pumping at all

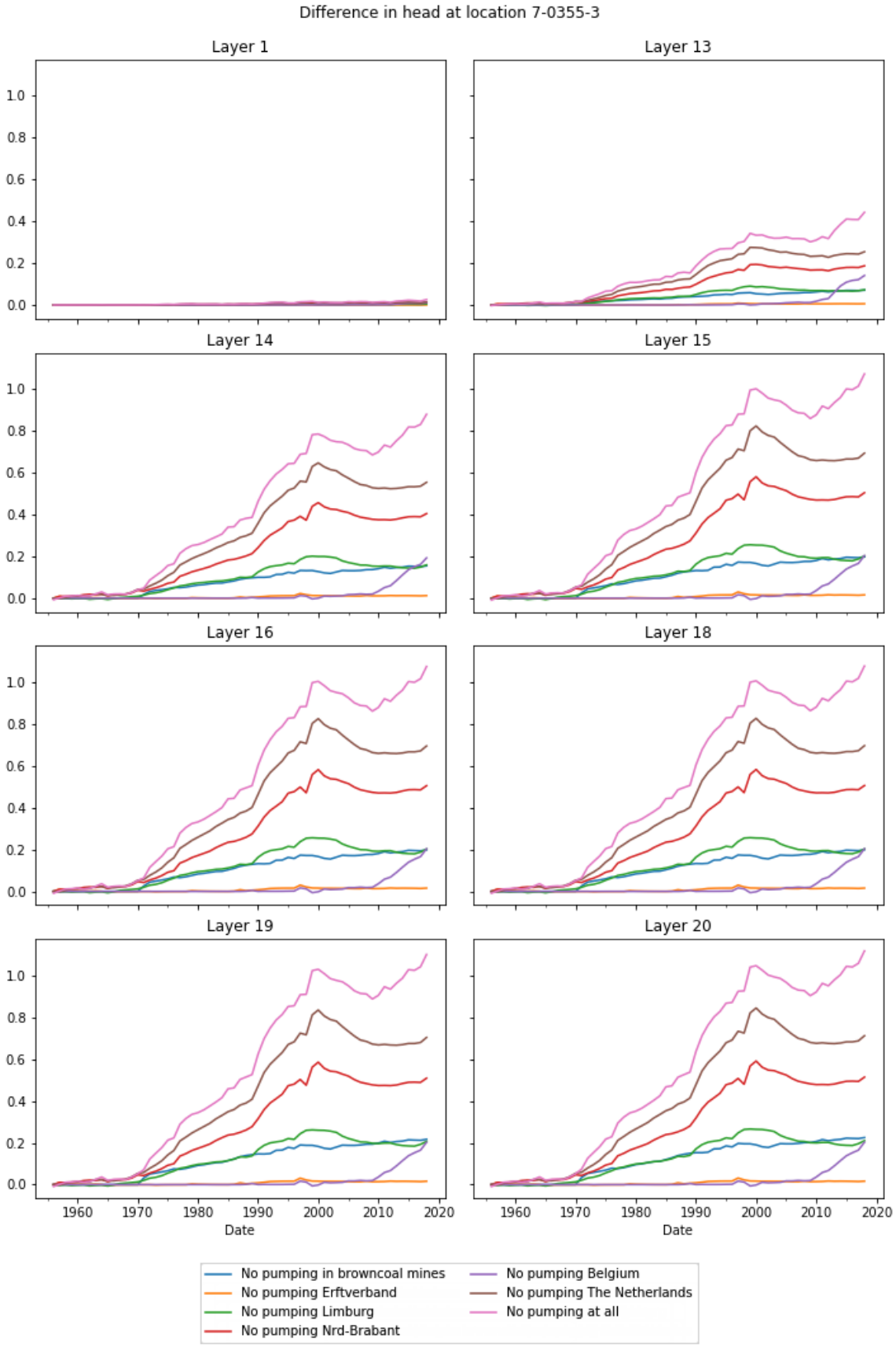
Difference in head at location 7-0355-3
Layer 1
Layer 13
Layer 14
Layer 15
Layer 16
Layer 18
Layer 19
Layer 20
1.0
0.8
0.6
0.4
0.2
0.0
1960
1970
1980
1990
2000
2010
2020
Date
No pumping in browncoal mines
No pumping Erftverband
No pumping Limburg
No pumping Nrd-Brabant
No pumping Belgium
No pumping The Netherlands
No pumping at all

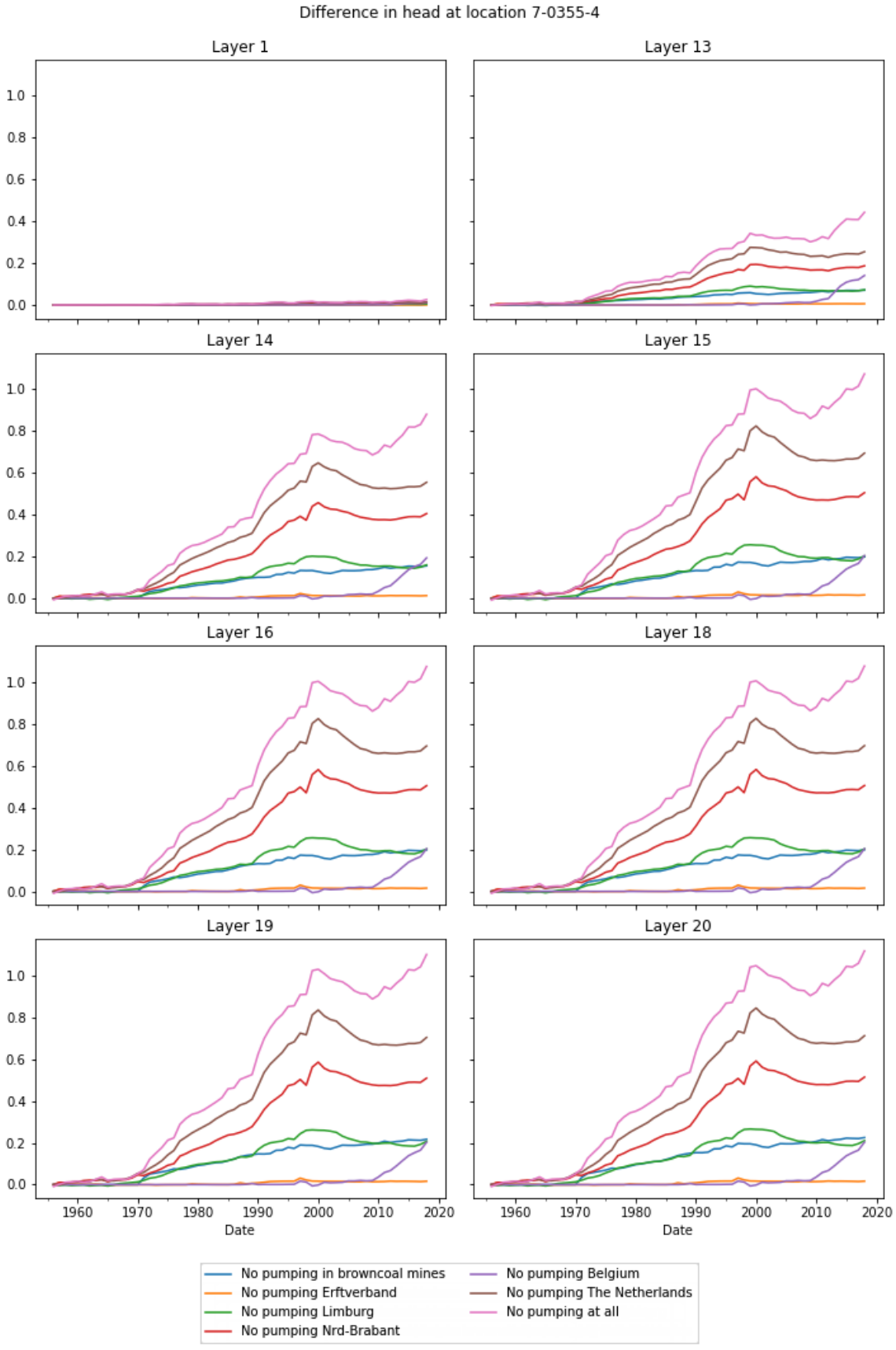
Difference in head at location 7-0355-4
Layer 1
Layer 13
Layer 14
Layer 15
Layer 16
Layer 18
Layer 19
Layer 20
1.0
0.8
0.6
0.4
0.2
0.0
1960
1970
1980
1990
2000
2010
2020
Date
No pumping in browncoal mines
No pumping Erftverband
No pumping Limburg
No pumping Nrd-Brabant
No pumping Belgium
No pumping The Netherlands
No pumping at all

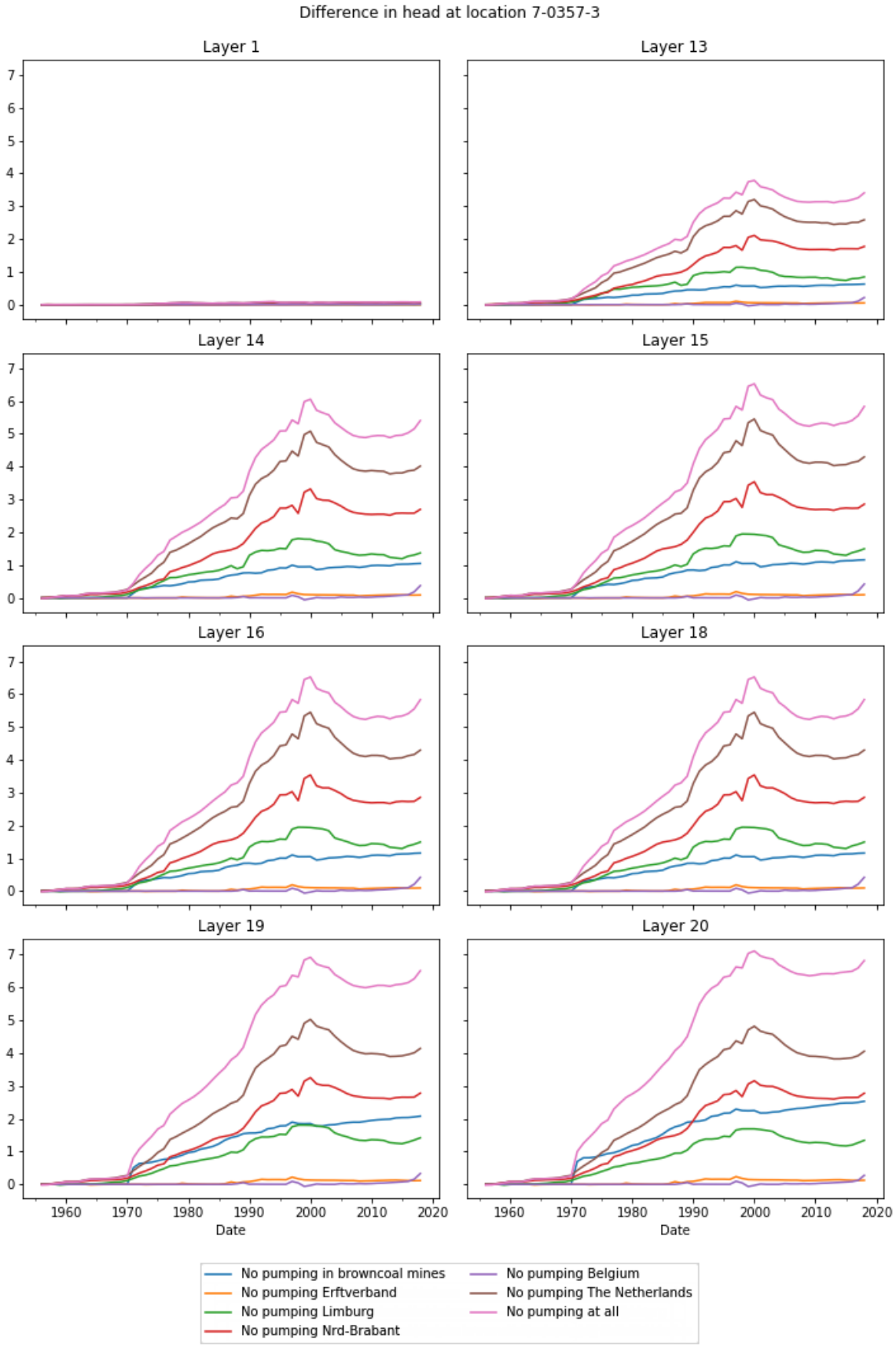
Difference in head at location 7-0357-3
Layer 1
Layer 13
Layer 14
Layer 15
Layer 16
Layer 18
Layer 19
Layer 20
0
1
2
3
4
5
6
7
1960
1970
1980
1990
2000
2010
2020
Date
No pumping in browncoal mines
No pumping Erftverband
No pumping Limburg
No pumping Nrd-Brabant
No pumping Belgium
No pumping The Netherlands
No pumping at all

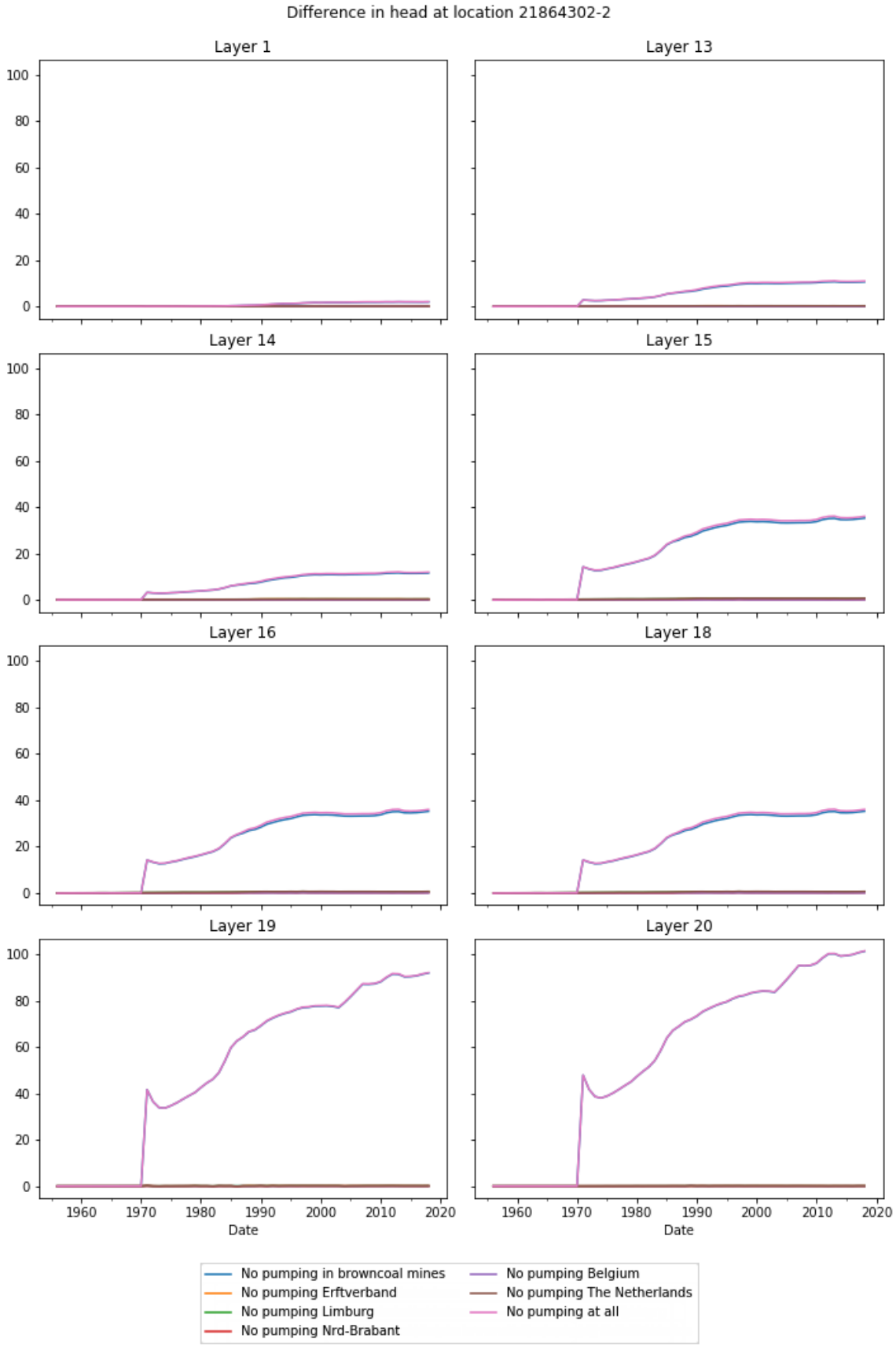
Difference in head at location 21864302-2
Layer 1
Layer 13
Layer 14
Layer 15
Layer 16
Layer 18
Layer 19
Layer 20
100
80
60
40
20
0
1960
1970
1980
1990
2000
2010
2020
Date
No pumping in browncoal mines
No pumping Erftverband
No pumping Limburg
No pumping Nrd-Brabant
No pumping Belgium
No pumping The Netherlands
No pumping at all

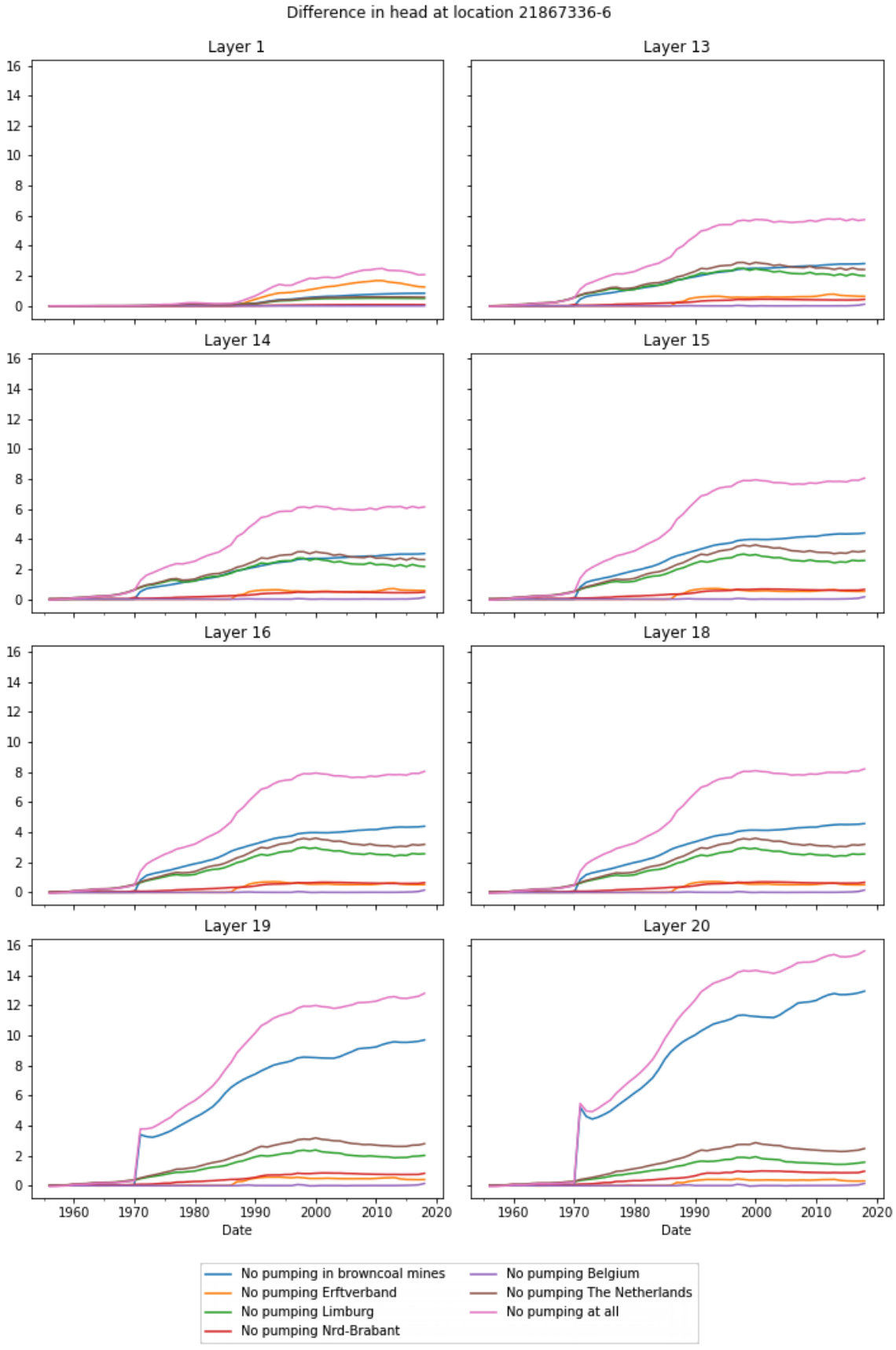
Difference in head at location 21867336-6
Layer 1
Layer 13
Layer 14
Layer 15
Layer 16
Layer 18
Layer 19
Layer 20
Date
Date
No pumping in browncoal mines
No pumping Erftverband
No pumping Limburg
No pumping Nrd-Brabant
No pumping Belgium
No pumping The Netherlands
No pumping at all

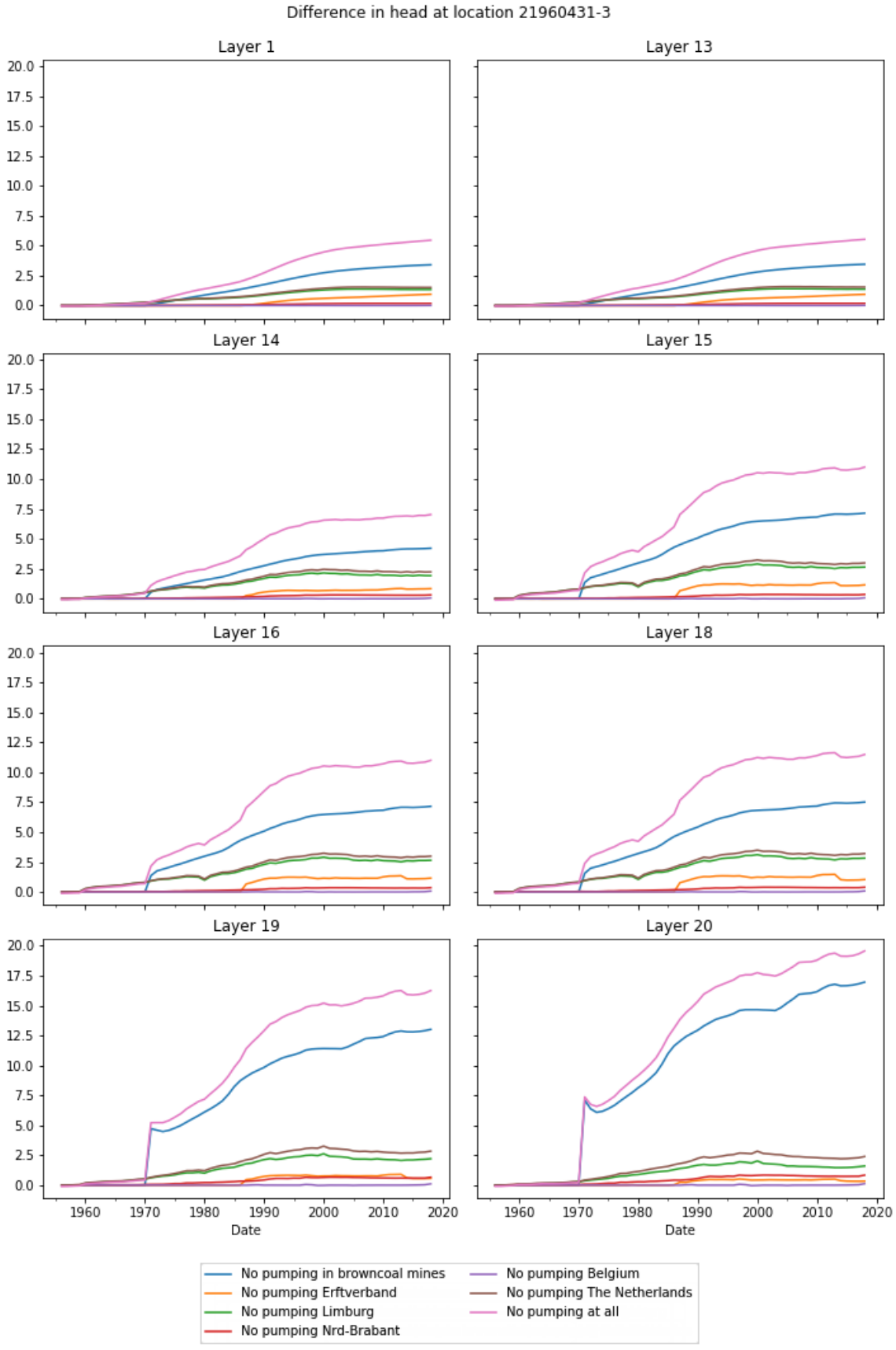
Difference in head at location 21960431-3
Layer 1
Layer 13
Layer 14
Layer 15
Layer 16
Layer 18
Layer 19
Layer 20
20.0
17.5
15.0
12.5
10.0
7.5
5.0
2.5
0.0
1960
1970
1980
1990
2000
2010
2020
Date
No pumping in browncoal mines
No pumping Erftverband
No pumping Limburg
No pumping Nrd-Brabant
No pumping Belgium
No pumping The Netherlands
No pumping at all

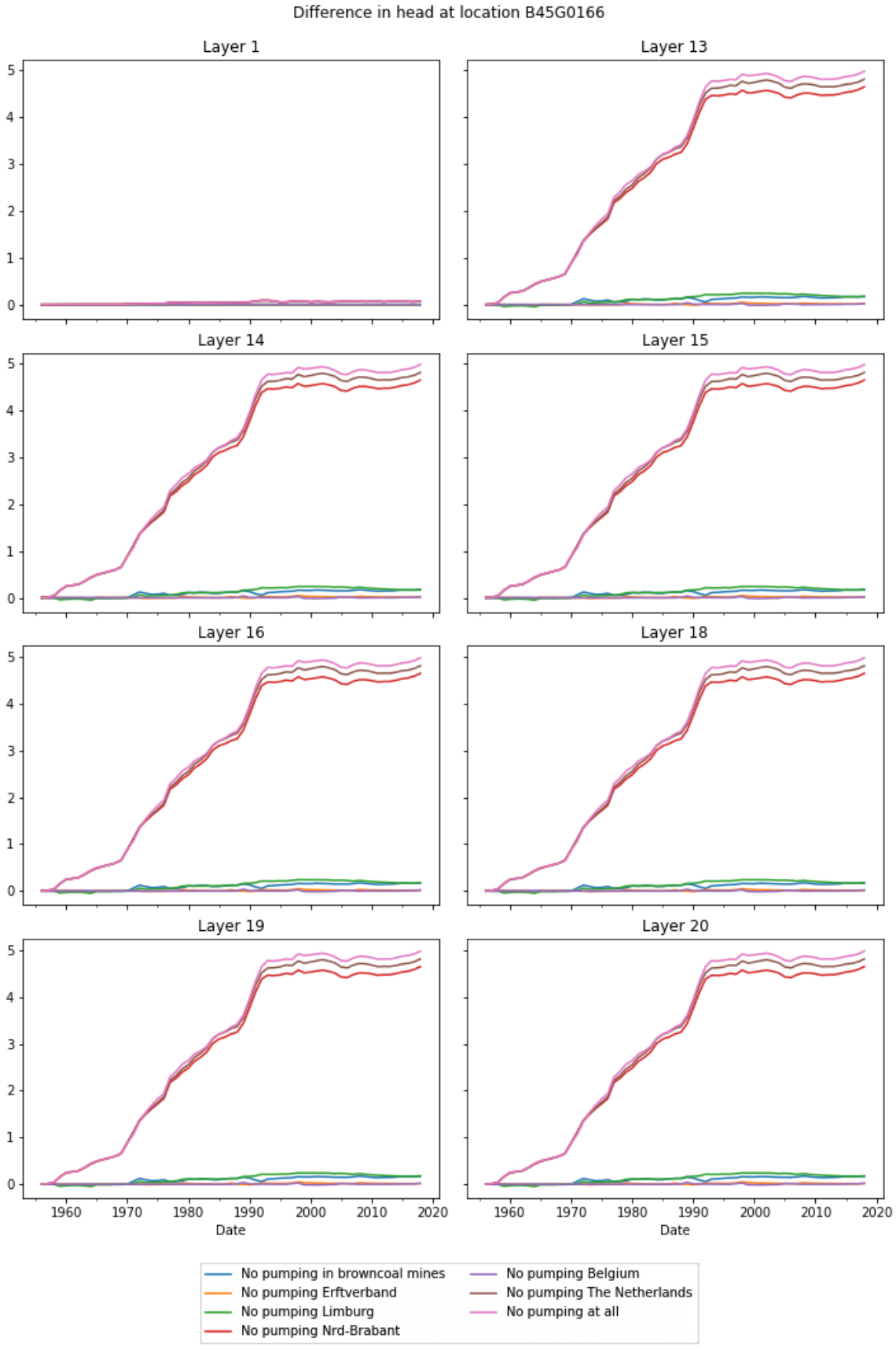
Difference in head at location B45G0166
Layer 1
Layer 13
Layer 14
Layer 15
Layer 16
Layer 18
Layer 19
Layer 20
0
1
2
3
4
5
1960
1970
1980
1990
2000
2010
2020
Date
No pumping in browncoal mines
No pumping Erftverband
No pumping Limburg
No pumping Nrd-Brabant
No pumping Belgium
No pumping The Netherlands
No pumping at all

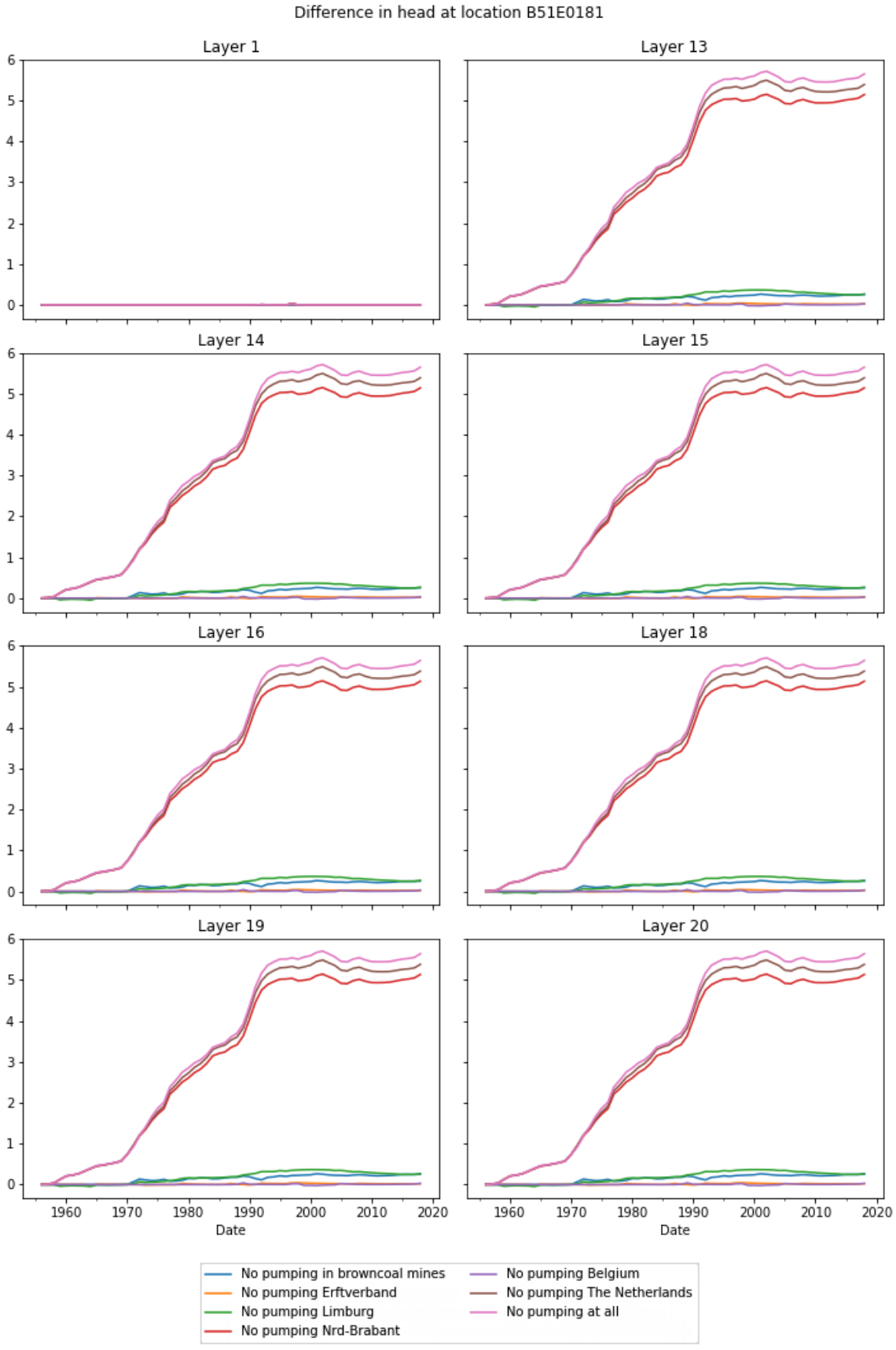
Difference in head at location B51E0181
Layer 1
Layer 13
Layer 14
Layer 15
Layer 16
Layer 18
Layer 19
Layer 20
0
1
2
3
4
5
6
1960
1970
1980
1990
2000
2010
2020
Date
No pumping in browncoal mines
No pumping Erftverband
No pumping Limburg
No pumping Nrd-Brabant
No pumping Belgium
No pumping The Netherlands
No pumping at all

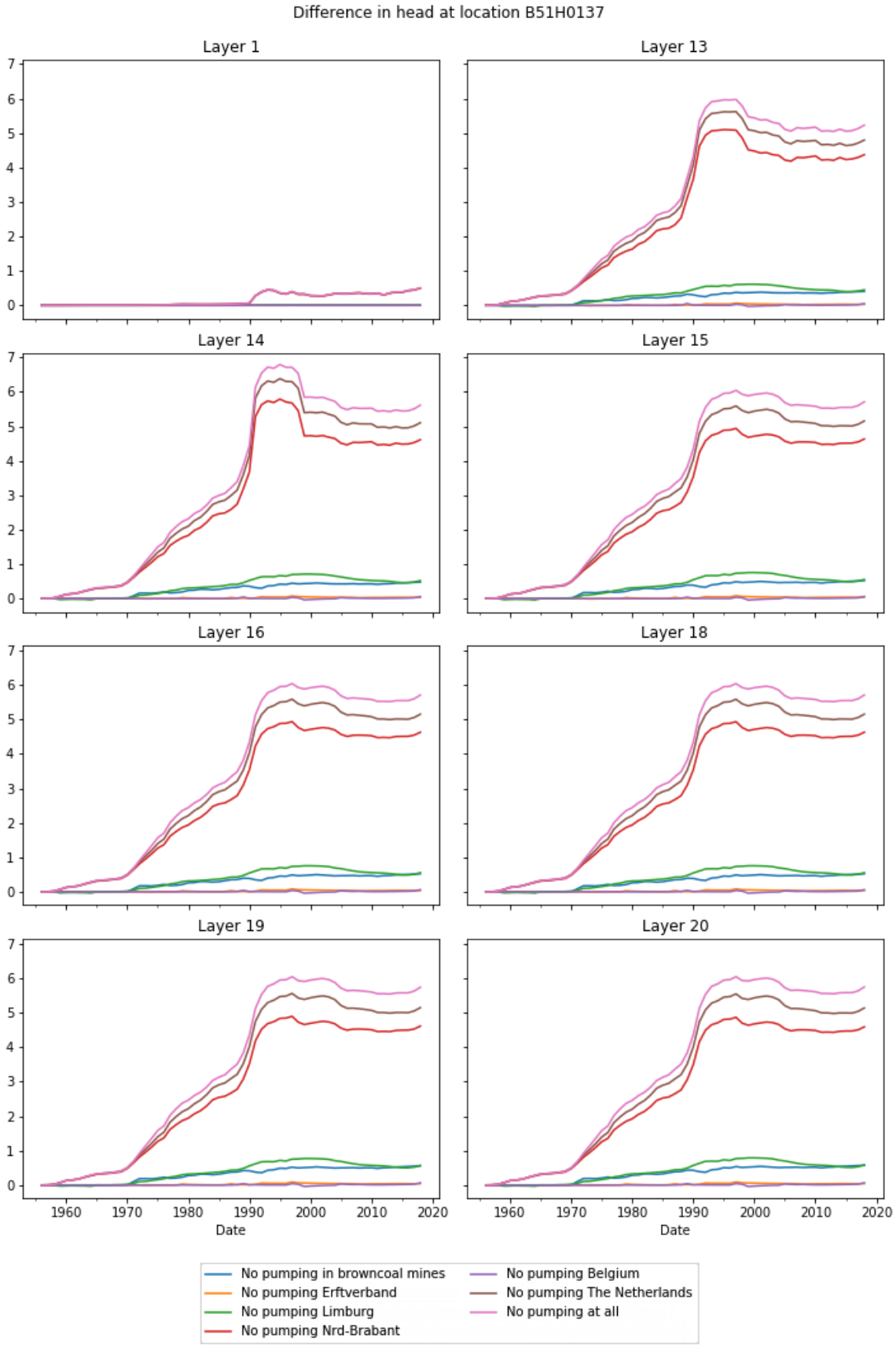
Difference in head at location B51H0137
Layer 1
Layer 13
Layer 14
Layer 15
Layer 16
Layer 18
Layer 19
Layer 20
Date
Date
No pumping in browncoal mines
No pumping Erftverband
No pumping Limburg
No pumping Nrd-Brabant
No pumping Belgium
No pumping The Netherlands
No pumping at all

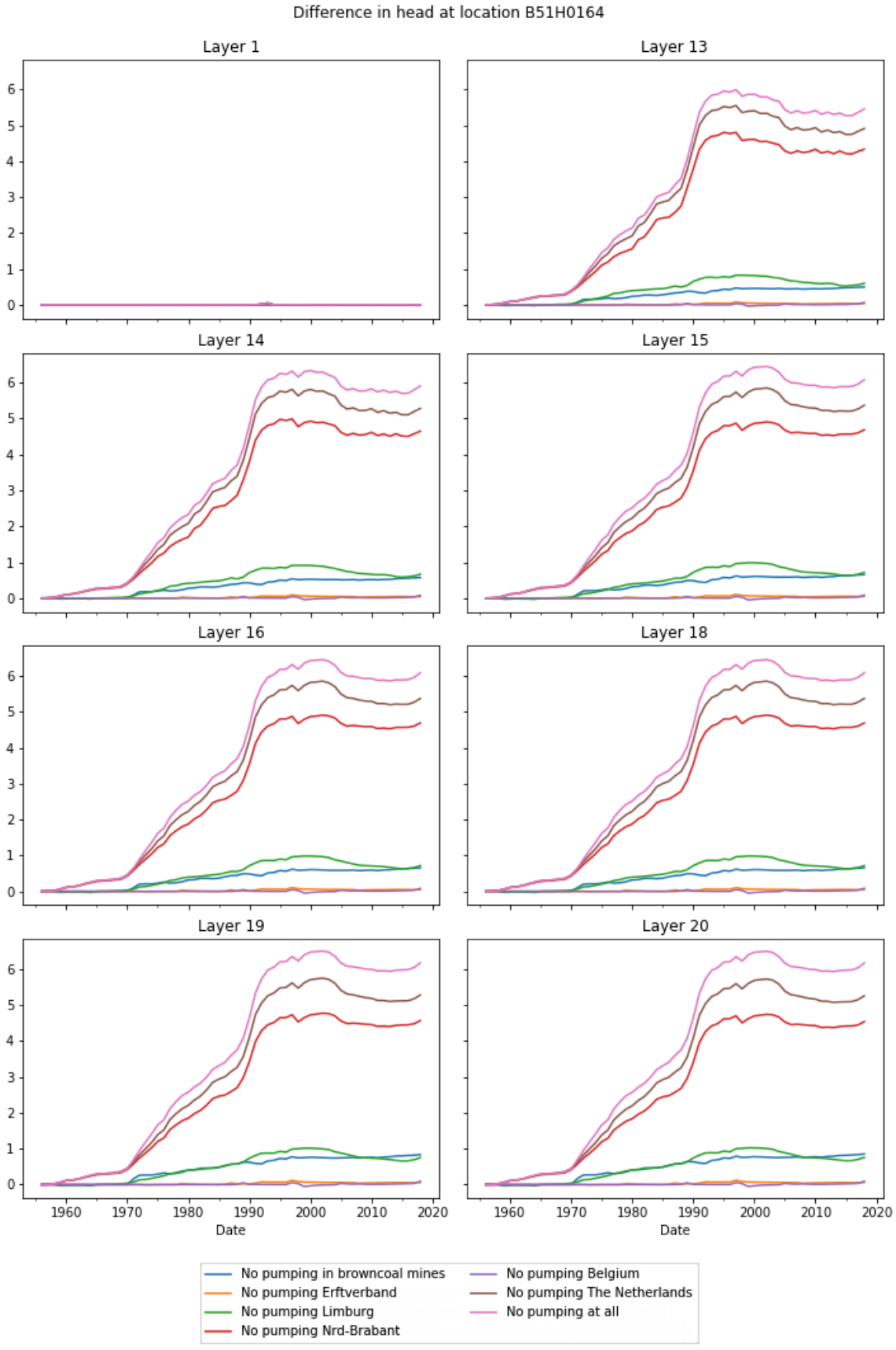
Difference in head at location B51H0164
Layer 1
Layer 13
Layer 14
Layer 15
Layer 16
Layer 18
Layer 19
Layer 20
0
1
2
3
4
5
6
1960
1970
1980
1990
2000
2010
2020
Date
No pumping in browncoal mines
No pumping Erftverband
No pumping Limburg
No pumping Nrd-Brabant
No pumping Belgium
No pumping The Netherlands
No pumping at all

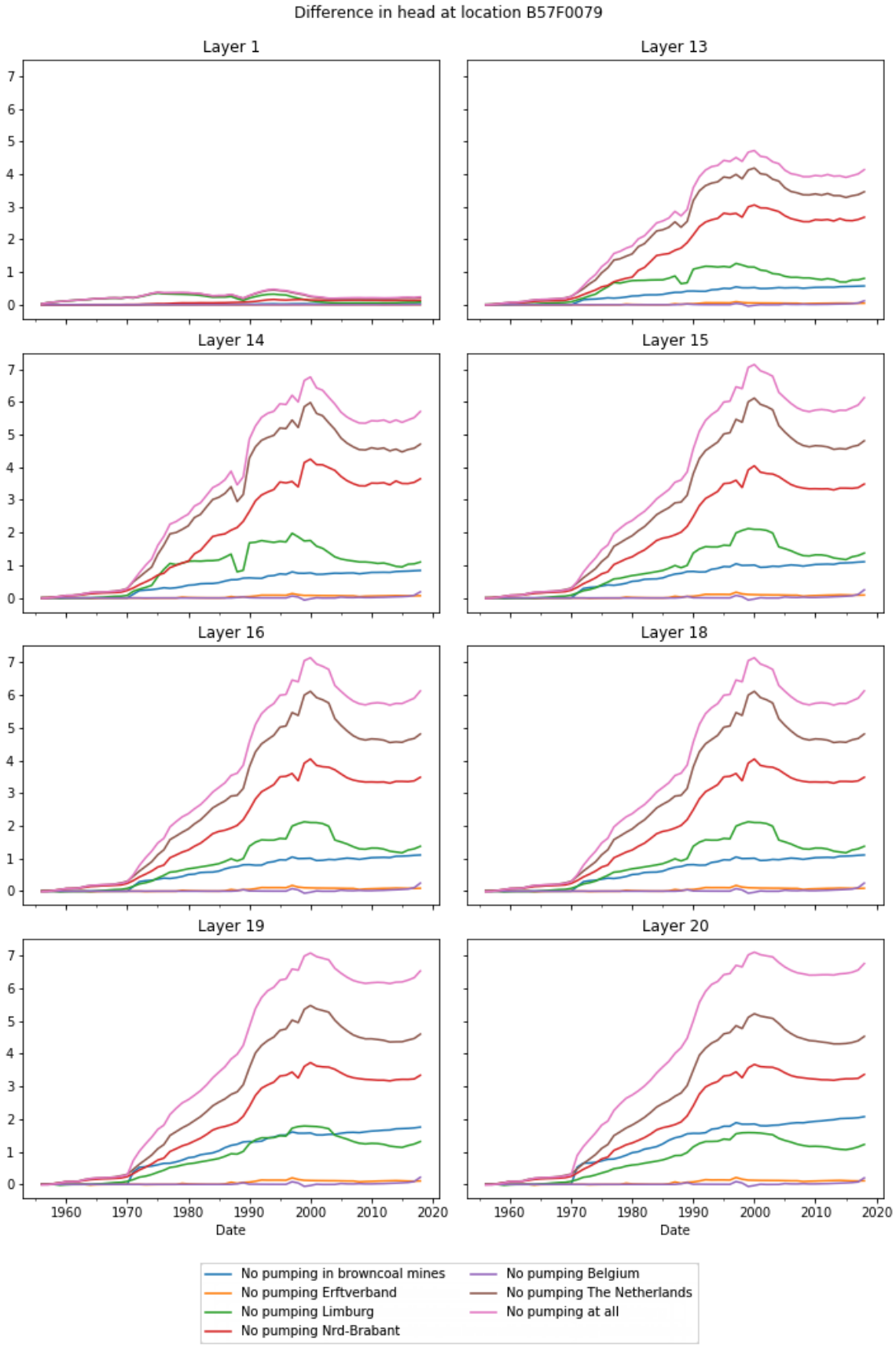
Difference in head at location B57F0079
Layer 1
Layer 13
Layer 14
Layer 15
Layer 16
Layer 18
Layer 19
Layer 20
0
1
2
3
4
5
6
7
1960
1970
1980
1990
2000
2010
2020
Date
No pumping in browncoal mines
No pumping Erftverband
No pumping Limburg
No pumping Nrd-Brabant
No pumping Belgium
No pumping The Netherlands
No pumping at all

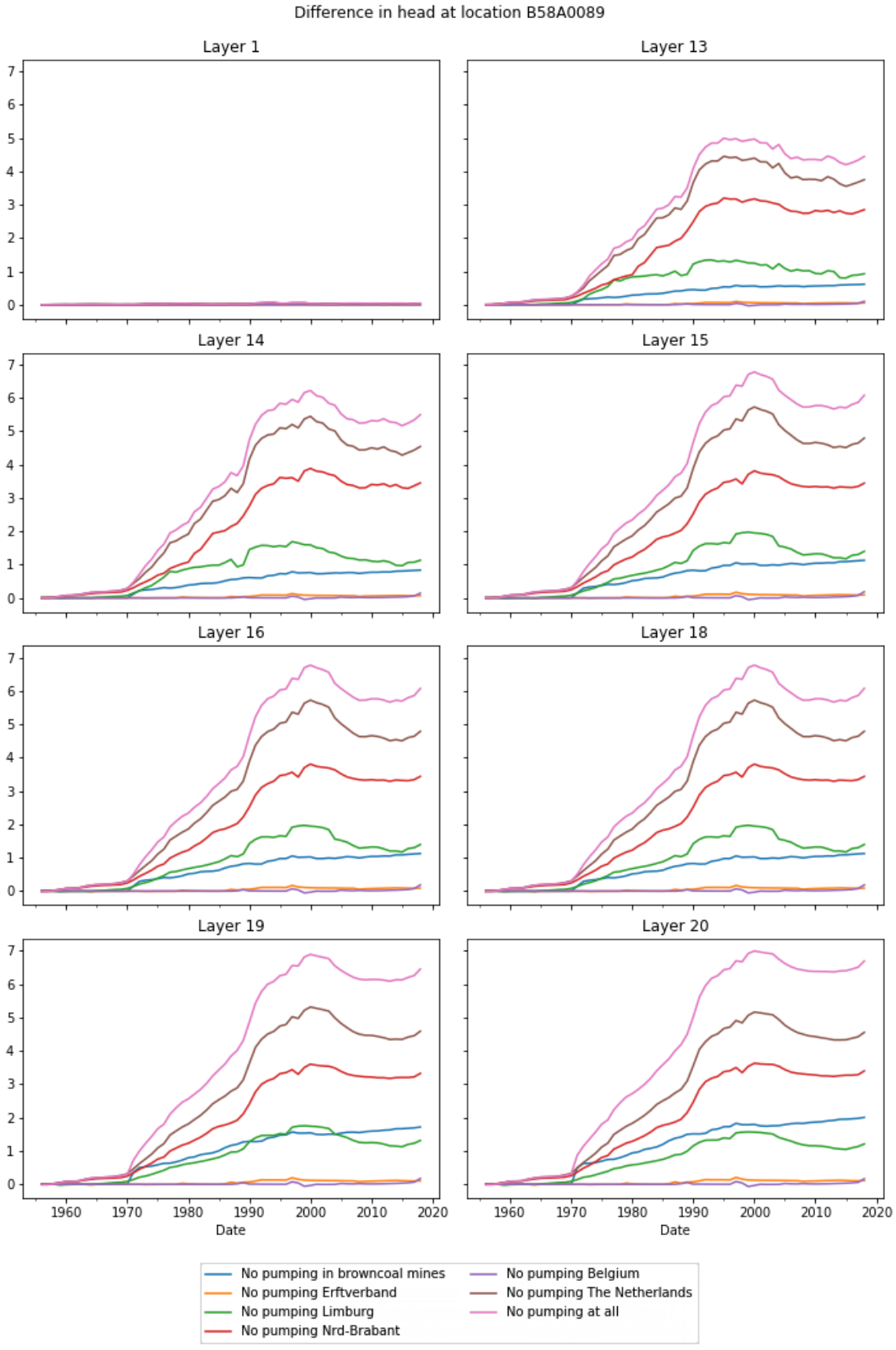
Difference in head at location B58A0089
Layer 1
Layer 13
Layer 14
Layer 15
Layer 16
Layer 18
Layer 19
Layer 20
Date
Date
No pumping in browncoal mines
No pumping Erftverband
No pumping Limburg
No pumping Nrd-Brabant
No pumping Belgium
No pumping The Netherlands
No pumping at all

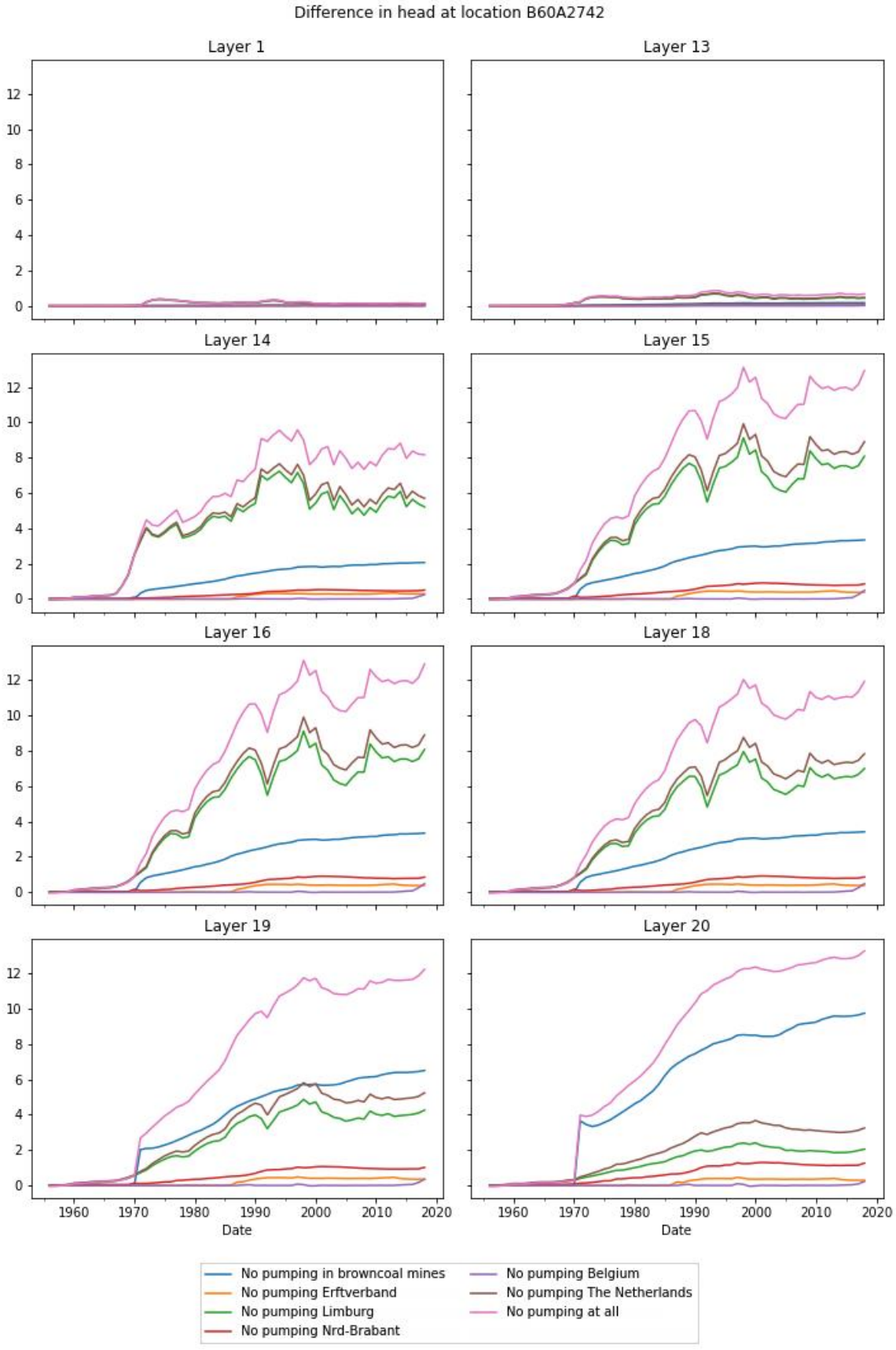
Difference in head at location B60A2742
Layer 1
Layer 13
Layer 14
Layer 15
Layer 16
Layer 18
Layer 19
Layer 20
0
2
4
6
8
10
12
1960
1970
1980
1990
2000
2010
2020
Date
No pumping in browncoal mines
No pumping Erftverband
No pumping Limburg
No pumping Nrd-Brabant
No pumping Belgium
No pumping The Netherlands
No pumping at all

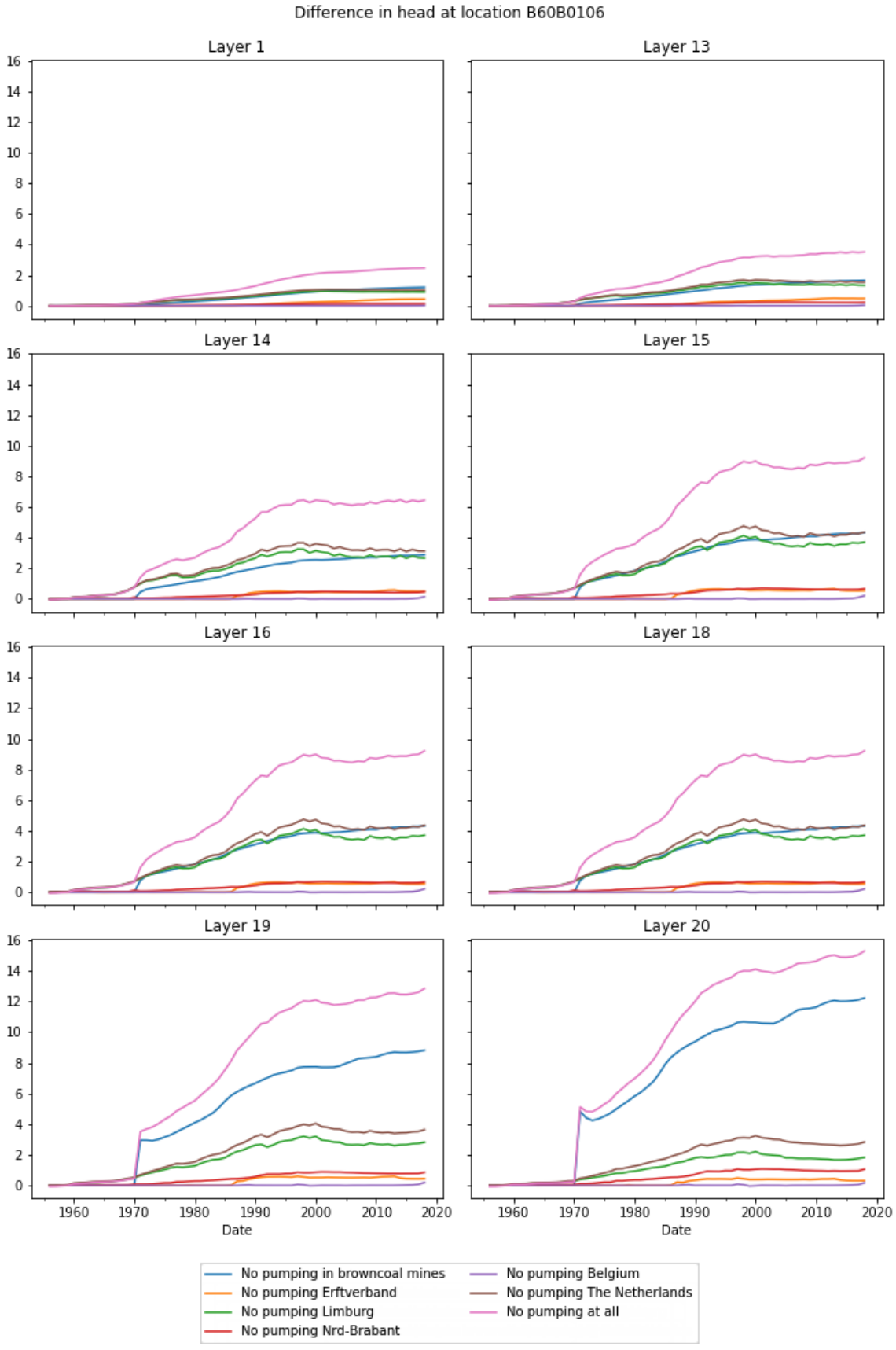
Difference in head at location B60B0106
Layer 1
Layer 13
Layer 14
Layer 15
Layer 16
Layer 18
Layer 19
Layer 20
Date
Date
No pumping in browncoal mines
No pumping Erftverband
No pumping Limburg
No pumping Nrd-Brabant
No pumping Belgium
No pumping The Netherlands
No pumping at all

A.12 Spatial Percentage of Influence

Here figures are presented that show the percentage that each influencer has on the groundwater level.

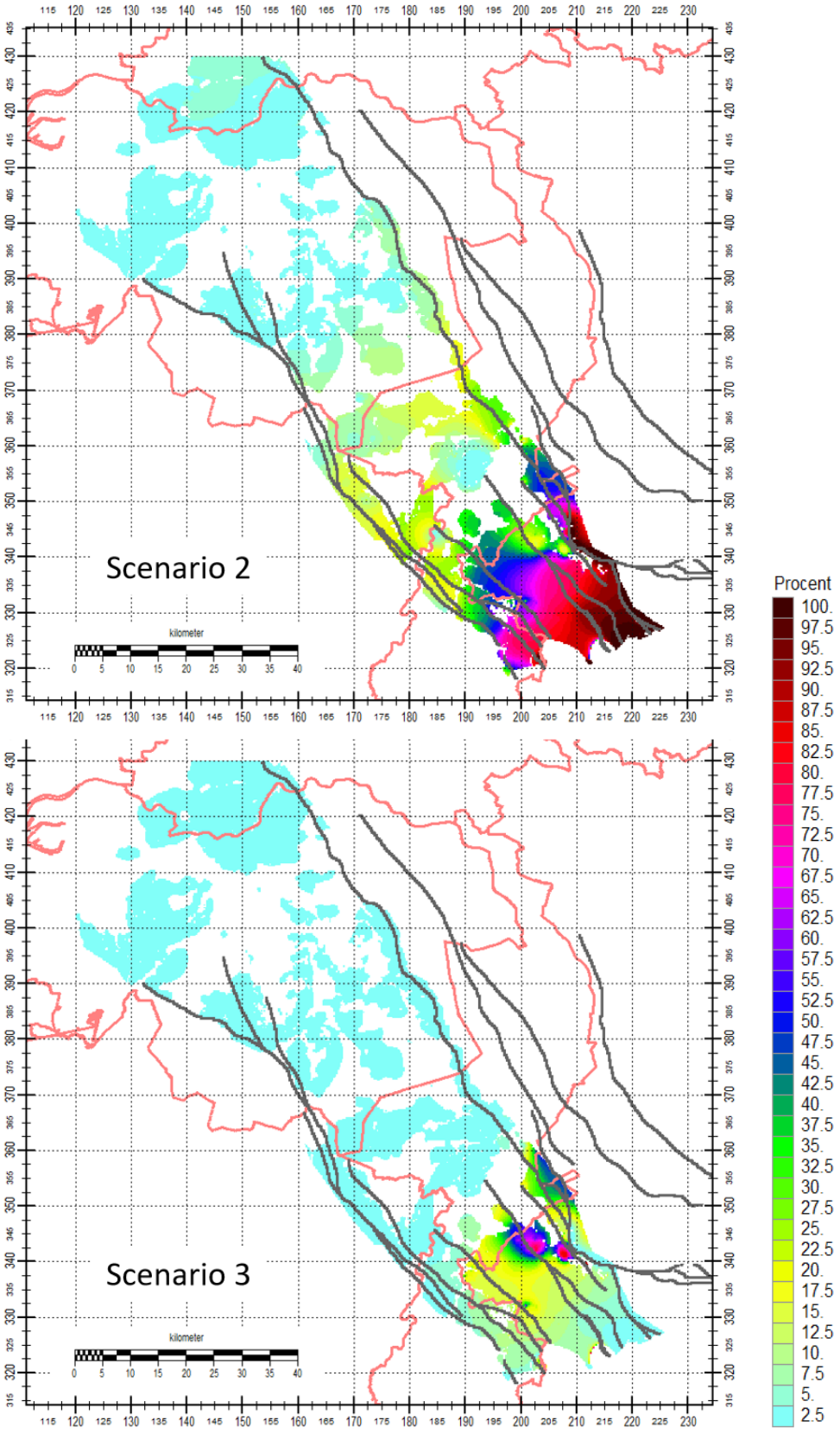

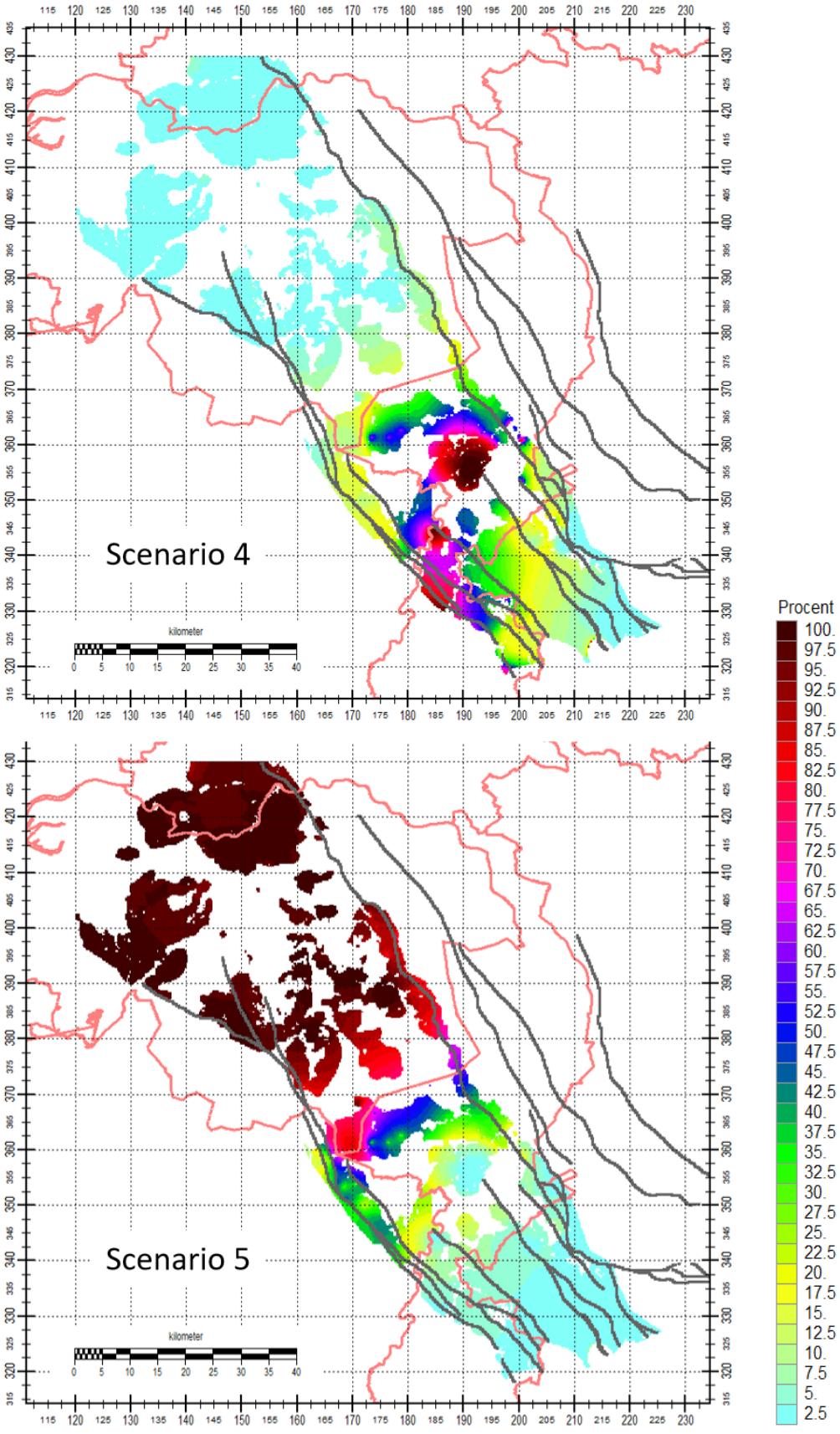
Scenario 4
kilometer
0 5 10 15 20 25 30 35 40
Scenario 5
kilometer
0 5 10 15 20 25 30 35 40
Procent
100.
97.5
95.
92.5
90.
87.5
85.
82.5
80.
77.5
75.
72.5
70.
67.5
65.
62.5
60.
57.5
55.
52.5
50.
47.5
45.
42.5
40.
37.5
35.
32.5
30.
27.5
25.
22.5
20.
17.5
15.
12.5
10.
7.5
5.
2.5

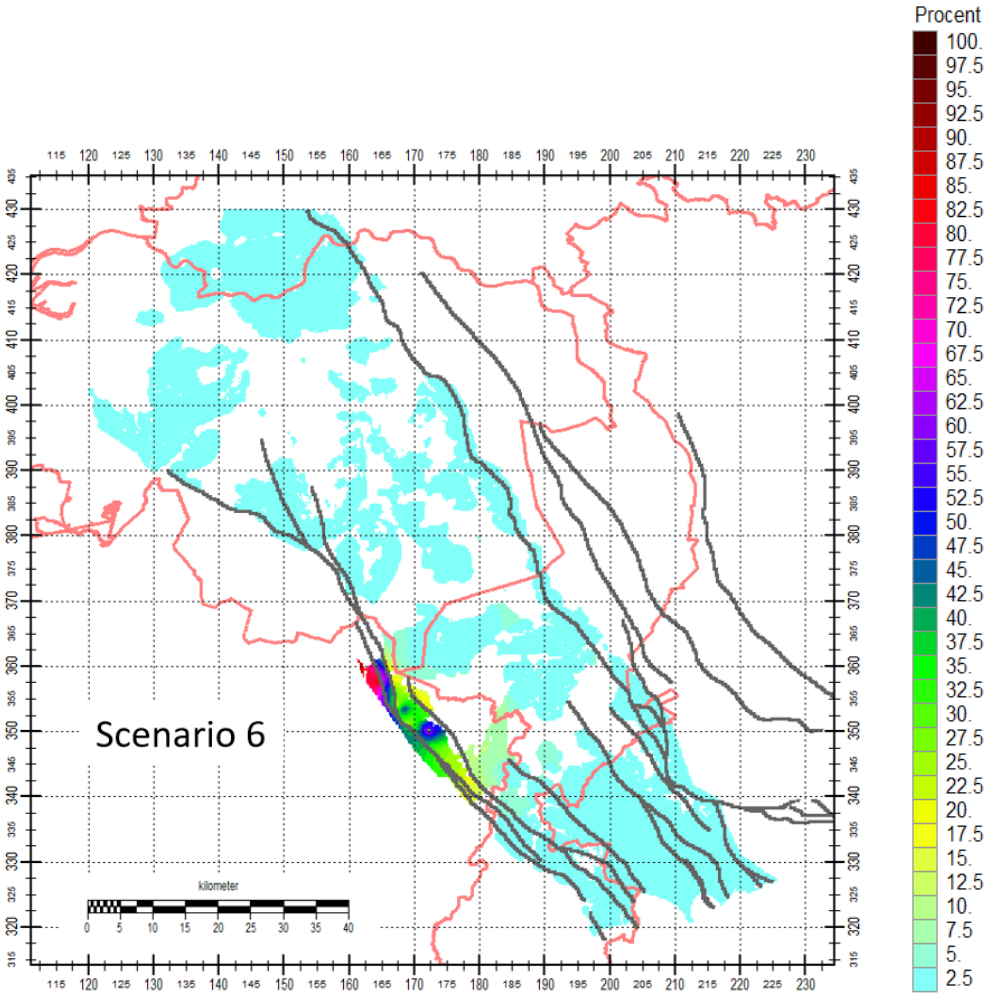
Procent
100.
97.5
95.
92.5
90.
87.5
85.
82.5
80.
77.5
75.
72.5
70.
67.5
65.
62.5
60.
57.5
55.
52.5
50.
47.5
45.
42.5
40.
37.5
35.
32.5
30.
27.5
25.
22.5
20.
17.5
15.
12.5
10.
7.5
5.
2.5
Scenario 6
kilometer
0 5 10 15 20 25 30 35 40

Procent
100.
97.5
95.
92.5
90.
87.5
85.
82.5
80.
77.5
75.
72.5
70.
67.5
65.
62.5
60.
57.5
55.
52.5
50.
47.5
45.
42.5
40.
37.5
35.
32.5
30.
27.5
25.
22.5
20.
17.5
15.
12.5
10.
7.5
5.
2.5
Scenario 5
Scenario 2
Scenario 6
Scenario 3
Scenario 4
Aquifer 2

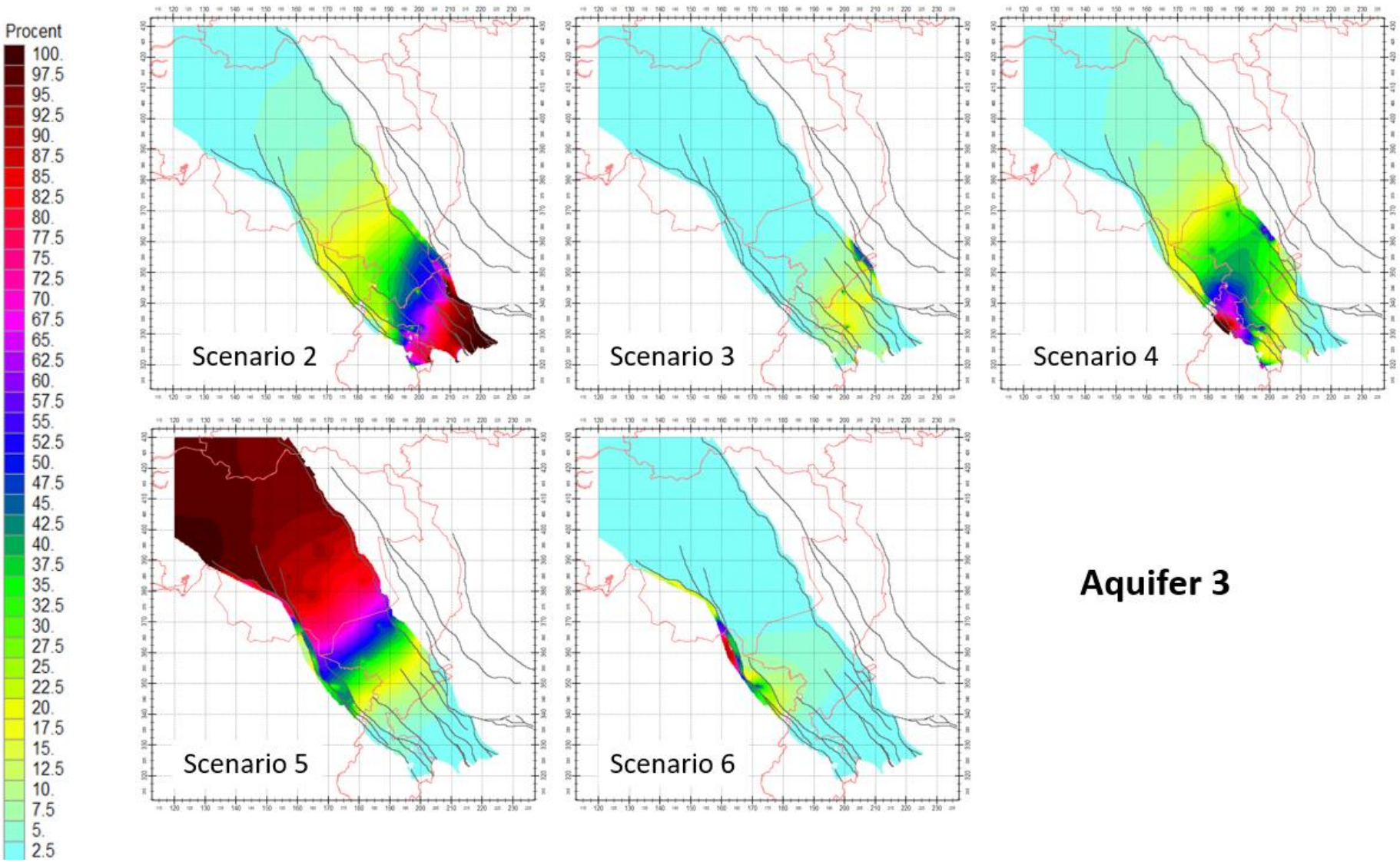
Procent
100.
97.5
95.
92.5
90.
87.5
85.
82.5
80.
77.5
75.
72.5
70.
67.5
65.
62.5
60.
57.5
55.
52.5
50.
47.5
45.
42.5
40.
37.5
35.
32.5
30.
27.5
25.
22.5
20.
17.5
15.
12.5
10.
7.5
5.
2.5
Scenario 2
Scenario 3
Scenario 4
Scenario 5
Scenario 6
Aquifer 3

A.13 Local effect near the Rode Beek and the Saeffelerbach

These figures show the local effect of all extractions on the groundwater level, the pressure heads in the 1st (model layer 14) and 2nd aquifer (model layer 15).

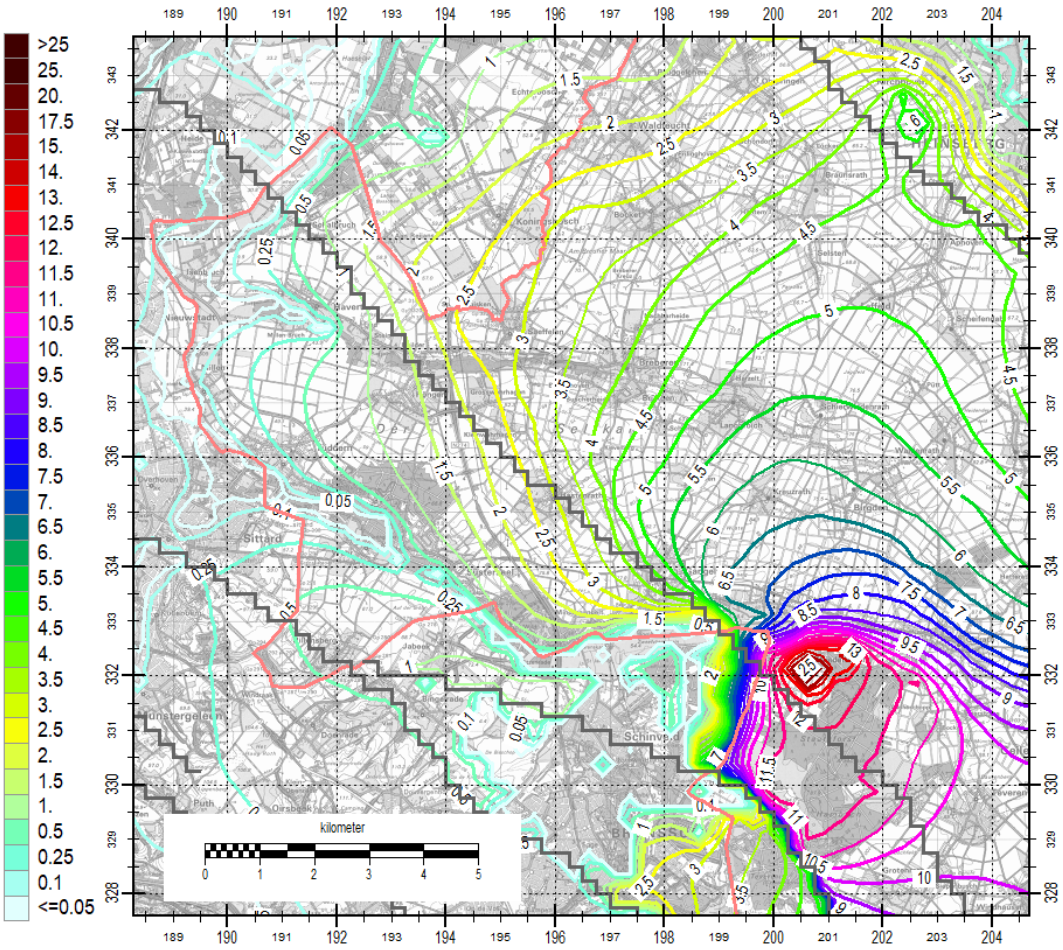

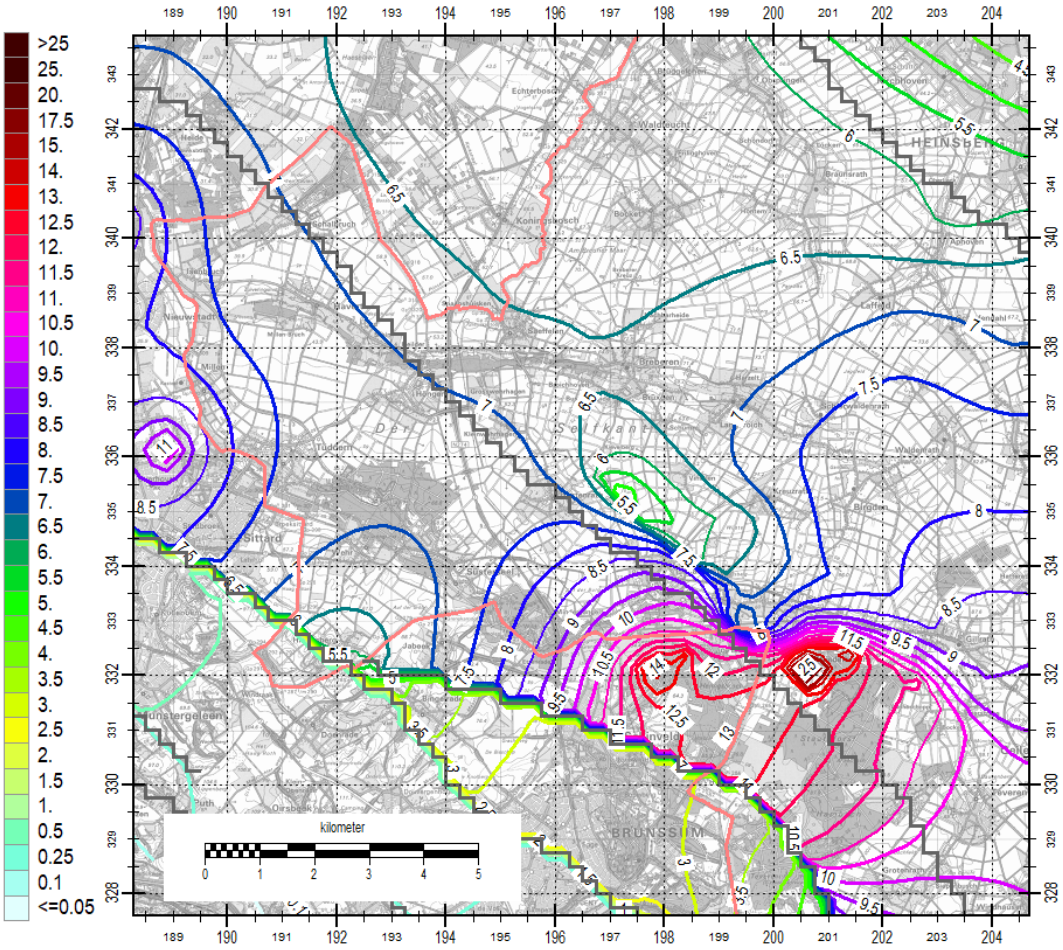
>25
25.
20.
17.5
15.
14.
13.
12.5
12.
11.5
11.
10.5
10.
9.5
9.
8.5
8.
7.5
7.
6.5
6.
5.5
5.
4.5
4.
3.5
3.
2.5
2.
1.5
1.
0.5
0.25
0.1
<=0.05
kilometer
0
1
2
3
4
5
HEINSBERG
BRUNSSUM
Sittard

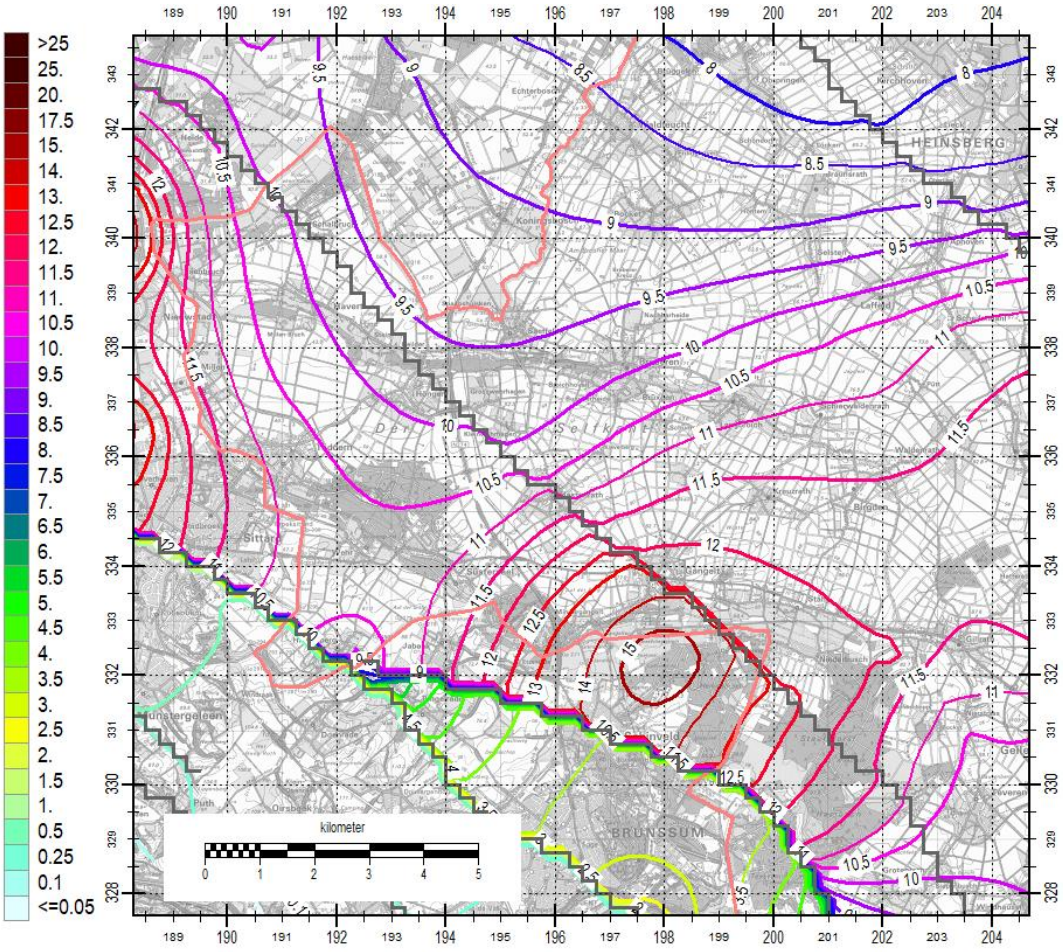
>25
25.
20.
17.5
15.
14.
13.
12.5
12.
11.5
11.
10.5
10.
9.5
9.
8.5
8.
7.5
7.
6.5
6.
5.5
5.
4.5
4.
3.5
3.
2.5
2.
1.5
1.
0.5
0.25
0.1
<=0.05
kilometer
0 1 2 3 4 5
HEINSBERG
BRUNSSUM
189 190 191 192 193 194 195 196 197 198 199 200 201 202 203 204
328 329 330 331 332 333 334 335 336 337 338 339 340 341 342 343